HHS Public Access

Author manuscript

Compr Physiol. Author manuscript; available in PMC 2018 February 13.

Published in final edited form as:

Compr Physiol. 2015 January ; 5(1): 45–98. doi:10.1002/cphy.c140002.

The Distal Convoluted Tubule

James A. McCormick and **David H. Ellison**

Division of Nephrology & Hypertension Oregon Health & Science University & VA Medical Center Portland, OR

I. Definition and morphology

The distal tubule of the mammalian kidney can be defined as the nephron segment between the macula densa region and the cortical collecting tubule. It comprises several morphologically and functionally heterogeneous subsegments, reabsorbs 5–10% of the filtered sodium and chloride under normal conditions, and participates importantly in net K^+ secretion. The segment also plays a central role in systemic calcium homeostasis, in systemic magnesium homeostasis, and in net acid secretion. Inherited disorders of distal cell function lead to systemic abnormalities of extracellular fluid (ECF) volume and potassium, calcium, and magnesium balance, confirming the importance of the distal tubule to human physiology and human disease.

The variable nomenclature sometimes applied to the distal nephron, and segmental and functional differences between mammalian species, have led to confusion about anatomical and functional properties. Although the definition of "distal tubule" is precise, the term has also been used to describe the thick ascending limb (or distal straight tubule) and distal convoluted tubule (see below). According to this anatomical definition, the connecting tubule and cortical and medullary collecting ducts form the collecting system. Early anatomists and physiologists, however, also described a "distal convolution", which can be distinguished from the proximal convolution and from straight tubules (171). This distal convolution corresponds to the distal tubule of the micropuncture literature and comprises the distal convoluted tubule and connecting tubule (468, 565). Some authors have referred to the entire region between the macula densa and the confluence as the "distal convoluted tubule" (339, 340), and when tubule segments were dissected for perfusion in vitro, it has then been divided into *bright, granular*, and *light* portions, according to its appearance.

Careful analysis of cell types along the renal distal tubule and of the segment's physiological properties, its hormonal responsiveness, and its response to physiological perturbation indicates that the renal distal tubule comprises four anatomically discrete subsegments (91, 229, 254). These include a short region of cortical thick ascending limb (cTAL), the distal convoluted tubule (DCT), the connecting tubule (CNT), and the initial portion of the cortical collecting duct (CCD). Here, the term *renal distal tubule* will be used to indicate the entire

Address for correspondence: David H. Ellison, M.D., Division of Nephrology & Hypertension, Oregon Health & Science University, 3181 SW Sam Jackson Park Road, CH12R, Portland, OR 97239, 503 494 4465, ellisond@ohsu.edu.

region between the macula densa and the CCD. The term *distal convoluted tubule* will be restricted to the segment comprising distal convoluted tubule cells.

Figure 1A shows the microanatomical organization of superficial and juxtaglomerular distal nephrons. In rats and rabbits, the post macula densa thick ascending limb of superficial nephrons ascends toward the kidney surface. The length of this post macula densa segment varies greatly. It is 0–500 μm in rabbits and 150 ± 20 μm in rats (105). This segment never reaches the kidney surface in normal rats, rabbits, or humans (254). In most species, there is an abrupt transition from TAL to DCT before the tubule reaches the kidney surface. After ascending toward the kidney surface, DCTs commonly make "hairpin" turns, after which they return close to the glomerulus (see Figure 1*A*). Although direct contact of the second loop of the distal tubule with a more proximal portion of distal tubule or the macula densa is uncommon, this second portion of the distal tubule frequently does make contact with the afferent arteriole (106). The physiological significance of this contact is not clear, but it may participate in resetting the tubuloglomerular feedback (345, 542, 543). The distal convoluted tubule has been shown to be 1.15 ± 0.05 mm long in the adult rat, with the entire renal distal tubule measuring 2.26 ± 0.11 mm (105). In all species, the DCT comprises distal convoluted tubule cells; in most species, intercalated cells begin to appear along the length of this tubule segment. In rat, mouse, and human, intercalated cells appear in the latter portion of the DCT and continue through the connecting and collecting tubules; in rabbit, intercalated cells are found only in the connecting and collecting tubules (254).

Distal convoluted tubule cells (see Figure 1B) are taller than TAL cells and demonstrate extensive amplification of the basolateral cell membrane (amplification is defined as the ratio of basolateral membrane area to apical membrane area). The amplification, twofold in rat and rabbit (254), results from extensive formation of narrow lamella-like lateral processes. These processes exhibit intermingling with neighboring DCT cells, providing extensive areas of cell-cell interaction. Encased within these basolateral processes are mitochondria, which impart a "palisading" appearance to the cells (231). Distal convoluted tubule cells contain the largest number of mitochondria per unit length of any cell along the nephron (233). In the basal portion of the cell, the lateral cell processes split into basal ridges that contain bundles of filaments, believed to anchor the cells to the basement membrane. Cell nuclei are uniformly located very close to the apical surface, where they often appear to be flattened by the luminal membrane. Mitochondria are not interposed between the nucleus and apical membrane but do fill the perinuclear region. The apical membrane is characterized by numerous short microvilli. Corresponding to the high density of mitochondria and to the extensive basolateral membrane amplification, the Na^+-K^+-ATPase activity is the highest in the DCT of any nephron segment (238, 433).

The CNT lies just distal to the DCT, arising abruptly in rabbits and gradually in most other species (254). In all species, it comprises predominantly two cell types, CNT cells and intercalated cells. The microanatomical organization of CNT differs between superficial and deeper nephrons (see Figure 1*A*). In superficial nephrons, the CNT is an unbranched segment that flows into the initial portion of the initial collecting tubule, before draining into a collecting duct. In the rat, the CNT of superficial nephrons was shown to be 0.49 ± 0.03 mm in length (105). The connecting tubules of mid cortical and juxtamedullary nephrons

generally join to form an 'arcade' before draining into a collecting duct, as shown in Figure 1A. These 'arcades' then ascend through the cortical labyrinth. As shown in Figure 1A, as they ascend, additional nephrons empty fluid into them, and it has been suggested that this serves to prevent the additional of dilute fluid into the collecting duct; as discussed below, connecting tubule cells express aquaporin 2 (246). These arcades usually run close to an interlobular artery (246). Only after one or more CNTs have joined do principal cells appear, indicating transition to the CCT. It has been suggested that some arcades probably exist in all mammalian species, but the percentage of nephrons emptying into the collecting duct via arcades, versus emptying directly, varies (465).

The appearance of CNT cells (see Figure 1B) is the same whether in superficial distal tubules or in arcades. Connecting tubule cells have been characterized as appearing intermediate between DCT and principal cells (232). In species such as the rat, where transitions from DCT to CNT and CCT are gradual, distinguishing DCT, CNT, and principal cells may be difficult, especially near the junctions between segments (226). However, it is now clear that CNT cells are distinct morphologically, functionally, and at the molecular level. Connecting tubule cells demonstrate basolateral cell membrane amplification, as do DCT cells. However, in CNT cells, more of the amplification results from infolding of the basal membrane rather than amplification of lateral cell processes (as in DCT cells) (226). Thus, in the CNT, there is less cell-cell contact than in the DCT. Mitochondria appear between the basal infoldings, but their number is significantly reduced compared with the DCT. The nucleus of CNT cells is apically oriented, but unlike in DCT cells, mitochondria may be observed between the nucleus and the apical membrane. The apical membrane of CNT cells exhibits fewer apical projections than does the apical membrane of DCT cells.

II. Electrophysiology

Electrical properties of the DCT, and CNT have been examined in vivo, in rats, using micropuncture techniques, and in vitro, in rabbit, mouse, and rat. In the rat, experiments performed in vivo showed that the transepithelial voltage throughout most of the superficial renal distal tubule is oriented with the lumen negative with respect to the blood (82, 237, 314). Wright (565) first showed that the transepithelial voltage becomes more lumen negative along the length of the distal tubule, a result confirmed by others (for references, see (400)). As the transepithelial voltage of the TAL is oriented with the lumen positive, with respect to the interstitium, the orientation of the transpiethelial voltage transitions somewhere along the DCT. TAL cells extend 100–300 μm beyond the macula densa in both rabbit and rat (231). Schnermann et al. (435) showed that the first 300 μm of rat DCT secretes NaCl in situ. They suggested that NaCl secretion creates a lumen-positive diffusion potential, owing to the higher permeability of these segments to Na^+ than to Cl^-. When Wright (565) plotted transepithelial voltage versus percent length along the superficial distal tubule, a sigmoidal relation was obtained (see Figure 2). The voltage was very low along the first 40% of the tubule length, rapidly increased in the region between 40 and 60%, and remained constant along the terminal 30% of tubule length. The region between 40–60% of distal length was shown by Dorup (105) to be the site at which intercalated cells appear in the rat and to comprise primarily DCT and CNT cells. This region is also the site at which all three subunits of the epithelial Na^+ channel first appear (524). Thus the transepithelial

voltage becomes negative in the region in which molecular pathways that mediate electrogenic Na^+ transport appear at the apical membrane. Based on a summary of the data, a model developed by Weinstein utilized a voltage of −5 mV, oriented with the lumen negative, for the middle portion of the DCT (554). A model of the CNT, also developed by Weinstein, estimated a value of −24 mV, oriented with the lumen negative, when aldosterone was present (555). It is this voltage that drives transepithelial K^+ secretion.

Figure 2*B* shows measurements of the transepithelial resistance of rat distal tubules, measured both in vivo and in vitro. Of note, the resistance is correlated inversely with the magnitude of the transepithelial voltage and therefore with the distance along the tubule. De Bermudez and Windhager (95) showed that the resistance of the distal tubule is reduced by arginine vasopressin, an effect that is more pronounced along the last 50% of distal tubule length than along the first half of distal tubule length. The decline in transepithelial resistance along the distal tubule probably reflects the larger component of electrogenic transport in more distal regions. Unfortunately, transitions between segments of rat distal tubules are gradual, so that inferences concerning properties of individual segments must be made cautiously.

In contrast, transitions between segments of the rabbit distal nephron are abrupt, making it possible to isolate specific nephron segments for study in vitro. Unfortunately, despite discrete segmentation of the rabbit distal nephron, a great deal of variability has been observed in studies of rabbit distal segments perfused in vitro; this is now believed to reflect difficulties in identifying and perfusing discrete segments. Two studies during the 1970s indicated that the voltage of the rabbit DCT is large and oriented with the lumen negative, with respect to the bath (180, 215). Subsequently, later studies, however, obtained voltages that are much lower (351, 451, 454, 525). There are several explanations for the differences in transepithelial voltage between studies performed before 1980 and those performed subsequently. In the early experiments, the perfused DCT segments were as long as 800 μm (180). As noted by Imai and colleagues (452, 454), DCT segments are usually <500 μm in length in rabbits, and it is likely that the longer DCT segments contained CNT cells as well as DCT cells. Velázquez et al. (525) harvested DCT from rabbits in the usual manner by cutting at the transition from TAL to DCT and at the junction with the CNT. Each DCT segment was then transected a second time at its midpoint. When the proximal segments were perfused in vitro, the transepithelial voltage was 0 mV and was amiloride resistant. In contrast, when the more distal segments (still “DCT” segments) were perfused in vitro, the transepithelial voltage was lumen negative (−4 mV) and could be inhibited by amiloride. These results suggest that the large transepithelial voltages obtained from early studies resulted, in part, from contamination by CNT cells. A second cause for variability of membrane voltages is the tubule perfusion rate. The transepithelial voltage of distal nephron segments varies inversely with tubule perfusion rate and with perfusion pressure (180). Although the mechanisms by which perfusion pressure and flow rate affect voltage are not understood fully, the same effect is observed in vivo, during perfusion of distal tubules (169). Regardless of the mechanisms by which luminal flow rate affects the transepithelial voltage, it appears that most measurements of transepithelial voltage in earlier studies were obtained using lower perfusion pressures. If one uses data from more recent studies, the values for rabbit tubules are similar to those of rodent tubules.

When CNT are perfused in vitro, they are usually obtained from arcade segments (see Fig. 1*A*), not from superficial distal tubules. Thus data on the properties of rabbit CNT cannot be compared directly with data on properties of "mid" or "late" segments of rat distal tubules. Nevertheless, both morphological and molecular information suggest that CNT from arcades are similar to CNT from superficial distal tubules (18, 84, 125, 367). The transepithelial voltage of CNT from rabbits perfused in vitro has ranged between 5 and 27 mV, oriented with the lumen negative with respect to the bath. As is the case for other tubule segments, the voltage of CNT varies inversely with perfusion pressure; the highest voltage (−27 mV) reported for this segment was obtained at a very low perfusion rate (215).

Claudins form the predominant permeability barriers across tight junctions. Along the DCT, paracellular solute transport is likely to be relatively modest (554), suggesting that paracellular permeability is low. Three claudins, 3, 7, and 8, have been reported to be present along the DCT (202), although claudin 7 was found at the basolateral membrane, rather than tight junctions. The appearance of claudin 8 appeared quite specific for the DCT (284).

The discussion above has focused primarily on a morphological or anatomical definition of the distal tubule. This nephron segment clearly plays important functional roles, as will be discussed below. The major ion transport pathways expressed by the cells of the distal tubule have largely been identified, and the hormonal receptors involved in regulating it have largely been identified.

III. Solute and water transport

A. Water transport

Distal convoluted tubule cells do not express aquaporin-2 (AQP2) (85); thus, the DCT forms the terminal diluting segment of the kidney. As AQP3 and AQP4 are typically expressed in cells that express AQP2, these also may not be expressed by DCT cells (85).

B. Sodium and chloride transport

1. Rates of Na^+ and Cl^- transport—Information about the quantitative contribution of the distal tubule to renal NaCl transport derives primarily from micropuncture experiments in rats. Sodium chloride delivery to the distal tubule depends on extracellular fluid (ECF) volume status. When ECF volume ranges from low to high, Na^+ delivery to the superficial distal tubule ranges from 4 to 20% of the filtered load (126, 240, 241, 314, 385). Because solute is reabsorbed by TAL cells, but water is not, the Na^+ concentration in the lumen of the first accessible segments of distal tubules ranges from 35 to 77 mM (168). It should be recalled, however, that solute delivery to distal segments accessible to micropuncture reflects the actions of a segment of TAL that lies distal to the macula densa (the post macula densa TAL) and a short segment of the DCT. To overcome these limitations, Schnermann and colleagues used Munich Wistar rats, which have post macula densa segments accessible at the kidney surface (435), and showed that luminal Na^+ and Cl^- concentrations rise as fluid flows from the macula densa into the DCT, owing to Na^+ and Cl^- secretion. Thus solute delivery to the most proximal portions of the DCT may be overestimated by measurements taken in superficial distal tubules. Under basal conditions, in the rat, transepithelial Na^+

reabsorption is approximately 200 pmol·min^{-1}·mm^{-1} (554). When Na^+ delivery to the DCT is varied, however, Na^+ transport also varies directly; thus Na^+ reabsorption is load-dependent. Khuri et al. (241) and Kunau et al. (257) increased distal Na^+ delivery by infusing saline or urea-saline into hydropenic animals. Both groups found that approximately 80% of the delivered Na^+ load was reabsorbed along the distal tubule. When volume expansion was more extreme, however, Kunau and colleagues found that fractional Na^+ reabsorption declined to 40% (257). Although this suggests that the distal tubule responds to extracellular volume expansion by reducing the fractional NaCl reabsorption, Diezi et al. (102) could not detect a change in distal fractional reabsorption, if the delivered load was kept constant, suggesting that the distal tubule is not subject to the effects of the 'physical factors' that alter transport along the proximal tubule.

Velázquez and colleagues (519) were the first to study the mutual dependence of Na and Cl transport along the DCT systematically. They found that Na^+ transport along the distal tubule is linearly dependent on the luminal concentration of Na^+, between 10 and 100 mM, when the luminal Cl^- concentration is maintained constant. Similarly, they found that Cl^- transport along the distal tubule is linearly dependent on the luminal Cl^- concentration, between 10 and 100 mM. In addition to dependence on the concentration of the transported molecule, however, these investigators also reported that Na^+ transport is dependent on Cl^- concentration and that Cl^- transport is dependent on Na^+ concentration; the molecular mechanism responsible for this mutual dependence is now known to be the thiazide-sensitive Na-Cl cotransporter (NCC, encoded by *SLC12A3*) (see below).

When luminal NaCl delivery increases, much of the increased NaCl transport along the distal tubule traverses the NCC, although some Na^+ traverses pathways that do not saturate. In microperfused rat distal tubules, raising the luminal NaCl concentration twofold increased transepithelial Na^+ transport by a factor of 3; this increase could be blocked entirely by luminal chlorothiazide (129). The dependence of transepithelial NaCl transport on luminal NaCl concentration probably results from a dependence of NCC on extracellular Na^+ and Cl^- concentrations, as modeled by Weinstein (554), although regulatory mechanisms also contribute.

2. Mechanisms of Na^+ and Cl^- transport—Pathways for Na^+ and Cl^- transport across the mammalian distal tubule have been investigated using functional, optical, electrophysiological, immunological, radioligand, and molecular techniques. These pathways are shown Table 1 and in Figure 3.

a. Na^+-K^+-ATPase: The Sodium-potassium-ATPase (Na^+-K^+-ATPase) is expressed at the basolateral membrane of DCT cells, CNT cells, and cells of the collecting tubule. It provides the primary driving force for Na^+ transport across all three segments by keeping the cellular Na^+ concentration low and the cellular K^+ concentration high (236). The Na^+-K^+-ATPase also contributes to making the inside of the cell electronegative with respect to the outside, both because it is electrogenic (moves 3 Na^+ out and 2 K^+ in) and because it generates large ion concentration gradients. Distal convoluted tubule cells express the highest Na^+-K^+-ATPase activity of any nephron segment (107, 117, 152, 233, 238), an observation that mirrors the extensive amplification of their basolateral cell membrane and the abundance of

mitochondria (233, 271). Connecting tubule cells also express high levels of Na^+-K^+-ATPase activity, but the activity of principal cells is much lower.

The Na^+-K^+-ATPase and the H^+K^+-ATPase share a great deal of structural homology. They are both composed of an α-subunit that is predicted to span the membrane 10 times and a β-subunit that spans the membrane once in a type II orientation. During the biosynthesis of these pumps, the β-subunits assemble with the α-subunits in the endoplasmic reticulum. Formation of the α-β complex appears to involve interactions between the cytoplasmic, extracytoplasmic, and transmembrane domains of the proteins and may be assisted through the involvement of chaperone proteins (111). Subunit assembly is required for the holoenzyme complex to reach the plasma membrane (111).

The Na^+-K^+-ATPase is also associates with an FXYD protein (reviewed in (154)), which has been characterized as a fine-tuning modulator of the Na^+-K^+-ATPase expressed in kidney tissues. This small single transmembrane domain protein interacts with the a subunit of Na^+-K^+-ATPase to increase affinity for ATP and decrease affinity for Na^+ allowing medullary cells to continue pump activity under reduced cellular ATP levels. The FXYD subunit is undetectable in kidney cell cultures grown under isotonic conditions and expression is induced with acute or chronic exposure to hypertonicity. The FXYD subunit demonstrates remarkable regulatory complexity including induction by chloride ions rather than sodium, the differential expression of at least 2 isoforms, involvement of separate MAP kinase signaling pathways for transcription (JNK) and translation (PI3K) as well as cell type regulation of expression. Mutations of this subunit, surprisingly, cause a disorder of magnesium wasting (see below) (413).

b. Thiazide-sensitive Na-Cl cotransporter: A dominant pathway by which Na^+ enters DCT cells across the apical membrane is NCC (see Figure 3) (18, 43, 367, 390, 586). Thiazide diuretics were shown nearly 40 years ago to inhibit Na^+ transport along the superficial distal tubule (258), but the nature of the transport pathway(s) inhibited by these diuretics remained obscure. As noted, Velázquez et al. (519) showed mutual dependence of Na^+ and Cl^- transport along the DCT. Stokes (474) reported that thiazides inhibit a coupled electroneutral NaCl cotransport pathway in the bladder of the winter flounder and suggested that it might be a related pathway. Ellison et al. (129) reported that a thiazide-sensitive electroneutral transport pathway mediates the majority of Na^+ and Cl^- transport by the 'early' distal tubule (DCT). Gamba et al. (151) isolated and cloned the electroneutral NaCl cotransporter from the bladder of the winter flounder; they also showed that this protein (now known as NCC) was structurally similar to a protein from the distal nephron of rats (150). The NCC was subsequently cloned from human (457), mouse (259), and rabbit (520). NCC is homologous to the bumetanide-sensitive Na-K-2Cl cotransporters (both secretory and absorptive isoforms (149), and to the K-Cl cotransporters (149). These transporters are members of the *cation chloride cotransporter* family; genes for this family are identified as members of the *SLC12* family; NCC derives from *SLC12A3* (149).

The mammalian NCC has a core size of 110 kDa (in rat, it is 1002 amino acid residues in length), but because it is glycosylated, runs between 125 and 180 kDa on Western blots (43, 390). It comprises 12 membrane-spanning domains, with amino and carboxyl termini within

the cytoplasm. The protein is glycosylated on two asparagine residues on the fourth extracellular loop (200); deletion of both glycosylation sites (but not either one alone) creates a protein that is not functional (200). Although the cation chloride transporters have not yet been crystallized, data obtained by crystallizing related amino acid polyamine organocation superfamily members, AdiC and ApcT, were used to model NKCC1 (461). The model, which probably shares several aspects with the closely related NCC, is consistent with the structure suggested above.

The site(s) at which thiazide diuretics, Na^+, and Cl^- bind to the transporter have remained obscure, owing to conflicting data. Tran et al. (499) showed that Cl^- competitively inhibits [^{3}H]metolazone binding to kidney membranes, suggesting that the diuretic binds to the anion site on the transporter. Chang and Fujita (70) proposed a kinetic model in which binding of ions and diuretics can be approximated by a state diagram. The transport protein is postulated to possess two ion-binding sites: one for anions and DCT diuretics and one for cations. Rate constants can be devised that permit the behavior of the model system to correspond to the behavior of the protein under a variety of physiological conditions. Alternatively, Monroy and colleagues (338) used data from NCC expressed in *Xenopus laevis* oocytes to show that the concentrations of both Na^+ and Cl^- affect the affinity of thiazides for NCC. The higher the concentration of both ions, the lower the thiazide-induced inhibition of NCC function. For example, the IC_{50} for metolazone inhibition of NCC was shifted by one order of magnitude to the left when either Cl^- or Na^+ was decreased from 100 to 2 mM (338); final answers concerning sites and mechanisms of diuretic binding to NCC await further structural data.

Expression of NCC is limited to the DCT in all species studied to date. While thiazide diuretics can inhibit transport along the proximal tubule (112, 140) and collecting duct (492), under some conditions, these effects are related to inhibition of transport proteins other than NCC (280). Although NCC expression is limited to the DCT, there are species-specific differences in the distribution of transport proteins along the distal tubule. In rabbit, NCC expression is limited to DCT cells and ends abruptly at the transition to CNT (18, 520). In human, rat, and mouse, however, expression of NCC extends from the proximal end of the DCT through a transitional segment (17, 43, 301, 302, 367). This transitional segment, referred to as the DCT2 or 'late DCT' (367), shares properties of the distal convoluted and CNT; it will be described more fully below.

Kinetic characteristics for NCC, with respect to its substrates, Na^+ and Cl^-, are now well defined. Before the protein was cloned, in vivo microperfusion data showed that the luminal $K_{1/2}$ concentrations for transport were 9 mM for Na^+ and 12 mM for Cl^-, when the counterion was kept constant (519). These values are slightly above those obtained by expressing the cotransporter in Xenopus oocytes, (338). These values are highly dependent on the experimental conditions used, and when modeling the kinetics of NCC, Weinstein integrated data from a variety of conditions to derive a best-fit model that incorporates varying concentrations of both ions (554); in this case, the apparent $K_{1/2}$ values for both Na^+ and Cl^+ are below 5 mM.

The role of NCC has also been studied using knockout approaches. A global NCC knockout exhibited hypomagnesemia and hypocalciuria, both cardinal features of human Gitelman syndrome (see below). The mice were reported to be normotensive at baseline, during anesthesia, although blood pressure was low when consuming a low salt diet (439). Abnormal sodium losses were not observed in those mice. A subsequent study showed that dietary KCl deprivation, which had little effect on plasma K^+ in wild type mice, caused substantial hypokalemia in $NCC^{-/-}$ mice (344). Interestingly, however, a mouse model that more closely resembles Gitelman syndrome, in which a Gitelman-mutant NCC was 'knocked in', did have substantial hypokalemia and hypotension at baseline (584). Reasons for the differences between the two models are unclear at this time.

c. Sodium proton antiporter: A second major apical Na^+ transport pathway of the DCT is NHE2, which is coexpressed with the NCC (68). Micropuncture studies suggest it transports substantial amounts of Na^+, but that it may be activate primarily when distal bicarbonate delivery is high (546) (see below, for further discussion). Although NHE3 has been detected at the apical surface of TAL cells, it does not appear to be expressed by DCT (9). The "housekeeping" isoform of the Na^+/H^+ exchanger, NHE-1, has been localized by immunocytochemistry to the basolateral surface of DCT cells in rabbit (29).

d. Other sodium entry pathways: At least in some species, the DCT also expresses the amiloride-sensitive Na^+ channel, ENaC. While early studies reported ENaC along the DCT (109), the method for identifying the DCT was not defined explicitly. In rats and mice, there is now clear evidence for a segment of the distal nephron in which ENaC and NCC are co-expressed, at the molecular level (17, 298, 434). This correspondence occurs in the segment defined originally by Bachmann and colleagues as the DCT2 (also called the 'late' DCT), based on coexpression of NCC with the Na^+/Ca^{2+} exchanger (367). The relative length of the segment in which NCC is co-expressed with ENaC, and its physiological role, remain subjects of debate. Most evidence suggests that the DCT2 is approximately one third as long as the DCT1. Of note, when rats are treated with thiazide diuretics chronically, to block NCC, cells of the DCT1 undergo apoptosis (300); similarly, when NCC is deleted genetically, the DCT1 does not develop (303). These data suggest that expression of NCC is essential for both the development and maintenance of DCT1 structure and function.

e. Chloride channels: As noted above, Na^+ exits DCT cells across the basolateral membrane via the ubiquitous Na^+-K^+-ATPase, (see Figure 3). Chloride, however, exits the cell primarily via two pathways, a KCl cotransporter and a chloride channel. Cellular chloride activity is maintained above electrochemical equilibrium in DCT cells by NCC. There is both functional and molecular evidence for a basolateral chloride channel in the DCT; the channel has a conductance of 9 pS and is inhibited by phorbol ester (307). This channel is probably a member of the ClC family of chloride channels. Rodent chloride channels are ClC-K1 and ClC-K2, which are homologous to the human channels ClC-KA and ClC-KB, respectively (242). Vandewalle et al. (516) detected CLC-K1 and CLC-K2 in microdissected Sprague-Dawley DCT segments; immunocytochemical analysis, using an antibody that recognized both CLC-K1 and CLC-K2, demonstrated abundant labeling of the DCT basolateral membrane (516). In contrast, Uchida et al. (502) did not detect expression

of the CLC-K1 by DCT segments. Yoshikawa et al. (590) used in situ hybridization, combined with immunocytochemistry with known markers, to identify sites of CLC-K expression. Whereas CLC-K1 was expressed in the medulla, CLC-K2 was expressed throughout the TAL, DCT, and CNT. Similar results have been obtained for humans for ClC-KB. Weinstein argues, based on known conductive properties of the DCT (306, 307) and on mathematical modeling, that the majority of transcellular chloride flux must traverse a coupled transporter, yet, there is strong evidence for a role of ClC-KB in mediating basolateral Cl exit from DCT cells, as patients with mutations in *CLCNKB* exhibit a clinical syndrome that includes some features of typical Gitelman syndrome, combined with features of Bartter syndrome (444).

f. Potassium chloride cotransporters: A second pathway for Cl^- exit from DCT cells is a K-Cl cotransporter. Functional evidence for K-Cl cotransport across DCT cells had been reported several years ago, where it was speculated to be either in the apical or basolateral membrane (128, 527). Jentsch and colleagues could not detect KCC4 in DCT cells, and found that its deletion did not affect intracellular chloride (38). They detected this isoform on the basolateral membrane of alpha intercalated cells, however, and found that mice lacking KCC4, develop metabolic acidosis (38). Gamba and colleagues recently confirmed that KCC4 is expressed at the basolateral membrane of alpha intercalated cells (332). More recently, however, Velázquez and colleagues found that KCC4 is expressed along rabbit DCT (523). In humans, KCC1 has been reported to be expressed widely, including along DCT (285). Based on conductive properties of the peritubular membrane of the DCT, Weinstein (554) found that DCT models require that the predominant C^{l-} exit pathway along this segment must be coupled; conductive Cl^- movement could not be sustained by known parameters.

g. Other transporters: An isoform of the anion exchanger, AE2, has also been detected along the DCT, and substantial bicarbonate reabsorption may traverse this pathway. Other Na^+ entry pathways have been detected in DCT cells in some species.

h. Connecting Tubule Transporters: Although the focus of this review is the DCT, a summary of mechanisms of Na^+ and Cl^- transport by CNT cells will be presented. Early studies showed that rabbit CNT isolated and perfused in vitro transport Na^+ and K^+ and exhibit a transepithelial voltage oriented in the lumen-negative direction (7, 215). Rates of Na^+ transport were reported to be ~20 $pmol \cdot cm^{-1} \cdot s^{-1}$, which is three or four times as great as rates in isolated CCD but similar to rates in isolated DCT segments perfused in vitro. Like DCT segments, CNT express the Na^+-K^+-ATPase at their basolateral surface. Although Na^+-K^+-ATPase expression levels are lower than in the DCT, they are higher than in the CCT (238).

Although early studies reported substantial effects of thiazide diuretics on transport along the connecting tubule (452, 454), molecular results have shown clearly that CNT cells do not express NCC (18, 367). In contrast, it is now very clear that ENaC is expressed at the apical surface of CNT cells, where is participates importantly in Na^+ transport (17, 301, 434).

A role of CNT cells in mediating transepithelial chloride transport has not been well established, but intercalated cells clearly do play a role. In this respect, type B intercalated cells express the anion exchanger pendrin (541), which has been recognized increasingly for its role in systemic NaCl homeostasis (11, 460).

i. Transport Models: Models of the distal tubule have been developed. Fujita and colleagues (69, 71) developed a model that incorporated the effects of both thiazide diuretics and amiloride. The model incorporated 40 initial parameters and could successfully predict the behavior of the tubule during exposure to thiazide diuretics and amiloride. A more recent model created by Weinstein (554) shared many properties, but it did not assume that cells are rigid. Further, Weinstein was able to use newer kinetic data for NCC derived using a mammalian form, rather than the flounder bladder form. It used values for electrolytes and pH present in the first segments of the DCT. It suggested a value of the transepithelial voltage of −5 mV. The model suggested a surprisingly large component of Na^+ transport along this segment by NHE2 of 121 $pmol \cdot min^{-1} \cdot mm^{-1}$, compared with transport by NCC of only 95 $pmol \cdot min^{-1} \cdot mm^{-1}$. It should be noted, however, that these rates were only along the most proximal portion of the DCT. After a short distance, NHE2 activity was modeled to decline substantially, so that later segments were primarily dependent on NCC. This would be consistent with the observation of Wang and colleagues that an inhibitor of NHE2 had little effect under usual conditions, but did when distal bicarbonate delivery was high (19).

Weinstein has incorporated several additional features in his DCT models (552, 554, 556). First, he showed the effects of concatenating the DCT with the CNT on diuretic effects. In focusing on effects of diuretics on urinary acidification, his models predicted that increasing distal Na^+ delivery (modeling ECF volume expansion) should have little effect on urinary acid excretion. In contrast, administration of thiazide diuretics should shift the predominant Na^+ reabsorptive pathway along the DCT from NCC to NHE2, thereby enhancing acid secretion, contributing to metabolic alkalosis. Most recently, Weinstein has concatenated the DCT, CNT and CD in his model, to explore the basis for maintaining K^+ excretion during anti-natriuresis. Potassium excretion is maintained constant in the high aldosterone state of volume contraction because angiotensin II dependent activation of DCT sodium reabsorption reduces sodium delivery to the CNT, while ENaC and Na^+/K^+-ATPase are activated by aldosterone. As a consequence, sodium/potassium exchange remains constant. In contrast, states of potassium loading will stimulate K^+ secretion along the CNT, while maintaining distal Na^+ delivery; this combination will lead to kaliuresis (552–556).

3. Regulation of Na^+ and Cl^- transport

a. Dietary salt, aldosterone, and angiotensin II: One of the major advances of the past two decades has been the realization that NaCl transport by the DCT is adjusted to meet physiological needs. Many of the important regulatory factors are shown in Figure 4. Prior to 1985, most investigators believed that rates of Na^+ transport along the distal tubule were modulated primarily by delivered load, not by hormones and cytokines (227, 228). Most subsequent work, however, has suggested that NCC is strongly activated by dietary NaCl deprivation, and that this effect contributes importantly to homeostasis. In 1989, Ellison and colleagues showed that dietary NaCl restriction increases thiazide-sensitive Na-Cl

cotransport by perfused distal tubules (126). As perfusion controlled rates of Na^+, Cl^-, and fluid delivery, these results established that the activity of the transporter is enhanced. Fanestil and colleagues reported that dietary NaCl restriction did not increase the density of [^{3}H] metolazone binding sites in kidney (130), where [^{3}H]-metolazone binding sites were taken surrogates for the number of thiazide-sensitive NCCs. Gamba and colleagues (341) reported that the same intervention failed to increase NCC mRNA, whereas in 2012, Lai (263) found a twofold increase in NCC mRNA, using the same intervention. Nevertheless, Kim and colleagues (244) found that dietary NaCl restriction increased the abundance of NCC protein, a finding now widely confirmed. This increase was later shown to occur within 3 days (317) and persist for at least 10 days. McDonough and colleagues (424) showed that dietary NaCl loading caused NCC to redistribute from an apical compartment to an intracellular one. Uchida and colleagues (78) and Vallon and colleagues (503) showed that dietary NaCl restriction increased the abundance of both total and phosphorylated NCC, with an exaggerated effect on the phosphorylated (activated) moiety. Palmer and colleagues (146) could not detect any effect of dietary NaCl restriction on total NCC abundance, but did find a substantial effect on NCC located at the plasma membrane. Taken together, these results strongly suggest that NCC is activated during dietary NaCl restriction, that this effect occurs at the protein, and perhaps message level, that the abundance of the phosphorylated apical membrane associated form of the transporter is especially increased, and that these effects have physiological relevance.

i. Aldosterone: Given the modulation of NCC activity by dietary salt, it is not surprising that effort has focused on the role of the renin/angiotensin/aldosterone system in signaling to NCC. Here, we will address the roles of angiotensin II and aldosterone on NCC abundance and activity. Hierholzer et al. (190) showed that adrenalectomy increases the tubule fluid-to-plasma Na^+ ratio in distal tubules, along the entire length. In retrospect, these data suggest that aldosterone activates transport along the DCT, *especially the DCT2,* as well as the CNT, but this conclusion was long ignored. Studies using isolated dissected rabbit kidney tubules detected minimal binding of [^{3}H]-aldosterone to DCT segments (108, 135–137), leading many to conclude that the DCT is not part of the aldosterone-sensitive distal nephron (ASDN). Yet [^{3}H]-aldosterone binding was detected along the DCT, at higher aldosterone concentrations (1.5–20 nM) (136). Similar results were obtained in rats, in which binding to DCT segments was detectable at 2 but not 0.2 nM [^{3}H]aldosterone (136). The metabolic enzyme 11β-hydroxysteroid dehydrogenase type 2 (11HSD2) plays a central role in insuring that most mineralocorticoid receptors (MR) are not bound by cortisol (or corticosterone, in rodents) by metabolizing glucocorticoid hormones. Bostanjoglo et al. (43) showed that 11HSD2 colocalizes with NCC in rat distal tubules. In rabbit, Velázquez et al. (520) showed that 11HSD2 message colocalizes with NCC (520). In the rat, although 11HSD2 was expressed by DCT cells, expression was not uniform (43). It was present at low to undetectable levels in the DCT1 (the most proximal portion of the the DCT) and at higher levels along the DCT2 (the more distal portion of the DCT). Even along the DCT2, however, expression of 11HSD2 was lower than expression along the CNT. In the mouse, the segment co-expressing 11HSD2 with NCC appears to be shorter than in rat, but an area of dual expression is clearly present (55).

More recent studies using PCR and immunofluorescence provide additional interesting insights into steroid hormone action along the DCT. Ackermann and colleagues (3) used RT-PCR to show GR is expressed all along the nephron. MR, in contrast, were expressed only along the TAL, DCT, CNT, and CD. This group also used immunofluorescence to show co-expression of both GR and MR in nuclei from DCT segments that express NCC. When animals were placed on a high NaCl diet, to suppress endogenous aldosterone secretion, MR was no longer expressed in the nucleus the DCT2 (where 11HSD2 is expressed). In contrast, high NaCl diet did not suppress MR nuclear localization along the DCT1. Together, these data suggest that MR plays an important role all along the DCT and CNT. Along the DCT1, it appears likely that MR are occupied predominantly by glucocorticoids, as there is little 11HSD2 to degrade glucocorticoids there. In contrast, it appears that MR along the DCT2 are likely responsive primarily to aldosterone, because 11HSD2 is more highly expressed here, making this segment more responsive to ECF volume status.

Abundant functional data confirm the importance of mineralocorticoid hormones in regulating NaCl transport by DCT. Chen et al. (74) and Velázquez et al. (517) reported that mineralocorticoid and glucocorticoid hormones increase the number of [^{3}H]-metolazone binding sites when administered to adrenalectomized animals. The combination of glucocorticoid and mineralocorticoid hormones increased the number of receptors more than did either hormone alone. Velázquez et al. (517) showed that aldosterone strongly simulates thiazide-sensitive NCC activity. In those experiments, thiazide-sensitive Na-Cl cotransport was barely detectable in adrenalectomized rats. Doses of of either aldosterone in the upper physiological range or dexamethasone increased transport capacity by up to 20-fold (517). The increase in ion transport did not result only from increases in luminal NaCl delivery, because they persisted when the luminal NaCl delivery was controlled by microperfusion.

Kim et al. (244) showed that aldosterone increased expression of thiazide-sensitive NCC, as determined by Western blot and immunocytochemistry of rat kidney cortex. Abdallah and colleagues reported that chronic furosemide infusion, which increases distal solute delivery, increases angiotensin II and aldosterone concentrations, and reduced serum K^+ concentration increases NCC abundance (1). This effect was attenuated, though not prevented, by spironolactone. As noted above, Uchida and colleagues (78) reported that dietary NaCl restriction increased the abundance of pNCC; they found that this effect could be inhibited by spironolactone and concluded that mineralocorticoid actions were primarily responsible. Van der Lubbe (513) showed that the effects of aldosterone on pNCC abundance occurred, even when circulating angiotensin II levels were suppressed by losartan, proving that the effects are not exclusively through angiotensin II.

There is some evidence for mechanisms by which aldosterone stimulates NCC. SGK1, a key early aldosterone signaling protein, is expressed along the DCT (334) and can activate NCC. Mice in which SGK1 has been knocked out constitutively do not fully activate NCC, in response to a low NaCl diet (139). Even more strikingly, mice in which SGK1 is deleted during adulthood (using the Pax8/rTA system) have an 80% reduction in NCC protein abundance, without any change in NCC message (133). Recently, some information about mechanisms of aldosterone's effect on NCC has begun to emerge. Two different mechanisms of SGK-1 action on NCC have been considered. " then state Rozansky et al.

showed that SGK1 supresses the inhibitory activity of WNK4 on NCC as expressed in Xenopus oocytes (see section III.b.iv.). More recent studies by Staub et al. revealed SGK-1 modulates NCC in a similar fashion it modulates ENaC. Rozansky and colleagues (419) showed that SGK1 suppresses the inhibitory activity of WNK4 on NCC, as expressed in oocytes (see section III.b.iv.). More recently, studies by Staub et al. (13, 134, 415) revealed that SGK1 modulates NCC much like it regulates ENaC. Those investigators showed that NEDD4-2 can associate with NCC, via a non canonical motif, and enhance its ubiquination. Ubiquitination is a common signal for proteins to be removed from the plasma membrane. When NEDD4-2 is genetically deleted along the nephron, NCC abundance rises substantially, NCC is more active functionally, and salt-sensitive hypertension results (416). Although these effects suggest a direct effect of aldosterone on NCC abundance and activity, it remains possible that the hypokalemia often induced by aldosterone contributes to activation (503, 514), during exogenous infusion, and from angiotensin II (62), during ECF volume contraction.

Interestingly, the DCT has also been proposed to contribute to the phenomenon of aldosterone escape. Although aldosterone is a potent sodium-retaining hormone and contributes importantly to NaCl retention during ECF volume depletion, aldosterone's effects on NaCl excretion wane, when aldosterone concentrations are high inappropriately, as during exogenous infusion or primary hyperaldosteronism; this effect has been termed aldosterone or DOCA escape; this phenomenon should be distinguished from the secondary rise in aldosterone concentration that occurs during chronic pharmacological blockade of angiotensin II signaling (438). Escape from aldosterone corresponds temporally to a reduction in the abundance of the NCC (550). Thus, while effects along the more proximal segments play a major role in this phenomenon (250), it appears that effects on NCC abundance also contribute. Thus, the increase in NCC and pNCC abundance that occurs secondary to aldosterone infusion wanes over time, as chronic treatment of rats with aldosterone led to secondary declines in NCC abundance (550). This phenomenon was shown to be independent of NO, which is also known to modulate NCC (501).

ii. Angiotensin II: There is also compelling evidence that angiotensin II increases the abundance and activity of NCC. As noted, dietary NaCl restriction, which stimulates both angiotensin II production and aldosterone secretion, increases NCC activity (127). Brooks and colleagues and Terker and colleagues (493) both found that NCC abundance is normal in AT1 receptor knockout animals, but these mice have reduced NCC abundance (by 44%) when consuming a low salt diet (51). Beutler and colleagues detected no effect of candesartan on NCC abundance, during dietary NaCl restriction (27), but Ecelbarger and colleagues found that chronic treatment with candesartan decreased NCC abundance and the magnitude of the diuretic response to hydrocholorthiazide (310). Kwon and colleagues (261) reported that 7 days of angiotensin infusion did not affect membrane NCC abundance, whereas Van der Lubbe (512) found that angiotensin II infusion did increase NCC abundance and did so in the absence of changes in mineralocorticoid levels. Gamba and colleagues showed that angiotensin II increases NCC activity, when expressed in oocytes, in a manner that required WNK4 (see below) (423); the same group went on to show that mice deficient in WNK4 could not respond to angiotensin or low salt diet, suggesting that WNK4

plays a key role in the angiotensin II effect (62). During angiotensin II infusion, a high salt diet leads to a secondary decrease in the abundance of NCC (501), suggesting some escape from its effects, but a recent study of chronic angiotensin II infusion showed that proximal sodium transporting proteins down regulated, whereas distal ones remained activated (354). The mechanism for this process remains unknown, but it was shown to be independent of nitric oxide signaling.

To transport ions, NCC must be phosphorylated (see Figure 4C and 4C). When expressed in oocytes, mutations that disrupt phosphorylation at T58 (rodent numbering) reduce transport activity substantially, mutations at S71 have moderate effects, and mutations at T53 have only modest ones. Mutation of all three residues essentially eliminates function, and the response to intracellular chloride depletion (376), and in vivo, phosphorylation appears to be cooperative, as many investigators have observed concordance between phosphorylation at the three sites. In oocytes, mutation of the three key residues does not affect the abundance of NCC at the plasma membrane, suggesting that they affect substrate turnover (376); this conclusion, however, was disputed by Alessi and colleagues, who observed membrane translocation of NCC when an aspartic acid mutation was introduced at T60 (409). Despite this, it seems clear that the phosphorylation-defective NCC lacks the ability to transport NaCl, even if it gets to the membrane. As will be discussed below, serine/threonine protein kinase 39 (SPAK) is one of the most important kinases contributing to activation of NCC by phosphorylation and both SPAK and OSR1 have been shown to phosphorylate NCC at these three residues, in vitro (Figure 4B) (408). Interestingly, the centrality of phosphorylation at T60 in humans (T58 in rodents) is confirmed by the phenotype of individuals who inherit a mutation of that residue; those individuals manifest classic Gitelman syndrome (291, 312, 445, 446), indicating severe transporter dysfunction.

Although many aspects of NCC regulation remain conjectural, Figure 4C shows schematically possible steps required to regulate NCC. Once synthesized, the protein must move to the plasma membrane. Most evidence suggests that NCC is not phosphorylated until it is inserted into the plasma membrane, as several groups have reported that phosphorylated NCC is never detected in subapical vesicles or intracellular sties (274, 382). As noted, Gamba and colleagues showed, in oocytes, that trafficking of NCC to the plasma membrane is not affected when all three crucial phosphorylation sites are mutated (376). Fenton and colleagues recently developed a novel MDCK line that expresses NCC (417). They found that NCC trafficking to the plasma membrane was constitutive and did not change when NCC was either stimulated (by low chloride hypotonic environment) or inhibited. Those workers also found that NCC is removed from the plasma membrane by clathrin-dependent mechanisms, and appeared to be dependent McCormick and colleagues, who found that SPAK deletion did not affect the ratio of apical to intracellular NCC (326). Yang and colleagues also reported that phosphorylation of NCC at T58 prolonged its residence in the plasma membrane of MDCK cells, (581), a finding confirmed by Fenton and colleagues. This suggests that phosphorylation should have an effect on the relative abundance of NCC in the membrane; in support of this, Yang and colleagues reported that patients who inherited a T60M mutation in NCC excreted less NCC in their urine (581), but it should be noted that deletion of NCC causes striking atrophy of the DCT, and that total NCC abundance is generally low in this situation (303), so that reduced excretion may

reflect reduced abundance and not altered trafficking. Interestingly, early work on WNK4, using oocytes, suggested that it regulated NCC primarily by altering trafficking to or from the plasma membrane (561, 577). This was later extended to mammalian cells, showing the WNK4 appeared to affect NCC trafficking to the plasma membrane, by altering its movement into lysosomes, thereby targeting it for ER associated degradation (353, 476–478). This observation, also made in vitro, appears at odds with the recent work. Thus, many details of NCC regulation within the cell remain to be solidified.

Work by McDonough and colleagues (274, 275, 354, 425, 426) also shows that NCC abundance in the apical membrane is modulated acutely by arterial pressure and angiotensin II. That work, using in vivo models, shows a shift in NCC protein from an apical compartment to a subapical one, in response to acute hypertension, with a shift in the opposite direction, upon treatment with angiotensin converting enzyme inhibitors. Gonzalez-Villalobos and colleagues suggested that the origin of the angiotensin II during either angiotensin II infusion or inhibition of nitric oxide synthases is renal angiotensinogen (167). This provocative hypothesis requires additional investigation, however, as there are other data suggesting that liver angiotensin II production dominates, and there are some concerns about the model (308, 318).

As phosphorylation of NCC is essential for its activity, the abundance of phosphorylated forms of NCC is often taken as a surrogate for its activation status. More recently, most studies of the effects of physiological perturbations on NCC activity have analyzed the abundance of phosphorylated moieties of NCC, an approach that appears more sensitive than determination of total NCC. Most of these have indicated that angiotensin II stimulates NCC activity. Thus, it appears that both angiotensin II and aldosterone can stimulate NCC activity and phosphorylation. At least angiotensin II can also increase NCC abundance at the plasma membrane. The combination of both stimuli also appears to be more potent than either one alone (note the 4 fold increase in NCC abundance at 10 days, when mice consume a low NaCl diet, compared with the waning effects of infused angiotensin II or aldosterone (51). Although these are both strongly salt retaining factors, the effects of both angiotensin II and aldosterone can wane, if hypertension develops, as occurs during aldosterone escape. Although the mechanisms for this effect remain obscure, the phenomenon of NCC trafficking away from the plasma membrane during acute hypertension has been reported (275).

b. Dietary K^+: During the past several years, it has become apparent that NCC is also modulated by dietary potassium intake; this is now believed to play an important role in modulating systemic potassium balance. Vallon and colleagues reported that dietary K^+ intake alters the abundance of phosphorylated NCC in rodents (503), with dietary KCl restriction leading to increased pNCC and dietary KCl loading leading to decreased pNCC. These investigators postulated that the activation of NCC in the setting of dietary KCl restriction likely limits Na^+ delivery to the ASDN, thereby reducing K^+ loss, by impeding K^+ secretion. Frindt and Palmer (145) reported that dietary KCl loading reduced the amount of NCC at the apical membrane, further supporting a role for NCC in this regard. As NaCl restriction also activates NCC, van der Lubbe et al. tested the effects of modulating K^+ intake in the setting of dietary NaCl restriction. They found that, even when dietary NaCl

was low, KCl added to the diet reduced the abundance of pNCC decreased (514). Loffing and colleagues (464) recently showed that gavage with high K^+ food rapidly decreases the abundance of pNCC, an effect that occurs within 30 minutes. In this situation, the investigators were able to vary both the K^+ and the anion independently, and reported that the effects of high K^+ gavage to rapidly dephosphorylate NCC were independent of the anion employed. Loffing and colleagues suggested that the effects of K+ were related to a gut hormone, as they could not mimic them in vitro (464), but McDonough and colleagues recently reported that infusions of KCl reduce NCC abundance and phosphorylation, suggesting that the effect may be direct (403).

Two recent studies have suggested that the nature of the accompanying anion may in fact alter the response to potassium loading. Two groups reported that potassium loading with a non-chloride anion led either to an increase or little change in NCC and pNCC abundance (533). Although several investigators have suggested that NCC inhibition will increase distal K+ secretion by increasing Na^+ delivery, Hunter and colleagues recently reported that acute thiazide administration did not increase kaliuresis or ENaC-mediated sodium transport (210). Wade and colleagues reported that the effects of dietary potassium deprivation to increase apical NCC abundance are observed along both the DCT1 and DCT2, even though reciprocal changes in ROMK apical abundance only occur along the DCT2 (535). Together, these results suggest that NCC abundance and activity are modulated by both dietary and serum potassium. Although the mechanisms of these effects remain to be explored, they are likely to be physiologically important.

c. Sympathetic nervous system: There is some evidence that NCC is involved in sympathetic nerve control of sodium reabsorption and blood pressure. In a rat model of salt-sensitive hypertension in which renal sympathetic nerve activity was increased by ablation of sensory neurons with capsaicin, NCC activity and abundance increased (281), although the NCC western blots showed a sharp band for NCC, typically associated with a lack of specificity. A more recent study examined the possible mechanisms by which sympathetic activation might lead to increased NCC activity. Infusion of norepinephrine into mice caused salt-sensitive hypertension that was associated with increased expression of total and pNCC (347). WNK4 mRNA and prote in levels were reduced by norepinephrine infusion, suggesting that stimulation of β-adrenergic receptors reduces WNK4 expression leading to NCC activation (see a discussion of WNK regulation of NCC, below), sodium retention, and salt-induced hypertension (347)). Downregulation of WNK4 expression was reported to require the glucocorticoid receptor, since these effects were not observed in glucocorticoid receptor knockout mice. Chromatin-immunoprecipitation and luciferase reporter assays data suggested that isoproterenol-induced transcriptional modulation of the *WNK4* gene is mediated by histone acetylation via inhibition of HDAC8 activity (347). Recently, Terker and colleagues confirmed that norepinephrine infusion causes salt-sensitive hypertension and activates NCC, but they did not observe a decrease in WNK4 abundance (493). They then developed an acute norepinephrine model, allowing them to show that the effect was independent of angiotensin II receptors and occurred even when SPAK was ablated.

d. Sex Steroids: Chen et al. (74) reported that the densities of [^{3}H]-metolazone receptors were higher in kidneys from female than male rats. This observation correlated with an increased sensitivity to thiazide diuretics in female animals. They noted that ovariectomy reduced the number of ^{3}[H]-metolazone receptors, suggesting that estrogens increase expression of activated NCC. Verlander et al. (529) reported that estrogen increases the amount of NCC protein in rat kidney cortex and increased the complexity of the apical plasma membrane of the DCT. In preliminary results, in contrast to this, Ecelbarger and colleagues reported that estrogens reduced NCC abundance in diabetic ovariectomized mice (406). Similar results were reported recently with regard to estradiol effects in ovariectomized rats, where treatment reduced both aldosterone and the abundance of NCC (189).

e. Arginine vasopressin: Arginine vasopressin (AVP) is a well-known regulator of water reabsorption along the collecting duct, but it also activates ENaC-mediated Na^+ reabsorption (217), and expression and phosphorylation of NKCC2 along the TAL (159). These effects of AVP are mediated by type 2 AVP receptors (V_2R), which are also expressed along the DCT (349), raising the possibility that AVP stimulates NCC along this segment. Ecelbarger and colleagues initially reported that chronic (7 days) infusion of the V2 receptor-specific agonist 1-deamino-[8-D-arginine]-vasopressin (dDAVP) in rats increased expression of total NCC by more than two-fold (113). However, in two subsequent studies, they found that dDAVP alone did not increase NCC expression unless the animals were also water-loaded (114, 462); another group also reported that chronic infusion with dDAVP had no effect on total NCC expression, although these animal were also sodium-restricted (262). A more recent study in mice showed that infusion of dDAVP for 3 days increased total NCC (428), as did a study in which mice were treated with dDAVP following overnight water-loading (410)

While there is some variability in findings with regard to effects of dDAVP on total NCC, effects on NCC plasma membrane abundance and phosphorylation, better correlates of NCC activity, are more consistent. First, a study using Brattleboro rats, which do not produce vasopressin and thus have central diabetes insipidus, found that acute administration dDAVP increased both apical membrane expression of NCC and its phosphorylation at SPAK/OSR1 target residues (350). Treatment of isolated tubules *in vitro* confirmed the effect of dDAVP was direct, and not secondary to other pathways such as the RAAS. Another study reported similar effects on NCC phosphorylation, but no effect on NCC distribution (383). An increase in levels of SPAK/OSR1 phosphorylation suggested that the effect of dDAVP on NCC phosphorylation is mediated via this pathway. Subsequently, it was shown that NCC phosphorylation in response to the vasopressin V2 receptor agonist dDAVP was attenuated in mice lacking SPAK (428). Another study examined the role of adenylyl cyclase 6 (AC6) in regulating NCC under baseline conditions, and following short-term dDAVP administration (410). These experiments made use of AC6 knockout mice, and showed that AC6 is not essential for basal phosphorylation of NCC or its membrane localization. However, the dDAVP-induced increase NCC phosphorylation and membrane abundance was completely abolished in AC6 knockout mice. These authors also reported a dDAVP-induced

increase in total NCC expression in wild type mice after water-loading overnight, which was also dependent on AC6.

f. Insulin: Obesity and increased insulin levels have been reported to stimulate several sodium transport proteins, including NCC (28, 239, 405). Ecelbarger and colleagues also reported that treatment with the insulin-sensitizing drug rosiglitazone reduced the natriuretic response to thiazides in both lean and obese mice (239). Three groups have reported evidence that insulin stimulates NCC via phosphoinositol 3-kinase (PI3K)-dependent pathway. Sohara et al. (363, 459) reported that insulin induces phosphorylation of SPAK and NCC in mpkDCT cells, and found that knocking down WNK4 inhibited this. They also observed that intraperitoneal injection of insulin is associated with increased phosphorylation of SPAK and NCC in the kidney of wild-type mice but not in a WNK4 hypomorphic mouse. Komers et al. (251) demonstrated in obese Zucker rats that the abundance of pNCC is increased, as is the response to hydrochlorothiazide. They also observed that insulin's effect on phosphorylating NCC can be prevented by PI3K blockers in vitro. Finally, Chavez-Canales et al. (73) showed that insulin increases the activity of NCC in Xenopus laevis oocytes. Again, inhibition of PI3K prevented the insulin effect on NCC. It was also observed by using a kidney ex vivo perfusion technique that insulin perfusion into the kidney induces phosphorylation of the cotransporter.

g. Systemic pH: Although DCT cells do not participate directly in modulating acid/base status, NaCl transport activity appears to be affected by changes in pH. Fanestil and colleagues reported that bicarbonate administration increased the number of [^{3}H] metolazone binding sites (presumed to reflect NCC molecules) (131), whereas acid-loading decreased them. Similar results were later obtained by Kim and colleagues, who used antibodies directed at the transporter itself to estimate abundance (243). These investigators speculated that the reduced NaCl transport that resulted during acidosis was likely to compensate for the increased activity of the proximal NHE3.

Another interaction between DCT cells and cells that modulate acid/base status has been noted more recently. Deletion of NCC leads to minimal salt wasting, owing to increased NaCl reabsorption both proximally and distally (439). It has recently been recognized that simultaneous deletion of the Cl/HCO3 antiporter pendrin, which in itself also causes a very mild phenotype, leads to quite substantial salt wasting and alkalosis (11, 460). Pendrin is expressed primarily by intercalated cells along the CNT and CCD. A few such cells appear along the later segments of the DCT.

h. Other peptide hormones: While regulation of NCC by angiotensin II and AVP is well established, two lesser-known peptide hormones have been reported to increase the density of [^{3}H]metolazone binding sites in rat kidney. Amylin is a peptide secreted by β-cells of the pancreas in response to nutrient stimuli. Administration of this peptide increased the density of [^{3}H]metolazone binding sites 32–58% (35). Administration of the structurally related peptide adrenomedullin also increased [^{3}H]metolazone density by ~30% (35). The physiological significance of these observations remains unclear.

C. Signaling to NCC: WNKs, SPAK/OSR1, Cullin 3, Kelch-like 3

The discovery in 2001 that mutations in members of the With No Lysine [K] (WNK) kinase family (WNK1 and WNK4) can cause the inherited disorder *Familial Hyperkalemic Hypertension* (FHHt, also known as Gordon Syndrome and Pseudohypoaldosteronism type II) inspired renewed focus on the DCT. This syndrome, discussed in more detail below, is manifested uniformly by hyperkalemia, and often by hypertension. As this syndrome is highly responsive to treatment with thiazide diuretics, specific inhibitors of NCC, it was suspected that the genetic defects involved would involve NCC in some way. The study of the regulatory molecules involved in this disease has proven fruitful, if at times introducing confusion. The identification of the downstream WNK targets, the kinases SPAK and OSR1, which directly phosphorylate NCC at several amino-terminal residues, has further extended our knowledge. More recently, the Lifton group and the Jeunemaitre groups identified additional genes that cause FHHt, encoding the proteins Cullin 3 and Kelch-like 3 (KLHL3). Cullin 3 and KLHL3 are components of a ubiquitin ligase complex, and their roles in modulating the WNK-SPAK/OSR1 kinase system are just beginning to be elucidated. A simplified scheme of regulation by WNK kinases, cullin 3 and KLHL3 is shown in Figure 4.

The first member of the WNK family was identified by Cobb and colleagues from a rat brain cDNA library during a search to identify novel members of the MAP/extracellular signal-regulated protein kinase family (573). The WNKs were so-named because the lysine involved in binding ATP and catalyzing phosphoryl transfer is situated in subdomain I, rather than subdomain II, where it is located in other serine/threonine kinases. Four genes encode members of the WNK kinase family in mammals, with alternative promoter usage and alternative splicing resulting in the generation of multiple isoforms (325). WNK2 has not been reported to play a role in the regulation of NCC or other renal cation cotransporters or ion channels so will not be discussed here.

The WNK1 gene (*WNK1*) produces at least two major products (100, 365, 573) and many alternatively spliced forms (365, 530)). These include a full-length kinase-active WNK1 (WNK1), which is widely expressed, and a second truncated product. The truncated product is produced from a separate promoter and lacks the majority of the kinase domain; this product is, therefore, kinase-inactive. It appears to be expressed only by kidney tubule epithelial cells along the TAL, DCT, and CNT; KS-WNK1 expression is 80X higher than WNK1 along DCT, whereas it is only 10X higher along the next highest segment, the CNT (530). For this reason, the kinase-inactive isoform has been termed ‘kidney-specific WNK1’ (KS-WNK1), to differentiate it from the full length WNK1.

WNK4 is expressed by epithelial cells throughout the body, including cells of the distal nephron (79, 368, 560). Original reports suggested strong expression near tight junctions (560), but this has not been replicated. It is highly expressed by cells of the DCT and CNT, but expression extends distally into the collecting duct and, at lower levels, into thick ascending limb (364, 368).

WNK3 is a third member of the family that is also expressed by kidney epithelial cells and elsewhere in the body (197, 224, 411). In contrast to the renal expression patterns of KS-WNK1 and WNK4, WNK3 expression is not predominantly along the ASDN; instead it is

expressed throughout the nephron, from the proximal tubule to the collecting duct (411). Although mutations in WNK3 have not been reported to be associated with FHHt, WNK3 has been shown to regulate the same classes of ion transport proteins that are targets of WNK1 and WNK4 (see below).

1. WNK kinases, *in vitro*—The clinical features of FHHt identify it as a disease of renal electrolyte transport, so investigation of the effects of WNK kinases was first directed at their role in modulating renal ion transport proteins. It is now clear that WNK kinases modulate the trafficking of many transport proteins to or from the plasma membrane, at least *in vitro*. In view of the fact that most of the defects in FHHt can be corrected by treatment with thiazide diuretics (322), and FHHt presents as a "mirror-image" of Gitelman Syndrome (322), a disease that results from inactivating mutations of NCC (259, 457), it is not surprising that WNK4 was soon shown to regulate NCC activity, in vitro (166, 561, 578).

Initial studies overexpressed WNK kinases in Xenopus oocytes and cultured mammalian cells. These showed that WNK4 reduces NCC abundance at the plasma membrane, without a substantial effect on total NCC abundance (53, 165, 166, 560, 577). Immunoprecipitation studies showed that WNK4 and NCC associate in a protein complex involving the carboxyl termini of both proteins (53, 561, 580). The role of WNK4 kinase activity in modulating NCC activity has been controversial. Two groups reported that the effects of WNK4 on NCC are dependent on its kinase activity (166, 561) whereas another group found evidence of a kinase-independent action (580). Indeed, one group showed that a truncated form of WNK4 lacking the entire kinase domain inhibited NCC activity (479, 580).

Studies to determine the mechanism by which WNK4 reduces surface NCC expression suggest that WNK4 inhibits the insertion of NCC into the plasma membrane, rather than affecting endocytosis. Studies using both *Xenopus* oocytes (165) and mammalian cells (53) showed that the ability of WNK4 to reduce NCC surface expression is not affected by a dominant-negative dynamin, suggesting that clathrin-dependent processes are not involved. Furthermore, the effect of WNK4 on NCC was sensitive to inhibition of lysosomal proton pumps, suggesting that WNK4 reduces trafficking of NCC to the plasma membrane, ultimately leading to enhanced lysosomal degradation (53). This view was extended to show that WNK4 reduces both the antegrade movement of NCC to the plasma membrane and the total abundance of NCC in transfected cells. The same group showed that WNK4 diverts NCC to the lysosome, where it can be degraded, by increasing its interaction with the adaptor protein, AP3 (478).

WNK1 was reported to have little effect on NCC activity itself, but it blocked the WNK4 effect (165, 577). Subsequently, however, a much more complex signaling pathway has emerged (Figure 4c and 4d). First, it is now clear that WNK1 is expressed endogenously by oocytes and cells, complicating the interpretation of overexpression experiments. Second, WNK1 is capable of phosphorylating and activating SPAK and OSR1, thereby activating NCC, in vitro. Third, it appears that WNK1 splice forms that are highly expressed in the kidney are especially potent in this regard (530).

Among renal-enriched WNK1 isoforms, a splice isoform, generated from a unique promoter, or promoters) and lacking intrinsic kinase activity, is most abundant. In the DCT, this form is enriched over 80 fold, compared with the rest of the kidney (530). This form has been called kidney-specific WNK1 (KS-WNK1) because it appears to be expressed primarily in the kidney, and especially along the DCT. This kinase-deficient WNK binds to and inhibits WNK kinase activity and WNK effects on NCC, presumably through a dominant-negative mechanism (270, 479).

WNK3 is also capable of stimulating NCC strongly, at least *in vitro* (411, 579). This effect is associated with an increase in NCC protein abundance at the plasma membrane and with an increase in NCC phosphorylation (411). A synthetic kinase-inactive form of WNK3 exerts inhibitory effects on NCC that resemble the effects of WNK4 (411, 579). We confirmed those results and showed further that WNK4 binds to and inhibits WNK3 actions on NCC; conversely, WNK3 blocks WNK4 inhibition of NCC (579). Intriguingly, when WNK3 and WNK4 are expressed in varying ratios, together with NCC, the range of NCC activities is much greater than when NCC is expressed with either WNK4 or WNK3 alone. Furthermore, the net effect of expressing NCC with different molar ratios of WNK3/WNK4 is a finely graded regulation of NCC activity from negligible (when WNK4 abundance greatly exceeded WNK3) to very high (when WNK3 abundance greatly exceeded WNK4). As will be noted below, however, the importance of WNK3 in regulating ion transport along the DCT may not be great, under normal circumstances, as gene knockout models produce quite mild phenotypes (330, 371).

We also reported that FHHt-mutant WNK4 Q562E loses its ability to inhibit WNK3 (579); yet, as noted above, FHHt does not appear to result from loss-of-function. This raised the possibility that interactions between WNK4 and WNK3 might help to explain the FHHt phenotype. In support of this hypothesis, we found that WNK4 Q562E binds to and inhibits the effect of wild type WNK4 on WNK3. Thus, WNK4 Q562E appears to act as a dominant-negative WNK4 modulator, leaving WNK3 activity unopposed and NCC activity strongly stimulated. While the knockout models noted above minimize a role for WNK3 in the DCT, most of the same interactions likely occur between WNK4 and WNK1, and these may be more relevant. WNK kinases can interact with each other to form oligomers (495, 573, 576, 580), through a region near the carboxyl terminal tail (576). The interactions require conserved amino acid residues, including crucial histamine and glutamine residues (called the ‘HQ’ motif (495)); disruption of these HQ motifs inhibits their ability to activate the kinases SPAK and OSR1 (495). This suggests that WNKs may act predominantly as dimers (or oligomers) and engage in trans-phosphorylation (495).

Studies of WNK kinase effects on the DCT in vivo will be discussed after SPAK and OSR1 have been introduced.

2. SPAK and OSR1, *in vitro*—The WNK kinases can regulate ion transport via mechanisms that are both dependent and independent of their kinase activity. Extensive work has now shown that activity of cation-chloride transporters, including NCC along the DCT, is stimulated following phosphorylation of conserved serines and threonines at their cytoplasmic N-terminal tail (Figure 4b). The WNK kinases, however, do not directly

phosphorylate these residues. A yeast two-hybrid analysis revealed that the STE20-related kinases, SPAK (previously called PASK (proline-alanine-rich Ste-20-related kinase) and now called serine/threonine kinase 39) and OSR1 (oxidative stress responsive 1, *OXSR1*; this should not be confused with the gene *OSR1*) bind to the N-terminal regions of the cation-chloride cotransporters KCC3, NKCC1, and NKCC2 (388). Subsequently, WNK1 was shown to interact with both SPAK and OSR1, and to phosphorylate two conserved residues (T243/S383 in SPAK, T185/S325 in OSR1) resulting in WNK activation (343, 532). In turn, SPAK and OSR1 were shown to interact with and directly phosphorylate NCC (343, 408). The interaction occurs between the C-termini of SPAK/OSR1 and the N-terminus of NCC (which contains the motif RFXV that is conserved between cation-chloride cotransporters) (408) (see Figure 4b). Mutagenesis of the T60 phosphorylation site in NCC (T58 in rodents) confirmed that SPAK/OSR1-mediated phosphorylation stimulates NCC activity *in vitro*. Activity of NCC was greatly increased under hypotonic low chloride conditions, which maximally activate SPAK/OSR1 (343), compared with activity under isotonic conditions, and mutation of the T60 phosphorylation site in NCC prevented this activation (408). Thus, WNK1 and SPAK/OSR1 were proposed to form components of a signaling cascade that stimulates activity of cation-chloride cotransporters including NCC.

3. WNK, SPAK and OSR1, *in vivo*—Transgenic, knockout, and knockin mouse models have been generated to analyze the functions of WNK kinases, SPAK, and OSR1 *in vivo*. The first was a gene trap approach that disrupted the first *WNK1* intron (and presumably left the KS-WNK1 promoter region intact) led to the production of WNK1 knockout mice (592). Mice homozygous for the disrupted allele die before embryonic day 13 from cardiovascular defects (572). Heterozygotes were viable but had blood pressure that was lower than wild type mice, lending support to the idea that L-WNK1 is a stimulator of sodium reabsorption. A second heterozygous WNK1 knockout model, however, was found to have normal arterial pressure during both normal and salt restricted diets (484), raising questions about the first report. Consistent with normal pressure in heterozygotes, a group of patients who manifested Hereditary Sensory Neuropathy Type 2 were found to be compound heterozygotes for WNK1. While one allele exhibited mutations in the neuron-enriched HSNII exon, the other contained a premature stop codon in WNK1 expected to lead to a non-functional protein. These individuals were reported to have normal blood pressure (448).

Very recently, a new WNK1 model was developed, in which the first intron of the gene was deleted (531). This model mimics a cause of FHHt in humans, in which much of the same intron is deleted. These heterozygous mice exhibit increased full length-WNK1 specifically in the DCT and CNT, with elevated blood pressure and increased total and phosphorylated NCC. Thus, these mice provide substantial support for a role of WNK1 to stimulate NCC activity, at least when overexpressed. As WNK1 along the nephron is low and nearly uniform, at least at the message level. In contrast, KS-WNK1 is highly expressed by the DCT (530). Thus, this mutation disrupts the normal ratio of KS-WNK1/WNK1 in the distal nephron. As several WNK4 knockout and hypomorphic mouse models (discussed below) appear to lack the ability to stimulate NCC when challenged, these data suggest that full length-WNK1 plays no more than a modest role in stimulating NCC activity normally.

In vivo models designed to examine the role of WNK4 in regulating electrolyte homeostasis and blood pressure have resulted in sometimes confusing data, but a clearer picture of WNK4 actions is now emerging. Two WNK4 knockout mouse lines and one WNK4 hypomorphic line have been reported wnk4 (62, 369, 487). Under basal conditions, one knockout mouse had low plasma K^+ concentrations (−.54 mM (62)), whereas the other two did not. Similarly, the systolic arterial pressure, measured telemetrically was slightly reduced in one model (5.5 mm Hg (369)), but not in the other two. There was mild hypomagnesemia in both models in which plasma magnesium was reported, but unlike NCC knockout mice (see above) or humans with Gitelman syndrome (see below), there was no hint of hypocalciuria. In all three cases, the abundance of NCC and phosphorylated NCC was reduced substantially. This phenotype has sometimes been characterized as 'Gitelman-like', but as hypocalciuria is an essential diagnostic criterion for Gitelman syndrome in humans and is characteristic of NCC knockout mice, and as hypocalciuria is uniformly observed when SPAK is deleted (see below), the phenotype does not resemble Gitelman syndrome or mimic NCC knockout. Perhaps the best summary of these data is that, under basal conditions, WNK4 supports NCC phosphorylation; its deletion produces a tendency toward hypokalemic alkalosis and salt wasting but differs from that observed in the setting of NCC knockout or disruption.

The effects of WNK4 deletion are much more striking when knockout mice are challenged with dietary perturbations. Gamba and colleagues (62) showed that dietary NaCl restriction or angiotensin II infusion did not activate NCC in mice lacking WNK4. Uchida and colleagues recently reported that WNK4 knockout mice become hypotensive when challenged with dietary NaCl restriction (487), despite activation of WNK1. Thus, it appears that WNK4 is an important stimulus to NCC activity, maintains arterial pressure, and contributes to renal homeostasis under dietary stress.

Another way to study normal WNK4 function is to generate mice with additional copies of WNK4. Lalioti et al. generated mice carrying nominally two extra copies of wild type WNK4 (265). Under basal conditions, the mice were normokalemic, but had slightly low arterial pressure during wakefulness, and mild hypocalciuria. The abundance of NCC was not evaluated quantitatively, but immunofluorescence suggested that the density of DCT profiles expressing NCC was reduced. The abundance of WNK4 protein was not estimated in those mice, but a subsequent publication showed only a modest increase (449). Using a similar approach, Uchida and colleagues developed mice with WNK4 expression increased by approximately 2-fold. They found a minimal increase in NCC abundance and the mice were normotensive, but they did exhibit an increase in plasma potassium. In contrast to these models, Uchida develop another transgenic mouse with multiple copies of WNK4 and remarkably increased abundance. Those mice exhibited clearly increased SPAK phosphorylation, increased NCC and pNCC abundance, and a clear FHHt type phenotype. Thus, substantial increases in wild type WNK4 abundance appear to activate NCC and cause hypertension. Smaller increases may not, although the data remain contradictory in this regard.

There have been three mouse models described in which disease-causing WNK4 mutations have been expressed. Lalioti and colleagues made transgenic mice, carrying two copies of

the Q562E mutation (561). The mice had mild hyperkalemia, hyperchloremia, and increased arterial pressure. When challenged with a high K^+ diet, Q526E WNK4 mice became more hyperkalemic, with clearly impaired K^+ excretion. Histological analysis revealed that overexpression of Q526E WNK4 increased the luminal surface area of DCT profiles, as detected visually. Immunostaining indicated that expression levels of NCC were increased in Q526E WNK4 mice, but co-localization studies with segment markers indicated that NCC expression was still confined to the DCT. Little or no differences were observed in ROMK expression between wild type and transgenic mice on normal or high K^+ diet, or in levels of ENaC expression (265). Importantly, interbreeding of Q562E WNK4 mice with NCC knockout mice resulted in complete amelioration of all the defects observed in the Q526E WNK mice, suggesting that dysregulation of NCC is the key mechanism underlying FHHt. Another report described generation of a WNK4 D561A knock-in mouse (585). Unlike the mice generated by Lalioti et al., which express mutant WNK4 on a wild type WNK4 background, these mice express one mutant WNK4 allele and one wild type allele, closely mimicking the human disease. The phenotype of these mice was remarkably similar to the phenotype of the WNK4 Q562E transgenic mice; the investigators also noted that the phenotypic effects were completely corrected by thiazide diuretics, like in humans (585). In addition, however, these investigators reported substantially increased phosphorylation of the NCC, which implicates that signaling through SPAK is increased.

A third model of FHHt more recently reported is an inducible FHHt transgenic model, in which expression of Q562E WNK4 was switched on by administration of doxycycline (81). Induction of Q562E WNK4 led to an increase in blood pressure and plasma potassium, which were both reversed when doxycycline administration was stopped, suggesting that the effects of this mutation were regulatory in nature. Mayan and colleagues detected increased NCC abundance in the urine of patients with WNK4 Q562E, versus controls, providing further support for the relevance of these observations to humans (320).

One result of these studies has led to some confusion, however. As noted, wild type WNK4 has been shown to inhibit NCC activity both *in vitro* and in animals. Some (53, 166, 561), though not all (578, 580), investigators have reported that mutations of WNK4 abrogate its inhibitory activity. This has led some investigators to suggest that FHHt results from *loss of WNK4-mediated NCC inhibition* (53, 384, 561, 579). Yet, the WNK4 Q562E transgenic animals express mutant WNK4 on a background that includes two wild type WNK4 alleles (265); the knock-in animals express mutant WNK4 on a background of a single wild type allele (585). In both situations, *wild type WNK4 is present and expressed within the kidney*, suggesting that WNK4 mutations act as 'gain-of-function' rather than 'loss-of-function' mutations. At this point, it is not possible to reconcile all of the data concerning WNK4 effects on NCC, but they do suggest that WNK4 may exist in two forms, an inhibitory form, where it suppresses NCC activity, as detected in vitro and in the Lalioti transgenic model, and an activating form, in which it stimulates NCC.

The *in vivo* roles of WNK3 with regard to the regulation of electrolyte homeostasis and blood pressure are thus far less ambiguous. Two independently-generated WNK3 knockout models had similar phenotypes. The Uchida group found no differences in plasma or urinary electrolyte levels, or in expression of total or phospho-NCC at baseline, or following dietary

NaCl restriction, but salt restriction did cause a decrease in blood pressure (372). The mechanism causing this reduction in blood pressure is unclear. The lack of a significant phenotype may result from increased expression of WNK1 and WNK4 observed in the knockout mice. Similarly, Mederle and colleagues reported no differences in electrolyte levels in WNK3 knockout mice generated using a gene trap approach (329). WNK1 mRNA levels were significantly elevated in WNK3 knockout mice. One difference between this model and that of the Uchida group was that dietary NaCl restriction led to increases in pSPAK/OSR1, pNKCC2 and pNCC expression levels, and in hydrochlorothiazide-induced diuresis, that were greater in WNK3 knockout mice than in wild type mice (329). The reason for this difference may be that immediately prior to dietary NaCl restriction, the mice were injected with the NKCC2 blocker furosemide, which may have resulted in a more severe salt-deprivation. Thus, the majority of data are consistent with a minor role for WNK3 in the kidney at baseline; whether the role is altered by physiological or pathophysiological mechanisms remains unclear.

In vitro, there is abundant data indicating that WNK kinases interact functionally (479, 495, 536, 579, 580). There is less information *in vivo*, but recent data confirm that KS-WNK1 is expressed primarily along the DCT, as noted above. As dietary potassium loading appears to increase the abundance of KS-WNK1 along the DCT (270, 364, 536). This, in turn, may inhibit other WNKs, leading to inhibition of NCC activity. In vivo, the effects of disruption or overexpression of KS-WNK1 are generally consistent with the predictions based on its *in vitro* actions. Two groups have independently generated and characterized KS-WNK1 knockout mice, with similar findings. Both groups reported no effect of KS-WNK1 disruption on plasma electrolyte levels or systolic blood pressure on standard diets (181, 297), with one finding a slight increase in diastolic blood pressure and mean arterial pressure (181). One group reported an increase in sodium retention and blood pressure following Na^+ loading (297), while the other found no effect on blood pressure or electrolyte homeostasis after Na^+ or K^+ loading (181). Protein expression levels of total and pNCC were elevated in KS-WNK1 knockout mice (181, 297), but in contrast to wild type mice, Na^+ restriction did not increase the pNCC/total NCC ratio, and Na^+ loading did not decrease this ratio (181). KS-WNK1 knockout mice thus appeared to have lost their ability to regulate NCC phosphorylation. The lack of phenotype may be due to a compensatory reduction in expression of ENaC and a reduction in expression of ROMK and BKCa (which is expressed along the CD) (181). The increased expression level of ROMK was unexpected since *in vitro*, KS-WNK1 was reported to stimulate ROMK expression at the apical membrane by inhibition L-WNK1 (86, 270, 296, 536). Expression of total and pNKCC2 was also reported to be elevated in KS-WNK1 knockout mice (297), which is consistent with an effect of KS-WNK1 on transport along this segment; this has been described (77).

In transgenic mice overexpressing KS-WNK1, systolic and diastolic blood pressure was significantly lower than that of wild type mice on a standard Na^+ diet (297). Plasma aldosterone and angiotensin II levels were elevated, indicating a normal response to restore ECF volume. Na^+ restriction could not induce an increase in total or pNCC or total and pNKCC2; salt wasting was present in these KS-WNK1 transgenic mice. These mice also displayed hypokalemia with upregulation of ROMK and hence increased tubular K^+ secretion. One limitation of this study is that the KSP-cadherin promoter was used to drive

transgene expression; this promoter is active along the entire nephron, so the KS-WNK1 transgene was expressed along segments where KS-WNK1 is not normally expressed.

The observation that both SPAK/OSR1 and NCC phosphorylation was increased following dietary salt restriction provided indirect evidence that SPAK/OSR1-mediated activation of NCC *in vivo* (78). More direct evidence that SPAK and OSR1 regulate NCC activity *in vivo* has come from the generation of several mouse models. The first insights came from the generation of knock-in mice expressing a SPAK mutant (SPAK T243A) that cannot be phosphorylated and hence activated by WNK kinases (396). $SPAK^{T243A/T243A}$ mice displayed salt-sensitive hypotension, and hypomagnesemia and hypocalciuria. Plasma potassium levels were normal on a regular sodium diet, but reduced on a low sodium diet. In this model, the abundance of phosphorylated NCC and NKCC2 were both reduced. More recently, several groups described a Gitelman-like phenotype in mice in which SPAK expression has been completely ablated (176, 326, 583). Interestingly, the phenotype of these mice was somewhat different from that observed in the $SPAK^{T243A/T243A}$ mice. The knockout mice also exhibited reduced abundance of NCC and pNCC, but they exhibited an increase in the abundance of phosphorylated NKCC2 (326, 582). One group noted that the dominant forms of SPAK in kidney differ from that in brain, where the majority of SPAK is full length. Two shorter forms, one called kidney-specific SPAK, from an alternative promoter, and one called short SPAK, from an alternative translation site, are highly expressed in kidney, especially along the thick ascending limb (177, 326), where it appears to inhibit OSR1 actions. Surprisingly, despite being expressed at significant levels along the DCT (176, 326, 428), targeted disruption of OSR1 specifically in the kidney (global disruption is embryonic lethal) led to *increased* levels of pNCC (292). The phenotype of these mice was more reminiscent of Bartter Syndrome, in which NKCC2, expressed along the TAL, is inactivated. Activation of NCC is likely a compensatory response to promote sodium retention in response to reduced ECF volume. A simple interpretation of these data is that *in vivo*, SPAK plays a more important role in the regulation of NCC along the DCT, whereas the major target of OSR1 is NKCC2. Additional support for this idea comes from the observation that despite an increase in OSR1 expression along the DCT, NCC phosphorylation in response to the vasopressin V2 receptor agonist dDAVP was attenuated in mice lacking SPAK (428). There is evidence, however, that OSR1 does play a role in the DCT. Grimm and colleagues (177) suggested that disrupting SPAK affected the ability of OSR1 to traffic to the apical membrane, where it might phosphorylate and activate NCC. Thus, the actions of SPAK and OSR1 were suggested to be complementary in this segment. While the exact relative importance of SPAK and OSR1 along the distal tubule may differ between TAL and DCT, it does appear that the kinases may have complementary actions in the DCT.

4. Cullin3 and KLHL3—While mutations in either WNK1 or WNK4 lead to FHHt, mutations in these genes are only causative in a small portion of the reported cases. Identification of other genes that cause FHHt has been hampered by insufficient numbers of affected family patients to perform traditional positional cloning. Recently it has become possible to combine microarray technology with high throughput sequencing to enrich exonic sequences and identify mutations that alter protein coding. A major advantage of this

approach is that it permits the rapid identification of *de novo* disease-causing mutations or mutations in small kindreds. Whole exome sequencing of patients with FHHt, but *without* mutations in either WNK1 or WNK4 led to the identification of two genes that are mutated in the majority of individuals with FHHt (46, 305), *Cul3* and *KLHL3*. The proteins encoded by these genes, Kelch-like 3 (KLHL3) and Cullin-3, are known to interact with each other, and are involved in protein ubiquitination, a process which is classically considered to target proteins for proteasomal degradation, but may also modulate protein activity, interaction and localization. Cullin-3 acts as a scaffold for the ring ligase, which catalyzes the addition of ubiquitin to lysine residues; KLHL3 interacts with Cullin-3 and acts as an adaptor, binding the substrate for the ring ligase (Figure 4). The majority of mutations in KLHL3 are missense mutations, leading to single amino acid changes in regions that interact with substrates or with Cullin3. Mutations in Cullin-3 alter Cullin3 mRNA splicing, resulting in a Cullin-3 transcript in which exon 9 is skipped and 57 amino acids are deleted. It is unlikely that deletion of these amino acids leads to a non-functional Cullin-3 protein, since Cullin-3 knockout mice are embryonic lethal (458).

An interesting clinical observation arose from the discovery that mutations in *Cul3* and *KLHL3* cause FHHt. The severity of the disease is strongly correlated with the causative gene, with mutations in *Cul3* leading to early diagnosis (average of 9 years of age), more severe hyperkalemia and metabolic acidosis, and hypertension in 94% of individuals by 18 years of age. Also of note, while the majority of mutations that cause FHHt are dominant, a subgroup of those patients carried recessive mutations in *KLHL3*. The overall pattern for the severity of disease is related to the causative gene thus: *Cul3*>*KLHL3*>*WNK4*>*WNK1*. This pattern suggests that *Cul3* lies upstream of *KLHL3*, *WNK4* and *WNK1* in a pathway that regulates NCC activity and plays an important role in maintaining ECF volume and electrolyte homeostasis.

Several *in vitro* studies have recently begun to provide information regarding this new NCC regulatory pathway, with similar findings. First, KLHL3 was found to interact with both Cullin3 and WNK4 in HEK293 cells (537). KLHL3 induced ubiquitination of WNK4 and reduced WNK4 protein levels (537). Mutations in either KLHL3 or WNK4 that cause FHHt impaired their interaction and reduced WNK4 ubiquitination, leading to elevated WNK4 levels (537). KLHL3 was found to target WNK4 for ubiquitination and polyubiquitination, and a total of fifteen ubiquitination sites were identified throughout the WNK4 protein, including seven in the kinase domain and one in the second coiled-coil domain. Polyubiquitination and degradation of WNK4 was abolished by the KLHL3 FHHt-causing mutation R528H (450). Inhibition of WNK4 by KLHL3 was also observed to increase membrane expression of ROMK. Finally, while it was observed that expression of an FHHt-causing WNK4 mutant increases WNK4 expression *in vivo*, this may be unrelated to direct effects on WNK4 stability (450). Since changes in NCC activity determine the volume of the DCT, this increase in WNK4 expression could have been secondary to hypertrophy of the DCT following activation of NCC by the mutant WNK4.

Another study using HEK293 cells found that KLHL3 interacts with all full-length WNK isoforms and with Cullin-3, but not with SPAK/OSR1 or NCC (370). The majority of the dominant FHHt-causing KLHL3 mutations inhibited binding to WNK1 or Cullin-3, and *in*

vitro, wild type, but not R528H, KLHL3 ubiquitinated WNK1. KLHL3 binds to a site in WNK1 outside the catalytic region (residues 479–667); mutation of residues within the equivalent region in WNK4 causes FHHt (WNK4 E562K and WNK4 Q565E) (560). As noted by other groups, these mutants were unable to interact with KLHL3. siRNA (small interfering RNA)-mediated knockdown of CUL3 increased WNK1 protein levels and kinase activity in HeLa cells (370). The most recent study used the *Xenopus laevis* oocyte co-expression, and reported that co-expression of KHLH3 increased the ubiquitination and degradation of co-injected of WNK4, and FHHt-causing mutations in KLHL3 reduce its ability to reduce WNK4 abundance (570). Co-injection of a Cullin-3 fragment (residues 1–400) also reduced the effect of KLHL3 on WNK4 expression, possibly through a dominant-negative effect on an endogenous Cullin isoform. The functional effects of KLHL3 and Cullin3 are somewhat unclear in this study, since injection of wild type WNK4 with NCC increased NCC activity which conflicts with previous data (165, 578, 579). This issue was not addressed by the authors but may be related to differences in uptake conditions. Injection of KLHL3 either alone, or with WNK4, strongly inhibited NCC activity; injection of Cullin3 also inhibited NCC activity, but weakly (570). One caveat with this study is that the effects of KLHL3 FHHt-causing mutants on WNK4 expression correlated inconsistently with their effects on NCC activity. Wild type KLHL3 strongly inhibited WNK4 expression and activity. However, the mutant KLHL3 A77E had little effect on WNK4 expression levels, yet a similar inhibitory effect on NCC activity to KLHL3 R528C, which reduced KLHL3 levels almost as much as wild type KLHL3 (570). Thus, the precise relationship between FHHt-causing mutations in KLHL3 and WNK4 expression and ultimately NCC activity is unclear. The overall consensus from these studies is that KLHL3 stimulates WNK4 ubiquitination and degradation, and FHHt-causing mutations in either KLHL3 or WNK4 prevents these effects leading to increased activation of NCC.

c. Potassium Transport

1. Rates of K^+ transport—The majority of filtered K^+ is reabsorbed along the proximal tubule and loop of Henle; ~10% of filtered K^+ reaches the DCT. Early micropuncture work established the superficial distal tubule as an important site of K^+ secretion. Many studies indicated that K^+ secretion along the distal tubule accounted for most or all urinary K^+ excretion under a variety of conditions (400, 569). More recently, regulation of K^+ excretion has been studied largely using principal cells of the cortical (and initial) collecting tubule as the model system (158, 568). This largely reflects technical issues, and the fact that collecting duct shares most of the major K transport pathways with the connecting tubule and initial collecting tubule, yet there is now substantial evidence for a unique and dominant role of the distal tubule in mediating net potassium excretion (334). This review will not address the important role of principal cells and of the CCD in renal K^+ homeostasis, nor will it provide a detailed description of factors that regulate K^+ secretion by principal cells. Mechanisms and control of K^+ excretion by the kidney and by the collecting duct have been reviewed extensively (158, 568). Here, the important role that DCT and CNT cells play in K^+ homeostasis will be described.

Micropuncture studies indicated that the luminal concentration of K^+ along the first 20–30% of the superficial distal tubule is low (566). This portion of the tubule is lined by DCT cells

(105). In one study, when early distal tubules were perfused separately from late distal tubules, rates of K^+ secretion by early tubules were found to be low and did not reach statistical significance (466). These data suggested that the DCT does not contribute importantly to K^+ secretion. However, microperfusion of segments of the distal tubule that lay within the initial 40% of tubule length did secrete K^+ at low but significant rates under control conditions (518). These segments would be expected to comprise only DCT cells (105). When the luminal Cl^- concentration was reduced, rates of K^+ secretion rose substantially (see below). Thus, a large percentage of K^+ secretion occurs along the portion of the distal tubule comprising primarily DCT, CNT, and intercalated cells. Pathways that can participate in K^+ secretion have been identified along the DCT1, DCT2 and CNT. A second function of K^+ transport pathways along the distal tubule is to provide the electrochemical gradient required to permit cation reabsorption, via recycling of K^+ at the basolateral membrane through KCNJ10/KCNJ16 channels. K^+ secretion mechanisms at the apical membrane, and the role of K^+ transport pathways at the basolateral membrane in electrochemical gradient generation will be described below.

2. Mechanisms of K^+ transport—The rate of K^+ secretion along the distal tubule is determined largely by the transepithelial voltage, and luminal K^+ concentrations at the distal end of the superficial distal tubule are typically close to those predicted by the Nernst equation (565). The transepithelial voltage along the distal nephron is determined primarily by sodium reabsorption via ENaC. The absence or presence of ENaC expression along the distal tubule is the major determinant of K^+ excretion. As described above, ENaC is absent from the DCT1 (302), and accordingly, the transepithelial is near to 0mV (524). Along the DCT2, where ENaC is expressed (302) there is a small, amiloride-sensitive lumen negative transepithelial voltage (524). Finally, along the CNT and then the CCD, ENaC expression coupled with a lack of NCC expression (302) results in a substantial lumen negative transepithelial voltage. The lumen negative voltage generated by Na^+ entry at the apical membrane thus provides the driving force for K^+ secretion along the DCT2, CNT and CCD. Based on the effects of low luminal Cl^- concentrations to stimulate K^+ secretion, Velázquez et al. (518) proposed that a K^+-Cl^- cotransport pathway is expressed at the apical membrane of DCT cells, but no further evidence has been obtained. The majority of evidence suggests that the primary pathways of K^+ secretion are two K^+ channels, the renal outer medulla K^+ channel (ROMK1, also called Kir1.1) and BK (Maxi-K).

a. ROMK1: ROMK1 is a constitutively active channel that mediates basal K^+ secretion (see for extensive review (557)), and its activity is most likely regulated by effects on total expression and on membrane abundance, as well as by altering channel activation. Along the distal nephron, immunolocalization studies have shown ROMK1 expression at the apical membrane of DCT1 (despite its low rate of K^+ secretion), DCT2, and CNT cells (335, 518, 535, 574). ROMK1 displays a nonlinear current-voltage relationship, characterized by a larger inward current than outward current, (hence the alternative name inward-rectifying potassium channel 1.1 or $K_{ir}1.1$ (255). Functional ROMK1 channels are formed by a homomeric assembly of four subunits, each of which possesses two transmembrane domains.

b. BK channels: Patch-clamp studies using isolated rabbit CNT revealed a role for BK as a renal K^+-secretory channel. High flow stimulated a K^+ conductance sensitive to the BK channel blocker charybdotoxin (489). BK channels are relatively inactive under basal conditions, but increased fluid delivery to the distal tubule results in increased cell-surface shear stress, which increases intracellular Ca^{2+} levels, resulting in channel activation (295). BK channels display diverse tissue-specific properties (47, 427, 473) that partially arise from differential expression of splice variants of the pore-forming α-subunit (BK-α) and association with different accessory β-subunits (β1–4) (252, 327). BK-α is expressed along the distal tubule, but the distribution of the accessory β-subunits varies. Immunostaining of mouse kidney sections showed that BK-β1 subunit expression is restricted to the apical membrane of the primary cells of the CNT (175), suggesting BK-α/β1 channels play a role in flow-induced K^+ secretion. The BK-β4 subunit is expressed along both DCT and CNT, where it is restricted to intercalated cells. Expression of BK-β4 is cytoplasmic, so the function of BK-α/β4 channels, which are unlikely to play a role in flow-induced K^+ secretion (175), is unclear.

c. KCNJ10: KCNJ10 (Kir4.1) is another K^+ channel in the DCT. This channel participates in generating the primary K^+ conductance at the basolateral membrane. KCNJ10 subunits consist of two transmembrane helices and one pore-forming domain. In the kidney, KCNJ10 forms heterotetramers with KCNJ16 (Kir5.1), which is also expressed along the distal nephron (20). *In vitro*, KCNJ10/KCNJ16 display different biophysical properties to KCNJ10 homodimers (20), including reduced open probability, increased single-channel conductance, and altered pH sensitivity. KCNJ10 has been reported to be inhibited by activation of the CaSR (207), which also co-localizes to the basolateral membrane of the DCT. The CaSR also inhibits KCNJ15 (Kir4.2), also expressed along the DCT (219, 306), but does not interact with KCNJ16 (207). Therefore, it is also possible that KCNJ10 and KCNJ16 form functional heterotetramers along the DCT.

Mutations in KCNJ10 cause EAST (SeSAME) syndrome (see below); those identified so far have varying effects on channel activity, from complete inactivation (arginine-199STOP) to relatively little effect on activity (alanine-167valine). In addition, several mutations alter pH sensitivity, resulting in channel silencing at physiological pH, and the arginine-175glutamine mutation reduces affinity of the channel for PIP2. No diseases have yet been linked to mutations in KCNJ15 or KCNJ16, and the physiological relevance of heterotetramer versus homotetramer formation is unknown. Although KCNJ10 permits K+ movement across the basolateral membrane, this process appears to be crucial for transepithelial NaCl cotransport, as the disruption of such transport leads to phenotype that resembles loss of NCC. KCNJ10/*KCNJ16 heteromers* appear to form the only major K^+ conductive pathway across the basolateral membrane of the DCT (594), but Weinstein has suggested that little net K^+ movement occurs through them (554, 556). This suggests that the channel serves another crucial function, perhaps its role in setting membrane voltage.

d. Miscellaneous K^+ pathways: Several other K^+ channels and cotransporters are expressed along the DCT and CNT, but their role in the function of these nephron segments is unknown. Along the CNT and CCD, KCNK1, a double-pore K^+ channel is expressed at the

apical membrane (146, 377). In addition, the voltage-gated K^+ channel ERG1 has been localized to the apical membrane of the DCT and CNT (60), and KCNQ1 is expressed along the basolateral of the DCT and CNT, although expression along DCT1 was weaker (595). Finally, KCC4 has been localized to the basolateral membrane of the DCT (523).

3. Regulation of K^+ transport—Many factors regulate K^+ secretion along the distal tubule. Factors that act from the peritubular side to increase K^+ secretion along the distal tubule include elevations of plasma K^+ (468), aldosterone (141), vasopressin (142), and angiotensin II (545). A low H^+ concentration also stimulates K^+ secretion (467). Basolateral factors that inhibit K^+ secretion along the distal tubule include metabolic acidosis (467) and hypokalemia (468).

Factors that influence K^+ secretion along the distal tubule from the luminal side include the luminal concentrations of Na^+, K^+, and Cl^- and the luminal fluid flow rate (568). Luminal inhibitors of K^+ secretion include organic cations, such as amiloride (526), triamterene (52), trimethoprim (80, 172, 521), and pentamidine (247), as well as inorganic cations, such as Ca^{2+} (374).

Increases in distal flow rate and luminal Na^+ concentration both stimulate K^+ secretion by distal tubules. It is likely that reducing the luminal Na^+ concentration below a critical level inhibits K^+ secretion by its effects on cellular Na^+ concentration and activity of the Na^+-K^+-ATPase pump (168). This is supported by the parallel reductions in K^+ secretion and transepithelial voltage that occur when luminal Na^+ concentration is reduced below 40 mM (168). Good et al. (168), however, reported that the luminal Na^+ concentration in fluid entering the distal tubule usually ranges from 38 to 77 mM, even under conditions of low dietary NaCl intake. Thus the luminal Na^+ concentration would not limit K^+ secretion along the distal tubule unless severe ECF volume contraction reduced the luminal Na^+ concentration below 40 mM. It should be emphasized that the luminal Na^+ concentration can and does frequently decline below 40 mM along the collecting duct. If the same relation between Na^+ concentration and K^+ secretion holds in that segment, luminal Na^+ may be limiting to K^+ excretion, even under conditions of mild ECF contraction. Mathematical models have been developed by Weinstein showing the impact of both fluid flow rate and luminal Na^+ concentration (555, 556). These models are entirely consistent with the microperfusion data of Good and colleagues (169), in which the effect of luminal factors were studied largely in the absence of systemic perturbation. The summative models show, however, that if one assumes that transport in the DCT and CNT can be modulated independently (for example by angiotensin II and aldosterone), and the transport properties are appropriately scaled, luminal Na^+ concentration may play an important role (554–556). A role for luminal Na^+ concentration in modulating K^+ secretion derives from the observations that the human diseases GS and FHHt, exhibit increased and decreased K^+ secretion, likely related to increased and decreased luminal Na^+ (379).

Fluid flow rate also affects K^+ secretion along the distal tubule (169, 240). In a series of microperfusion experiments, when the luminal flow rate was increased from 6 to 26 nl/min, K^+ secretion nearly doubled (169). In contrast to the case of luminal Na^+ concentration, discussed above, this range of flow rates is well within the range observed under free flow

conditions of hydropenia and mild volume expansion. Thus the flow rate of fluid entering the distal tubule is likely to have an effect on K^+ secretion on a day-to-day basis. Before the discovery of the role played by BK channels in flow-mediated secretion, it was suggested that these effects resulted largely from changes in luminal K^+ concentration. When the flow rate is low, luminal K^+ concentrations increase dramatically along the length of the distal tubule, owing to continued secretion. In contrast, when the flow rate is high, luminal K^+ concentrations remain lower. The lower luminal K^+ concentration permits continued K^+ secretion along the length of the distal tubule (564). These factors almost certainly do play a role, but the striking effect of BK deletion in mice to abrogate flow-dependent K^+ secretion (391) suggests that these channels have a unique role.

Another factor that alters K^+ excretion in humans and animals is diuretic drugs. Loop and DCT diuretics (thiazides and others) increase urinary K^+ excretion and can cause hypokalemia. A factor that contributes to diuretic-induced K^+ wasting is contraction of the ECF volume and hyperaldosteronism (559). Another factor is the increase in distal flow rate. Loop diuretics inhibit K^+ reabsorption along the TAL and increase K^+ delivery to the DCT (203, 526). Thus a component of the K^+ wasting that results from loop diuretic administration reflects direct actions of the drugs, yet DCT diuretics such as the thiazides do not alter K^+ secretion directly (526), at least under normal conditions, and yet these drugs are potent kaliuretics. One factor contributing to this effect is that DCT diuretics increase Ca^{2+} absorption by the DCT. This reduces the luminal concentration of Ca^{2+} in the late distal tubule. Calcium acts in the distal tubule to inhibit K^+ secretion indirectly, by blocking Na^+ channels (375). This observation may explain part of the difference in kaliuretic potency of loop and DCT diuretics. In contrast to the effects of DCT diuretics, loop diuretics increase distal Ca^{2+} delivery, which would be expected to inhibit K^+ secretion.

Under some conditions, however, thiazide diuretics may inhibit K^+ secretion by the distal tubule. When the luminal concentration of Cl^- in the distal tubule is low, the relation between luminal Na^+ concentration and K^+ secretion changes. Velázquez et al. (527) showed that raising luminal Na^+ concentration from 40 to 150 mM stimulates K^+ secretion by distal tubules perfused with a Cl^--free solution (527). They showed that this effect occurred primarily along the early distal tubule and suggested that it reflected transport via an apical K^+-Cl^- cotransport pathway. Because there is little molecular evidence for a luminal K^+-Cl^- transport pathway, these effects of luminal Na^+ concentration on K^+ secretion are more likely to involve secretion via ROMK.

Organic cations may also affect K^+ secretion by the distal tubule. Amiloride blocks epithelial Na^+ channels and thereby reduces K^+ secretion along the distal tubule and collecting duct. Triamterene appears to act in much the same manner (52). More recently, it has been recognized that other organic cations, used primarily as antimicrobial substances, can also block epithelial Na^+ channels and cause K^+ retention. Both trimethoprim (80, 430, 522) and pentamadine (247) have been shown to block Na^+ channels, inhibit K^+ secretion, and cause hyperkalemia in patients. It is postulated that these drugs, like amiloride, enter the pore region of channels (377) leading to channel blockade. It seems likely that other organic cations may have similar “amiloride-like” effects on the distal tubule.

a. Regulation of ROMK1: The numerous mechanisms by which ROMK1 activity is regulated have been extensively reviewed (157, 414, 549, 557). Here, more recent regulatory mechanisms will be summarized. ROMK is modulated physiologically to enhance K^+ secretion appropriately. A recent study using well validated ROMK1 antibodies revealed significant effects of dietary K^+ supplementation. In renal cortex, total ROMK1 expression increased, and immunofluorescence indicated enhanced apical staining, along DCT2, CNT and CD (535). In contrast, although ROMK was expressed along the DCT1, dietary K^+ loading did not affect it; this is consistent with a lack of functional ROMK in the apical membrane of distal tubules, as documented by patch clamp studies (personal communication, WH Wang).

The PKA pathway plays a central role in mediating the effects of vasopressin on K^+ secretion along the TAL and distal nephron (61, 547). Activation of this pathway results in phosphorylation of ROMK1 at several sites, increasing ROMK1 activity (575); the importance of phosphorylation of ROMK1 by PKA is illustrated by the observation, in humans, that mutation of a PKA phosphorylation site causes Bartter Syndrome (455). Phosphorylation of ROMK1 stimulates channel activity by either increasing insertion of ROMK1 into the plasma membrane (589), or by a mechanism involving PIP2-dependent ROMK1 activation. Phosphorylation of ROMK by PKA does not directly activate ROMK1 channels in membranes that are depleted of PIP_2 (293), but lowers the concentration of PIP_2 necessary for activation of the channels, suggesting that PKA activates ROMK1 by enhancing PIP_2-channel interaction.

The PKC pathway is also important for regulation of K^+ transport in CD by PLC-activating hormones and growth factors, including prostaglandin E_2, bradykinin, and epidermal growth factor (12, 143, 183, 480). The effect of PKC on ROMK1 is complex because PKC exerts both stimulatory and inhibitory effects (287, 593). PKC-induced phosphorylation of ROMK channels is required for insertion of ROMK1 into the plasma membrane (287). Activation of PKC by phorbol 12-myristate 13-acetate (PMA) inhibits apical K^+ channels in CCDs (548). Stimulation of PKC decreased the sensitivity of ROMK channels to PIP2 (593), an activator of ROMK1 (208, 293); thus PKA and PKC regulate ROMK1 activity by enhancing or inhibiting PIP2-dependent ROMK1 activation respectively.

The aldosterone-inducible serine-threonine kinase SGK1 regulates the activity of a wide variety of ion channels and transporters (324). ROMK1 contains a consensus SGK1 phosphorylation site at serine 44, and ablation of this phosphorylation site (S44A) reduced ROMK1 activity in *Xenopus* oocytes; conversely, a phosphomimetic mutation, S44D, stimulated activity (589). These effects involved a decrease or increase in ROMK1 plasma membrane expression respectively. In vitro kinase assays confirmed that ROMK1 is a substrate for SGK1. SGK1 may therefore represent a pathway through which aldosterone is able stimulate K^+ secretion.

In addition to effects on activity of NCC and ENaC WNK kinases also modulate activity of ROMK1. WNK4 strongly inhibits ROMK1 activity *in vitro,* through a kinase-independent mechanism (225, 270). WNK4 reduces ROMK1 abundance at the plasma membrane, but in contrast to its inhibition of NCC, the effect is dynamin-dependent and involves clathrin-

mediated endocytosis (225). WNK4 and ROMK1 interact, but interaction is not sufficient to result in ROMK1 inhibition (185). FHHt-causing mutations in WNK4 (E559K, D561A and Q562E) increase this interaction and inhibit ROMK1 to a greater extent than wild type WNK4 (185, 225). Furthermore, deletion of the region containing these three amino acids prevents WNK4 inhibition of ROMK1, and a synthetic peptide of this region blocks the interaction between WNK4 and ROMK1, indicating it plays a key role in the WNK4-ROMK interaction (348). Taken together, these data suggest a possible mechanism for the hyperkalemia observed in FHHt, whereby potassium secretion is reduced by lower apical membrane expression of ROMK1. Direct phosphorylation of WNK4 by SGK1 reverses WNK4 inhibition of ROMK1 (412), with further complexity added by attenuation of the SGK1 effect by the protein kinase c-Src (591). In contrast to its effects on inhibition of NCC by WNK4, angiotensin II does not affect inhibition of ROMK1 by WNK4 (423).

Studies in *Xenopus* oocytes and HEK-293 cells have shown that WNK1 also inhibits ROMK1 activity. The effect is either dependent on intact kinase activity (270, 544), or independent on it, depending on the study (86). Three proline-rich motifs (PXXP) within amino acids 1-119 of WNK1 are sufficient to inhibit ROMK1 (185, 544). Time course studies of ROMK1 plasma membrane expression suggest that WNK1 increases endocytosis of ROMK1 in a dynamin-dependent manner (86), an effect involving interactions with the scaffolding protein intersectin (185). Interaction with intersectin occurs via the N-terminal proline-rich motifs of WNK1, and triple mutation of these motifs ablates this interaction, as well as preventing ROMK1 inhibition (185). WNK4 inhibition of ROMK1 also seems to require its interaction with intersectin, and interestingly, FHHt-causing mutations in WNK increase the interaction (185). Recently, direct evidence was provided that WNK1 stimulates ROMK1 endocytosis, and the clathrin adaptor molecule ARH is required (132). It remains to be determined whether ARH is a WNK1 substrate, and whether other WNK kinases modulate WNK1-ARH interaction.

KS-WNK1 alone does not affect ROMK1 activity, but reverses WNK1 inhibition of the channel (296). Two regions within KS-WNK1 have been identified that mediate its antagonistic effect on WNK1 regulation of ROMK1 (296). Not surprisingly, one region, including amino acids 31-253, contains the autoinhibitory domain; the other, which spans amino acids 1-77, contains the unique cysteine-rich sequence encoded by exon 4a. Both of these regions coimmunoprecipitate with amino acids 1-491 of WNK1, and mutational analysis revealed that the two essential phenylalanine residues in the autoinhibitory domain are required for region 31-253 to inhibit WNK1. In order for KS-WNK1 to inhibit WNK1, amino acids 120-491 of WNK1 are required, rather than the N-terminal proline-rich motif (296).

WNK3 has also been shown to inhibit ROMK1 activity in *Xenopus* oocytes, through an effect on plasma membrane abundance, rather than conductance or open probability (278). Interestingly, introduction of a mutation homologous to the FHHt-causing WNK mutation Q562E enhanced the inhibitory effect of WNK3, suggesting that this region may play an important role in the function of the WNKs in general.

Src-family protein tyrosine kinase phosphorylates ROMK1 at tyrosine 337, and phosphorylation at this site is increased by dietary K^+ restriction, or inhibited by a high K^+ diet (288); parallel changes have been observed in expression levels of c-Src and c-Yes (551). Activation of c-Src inhibits SGK1-mediated phosphorylation of WNK4, thereby restoring the inhibitory effect of WNK4 on ROMK channels and K^+ secretion (591) (see above). It has been proposed that this interaction between c-SRC, SGK1 and WNK4 may provide a mechanism to reduce K^+ loss during ECF volume (ECF) depletion, and increase it during high K^+ states, both of which would increase SGK1 expression via stimulation of aldosterone secretion (549). While K^+ supplementation inhibits c-Src expression, ECF depletion has no effect. Thus, during ECF depletion, high c-Src activity prevents the effect of SGK1 on K^+ secretion; under high K^+ conditions, suppression of c-Src permits SGK1 to stimulate K^+ secretion. The tetraspanin CD63 has been reported to increase c-SRC activity, enhancing c-SRC-mediated inhibition of ROMK1 (286).

The role of klotho in regulation of Ca^{2+} reabsorption is discussed in detail below; klotho has also been reported to regulate ROMK1 through the same mechanism. Treatment of cultured cells with the extracellular domain of Klotho increased plasma membrane expression of ROMK1 through removal of terminal sialic acids from the ROMK1 extracellular N-glycan. Removal of sialic acids allows binding of galectin-1 to ROMK1, preventing clathrin-mediated endocytosis or ROMK1 (65). Furthermore, injection of the extracellular domain of Klotho into rats stimulated urinary K^+ excretion (63).

b. Regulation of BK: Similar to the regulation of ROMK1, pathways that regulate BK channel activity have been described, but the *in vivo* relevance of these to K^+ secretion along the DCT and CNT is unclear. The pore-forming α-subunit (BK-α) of BK is phosphorylated by both PKA and PKC. Patch-clamp studies using isolated rat CCD revealed that application of PGE2 inhibited BK channel activity (223). Inhibition of P38 and ERK MAPK stimulated BK channel activity, and prevented PGE2 inhibition; this pathway may be mediated through PKC. Expression of the PGE2 synthetic enzyme cyclooxygenase II was stimulated during K^+ restriction, suggesting that this pathway may serve to reduce K^+ secretion through BK under this condition. Studies using microperfused rabbit CCDs showed that specific inhibition of PKA tonically inhibited flow-stimulated BK channel activity in principal cells, but not in intercalated cells (294), which may reflect differences in BK-β isoform expression. PKC also inhibits flow-stimulated BK activity, but this effect may be indirect, since PKC activation is required for mechanosensitive Ca^{2+} signaling.

The CYP-epoxygenases CYP2C23 and CYP2J2 are enzymes that metabolize arachidonic acids and are expressed in the CCD (309, 482). CYP2C23 in particular, has been shown to be the major isoform of CYP-epoxygenase responsible for formation of the arachidonic acid metabolite 11,12-epoxyeicosatrienoic acid (11,12-EET) in the kidney (198, 216). Dietary K^+ supplementation increased the expression of CYP2C23 but not CYP2J2, and increased 11,12-EET levels in isolated rat CCD tubules (483). Application of both arachidonic and 11,12-EET increased BK channel activity, even when CYP-epoxygenase was inhibited. Furthermore, inhibition of CYP-epoxygenase abolished iberiotoxin-sensitive and flow-stimulated, but not basal BK channel activity, in isolated microperfused rabbit CCD. In

summary, high dietary K^+ stimulates the renal CYP-epoxygenase pathway, which plays an important role in activating BK channels and flow-stimulated K secretion along the CCD.

c. Models of K^+ transport: As noted above, the DCT1 primarily reabsorbs Na^+ and Cl^- with relatively little transepithelial K^+ movement. Consistent with this function, functional K^+ channels have been detected along the basolateral membrane, but not along the apical membrane (289). Although ROMK (535) and KCNA1 (Kir1.1) (164) have been detected at the apical membrane by immunofluorescence, they appear to contribute little to apical K^+ conductance (121). In contrast, as noted, 40 pS K^+ channels along the basolateral membrane are detectable along DCT1. Weinstein has modeled the DCT1 (554, 556), using measured conductances for K^+ and Cl^- to estimate rates of transport. According to this model, the majority of K^+ movement across the basolateral membrane of this segment traverses an electroneurtral KCl cotransport pathway, rather than a K^+ channel. This suggests that the basolateral channels may primarily serve the function of maintaining an appropriate basolateral membrane voltage. Along the DCT2, K^+ clearly traverses conductive pathways in the apical membrane; ROMK is clearly one important pathway.

d. The aldosterone paradox: Several years ago, Halperin coined the phrase, 'aldosterone paradox' to describe the fact that aldosterone appears to enhance K^+ excretion, under some conditions, while favoring NaCl retention under others (290). These differential effects occur in situations where aldosterone secretion is stimulated respectively by hyperkalemia and by ECF volume depletion (and therefore angiotensin II). Although Weinstein has recently questioned whether the phenomenon is, in fact, paradoxical (556), the moniker has proved popular (14, 514). From a phenomenological standpoint, several factors appear to limit the tendency for K^+ secretion that would otherwise occur associated with exposure to high circulating aldosterone. When the ECF volume is low, GFR may be slightly reduced, and rates of proximal tubule reabsorption are enhanced. As a portion of the proximal effects results from angiotensin II, which stimulates Na^+/H^+ exchange, this will limit distal Na^+ delivery. The DCT appears to play a key role in switching from kaliuresis to antinatriuresis, in response to ECF volume depletion. As discussed above, this segment is highly responsive to angiotensin II. When angiotensin II stimulates NCC activity along the DCT, this further limits Na delivery to the DCT2 and CNT, thereby reducing K^+ secretion. This process has been modeled by Weinstein (556).

The key role of the DCT in modulating serum K^+ is illustrated by diseases of humans in which DCT function is disturbed. In Gitelman syndrome, wherein NCC is functionally deficient (259), K^+ wasting is often unrelenting. In contrast, in Familial Hyperkalemic Hypertension, where NCC activity is stimulating constitutively (379), hyperkalemia is constant. These disease processes point to the central role of the DCT in modulating systemic K^+ balance.

E. Calcium Transport

1. Rates of Ca^{2+} transport—Ca^{2+} ions play an essential role in many cellular processes. Three major processes maintain body Ca^{2+} within a narrow range: intestinal absorption, bone resorption and formation, and urinary excretion. Net intestinal absorption of Ca^{2+}

amounts to ~200 mg of the normal dietary intake of 1,000 mg. In the steady state, this net absorption is matched by urinary excretion. Since 10,600 mg of the ~10,800 mg (98%) of Ca^{2+} filtered daily must be reabsorbed by the kidney (90), this organ represents a key regulator of Ca^{2+} homeostasis.

The bulk of the filtered load of Ca^{2+} (60–70%) is reabsorbed in the proximal tubule largely by passive means through the paracellular pathway and only ~15% of the filtered load reaches the distal tubule. Reabsorption along the distal tubule occurs by active transcellular transport, since the luminal concentration of Ca^{2+} is below that of blood, and the transepithelial voltage is lumen negative (268). Furthermore, the passive permeability of the distal nephron for Ca^{2+} is very low (89). The amount of calcium reabsorbed by the distal tubule rises when the amount of Ca^{2+} delivered to it increases (89, 173). In rodents, rates are approximately 2–5 $pmol \cdot min^{-1} \cdot mm^{-1}$ (87, 89).

Although both Ca^{2+} and Mg^{2+} (see below) are reabsorbed along the distal nephron, including along the DCT, the sites of reabsorption overlap only partially. This segmental separation has implications with regard to side effects of drugs and for genetic diseases. Ca^{2+} reabsorption along the DCT1 appears to be minimal, as the molecular machinery, described below, is not present in this segment (103). In fact, the expression of the Na^+/Ca^{2+} exchanger by the DCT2 was used to first distinguish this segment, molecularly, from the DCT1 (366). Thus, the majority of Ca^{2+} reabsorption takes place along the DCT2 and the CNT, whereas Mg^{2+} reabsorption occurs predominantly along DCT1 (301) (see Figure 5). The reader is referred to other work for additional information about transport properties of the CNT (471).

2. Mechanisms of Ca^{2+} transport—The process by which Ca^{2+} is reabsorbed by the DCT and CNT is reasonably well-established, at the molecular level; they are shown schematically in Figure 5. The combination of a 1,000-fold inward concentration gradient and the cell-negative membrane potential provides a large electrochemical driving force favoring the entry of Ca^{2+} across both the apical and basolateral membrane. At the apical membrane, Ca^{2+} enters the cell through the transient receptor potential vanilloid 5 (TRPV5) Ca^{2+} channel. Ca^{2+} is extruded across the basolateral membrane and into the blood by the Na^+/Ca^{2+} exchanger (NCX1), and the plasma membrane Ca^{2+}-ATPase (PMCA1b) (311). An additional essential component of the Ca^{2+} transport mechanism is the intracellular Ca^{2+} binding protein, calbindin 28K. Like for Na^+ and K^+, a mathematical model for Ca^{2+} transport along the DCT2 and CNT has been developed (40).

a. TRPV5: TRPV5, originally identified as the epithelial Ca^{2+} channel, is a member of the TRP channel superfamily (101). The channel contains intracellular amino- and carboxyl-terminal tails, which flank the six transmembrane (TM) segments; there is an additional hydrophobic stretch between TM5 and TM6, which is predicted to form the pore. The amino-terminal tail contains six ankyrin repeats for both channel assembly and protein–protein interactions, and the carboxyl-terminal tail harbors three potential protein kinase C (PKC) sites. In cell systems, TRPV5 assembles into large homotetramers (41)

TRPV5 is constitutively active at low intracellular Ca^{2+} concentrations and physiological membrane potentials, with strong inward rectification (528). The channel is highly selective for Ca^{2+}, making it the most Ca^{2+}-selective member in the TRP superfamily (528). DTRPV5 is abundantly expressed along the DCT2 and CNT, where its deletion substantially reduced Ca^{2+} reabsorption, as TRPV5$^{-/-}$ mice excrete six- to tenfold more Ca^{2+} than wild-type littermates (195).

b. NCX1: The Na^+/Ca^{2+} exchanger plays a key role in transepithelial Ca^{2+} transport. NCX1 exchanges Na^+ and Ca^{2+} in a 3:1 stoichiometric ratio. Moreover, NCX1 is widely expressed in diverse tissues including the heart, brain, and skeletal muscle. In the kidney, the expression of NCX1 is restricted to the distal part of the nephron, particularly the DCT and CNT. In the DCT, it is only expressed by cells of the DCT2 (in rodents and humans) (122, 366). In the rabbit, where transitional segments are not observed, expression of Ca^{2+} transporting proteins, including the NCX1, is limited to the CNT. NCX1 has been estimated to transport approximately 70% of the Ca^{2+} across the basolateral membrane (194).

NCX is driven by both the Na^+ gradient across the basolateral cell membrane and by the intracellular voltage. Because the stoichiometry is $3Na^+/2Ca^{2+}$, the transporter carries a net positive charge into the cell. Ca^{2+} inside the cell can bind to the transport protein and activate it, allosterically. NCX has been modeled to comprise 9 TM domains. These are divided between an amino-terminal domain, including the first 4 TM domains, and a carboxyl-terminal domain, comprising the remaining four. The two domains are separated by a cytosolic loop comprising 500 residues, which includes two Ca^{2+} binding domains. CBD1 exhibits high Ca^{2+} affinity, whereas CBD2, exhibits lower affinity. When Ca^{2+} binds, large structural changes occur that strongly activate Ca^{2+} transport. Many regulatory proteins have been reported to bind to the carboxyl terminal domain. These have been reviewed (50).

c. PMCA1b: Plasma membrane ATPases are high-affinity Ca^{2+} efflux pumps that keep intracellular Ca^{2+} concentration very low in cells. The highest Ca^{2+}-ATPase activity in kidney is in the DCT segment. Although this protein likely plays an important role in transepithelial Ca^{2+} transport, it likely plays a less important role than NCX1, as it has been estimated to transport only ~30% of the total Ca^{2+} efflux (31). PMCAs belong to the type IIB subfamily within the large superfamily of P-type ATPases (475). In mammals, four separate genes code for the major PMCA isoforms 1–4, with alternative splicing generating a large number of specific PMCA isoforms. They appear to have 10 TM regions, with a long carboxyl-terminal tail and a central intracellular nucleotide-binding domain (475). The difference in expression pattern and abundance suggests that the different PMCA isoforms and splice variants fulfill different roles in cellular Ca^{2+} regulation.

d. Calbindin D28K and D9K: Within the cell, Ca^{2+} channel binds to Calbindin-D28k and D9k; these proteins are names for their apparent molecular weights, 28 and 9 kDa, respectively. These proteins rapidly buffer apical calcium influx, thus greatly enhancing the capacity for Ca^{2+} to enter cells from the lumen, without triggering intracellular signaling events (253). The calbindins then shuttle Ca^{2+} from the apical to the basolateral membrane, where the Ca^{2+} offloads to extruding mechanisms. In the rabbit and rat, calbindin-D28k is expressed predominantly in the DCT and CNT (490). One study has also shown significant

levels of expression in the CCD of rat (404). Calbindin D9K in rat is expressed in the cTAL, DCT, CNT, and CCD (32, 437). Initially, there was some confusion over the role that calbindin-D28k plays in systemic Ca^{2+} homeostasis, as mice deficient in this protein displayed few Ca^{2+} abnormalities. Nevertheless, this issue was resolved by experiments in which both calbindin-D28k and the VDR were knocked out. The double knockout mice had substantial abnormalities, with decreased expression of calbindin-D9k, as well (596). These results show clearly that calbindin-D28k plays an essential role in mediating Ca^{2+} transport across the DCT2 and CNT. The function of calbindin-D28k is illustrated by effects of intracellular calcium. When the intracellular calcium concentration is low, calbindin-D28k moves toward the apical membrane, associating with TRPV5. This process appears to be essential for preserving Ca^{2+} influx (266).

3. Regulation of Ca^{2+} transport—Regulation of Ca^{2+} transport along the DCT and CNT is likely to involve regulation at all three steps of the transcellular pathway (i.e. apical entry through TRPV5, shuttling by calbindins and basolateral extrusion through NCX1 and PMCAs). Regulation of TRPV5 activity in particular has been extensively characterized, and includes (i) regulation of TRPV5 expression, (ii) regulation of TRPV5 plasma membrane abundance and (iii) alteration of TRPV5 open probability.

Many of the regulators of TRPV5 expression levels also regulate expression of other proteins in the transcellular pathway i.e. NCX1 and calbindin-d28K and PMCA1b. Control of plasma Ca^{2+} levels within a narrow range is achieved by stimulation of the synthesis and release of calcitropic hormones including 1,25-Dihydroxyvitamin D_3 [$1,25(OH)_2D_3$], calcitonin (147) and parathyroid hormone (PTH), the latter two of which are release following sensing of Ca^{2+} demand by the Ca^{2+}-sensing receptor (CaSR). PTH and $1,25(OH)_2D_3$ in particular have been shown to be important activators of expression of the transcellular transport machinery in the kidney (reviewed in (103)) but several additional stimuli also play roles.

a. PTH: Isolated nephron segment RT-PCR and in situ hybridization have localized PTH receptor expression in rat kidney. Expression was noted in the glomerulus, proximal tubules, cortical thick ascending limb (cTAL), and the DCT, but not in the CCD (277, 407). The CNT was not addressed as a distinct segment in these studies. PTH acts both acutely (**see below**), and chronically though the genomic effects described here, to stimulate calcium reabsorption. In rats, PTH supplementation was observed to increase renal expression of TRPV5, Calbindin-d28K, NCX1 and PMCA1b (505). The same effects were observed in primary cultures of rabbit CNT and CCD (505). Parathyroidectomy, which reduces PTH levels, had the opposite effect (with the exception of unchanged PMCA1b levels), and replacement of PTH reversed this effect (505). In addition, knockout mice lacking the CaSR, which couples plasma Ca^{2+} levels to PTH secretion, display elevated PTH levels and a concomitant increase in TRPV5 expression (505).

b. Vitamin D: 1,25-Dihydroxyvitamin D_3 [$1,25(OH)_2D_3$] is a primary regulator of calcium and phosphorus homeostasis, acting through effects on gene expression in intestine, kidney, and bone, and through feedback inhibition of PTH production at the parathyroid glands. $1,25(OH)_2D_3$ binds to the vitamin D receptor (VDR), a member of the nuclear receptor

superfamily of steroid/thyroid hormone receptors, which then acts as a transcription factor to modulate expression of target genes. In human kidney, the VDR is expressed at high levels along the DCT, and CCD, with lower but significant expression in the proximal tubule (256). Rats raised on a vitamin D-deficient diet display a significant reduction in plasma Ca^{2+} levels associated with lower renal TRPV5 expression, but supplementation with $1,25(OH)_2D_3$ reversed this effect (193). The enzyme 25(OH) vitamin $D_3$1α-hydroxylase (CYP27B1) [1α (OH)ase] is responsible for the final and key step of $1,25(OH)_2D_3$ synthesis, and its targeted disruption in mice also reduces TRPV5 expression. In addition, expression of calbindin-d28K and NCX1 are reduced (PMCA1b expression is unchanged) (192); Ca^{2+} supplementation reversed these effects, and also increase PMCA1b expression. The final demonstration of the central importance of vitamin D in regulating expression of the renal transcellular pathway proteins comes from ablation of VDR in mice, which display reduced TRPV5 expression (507), or knockdown of VDR by microRNA in a rat cell line, which reduces expression of TRPV5, Calbindin D28K, NCX1 and PMCA1b (571). The observation that dietary Ca^{2+} supplementation reverses the effects of both VDR and 1α (OH)ase knockout on transcellular pathway proteins suggests that dietary Ca^{2+} regulates their expression independently of $1,25(OH)_2D_3$.

c. Sex steroids: It is well established that estrogen deficiency in postmenopausal women is associated with an increased risk for osteoporosis. Studies in normal humans have shown that males display a greater degree of urinary Ca^{2+} excretion than females (94, 342). These observations indicate that sex steroid hormones may play a role in regulating the transcellular pathway. Estrogens exert a stimulatory effect on expression of Ca^{2+} transport proteins. In mice lacking the estrogen receptor-α (which is expressed in DCT and CNT), levels of TRPV5, Calbindin-d28K, NCX1 and PMCA1b are all reduced (508). While ovariectomy of rats itself had no effect on expression levels, estrogen replacement in ovariectomized rats increased expression of all four proteins (504). The effect on at least TRPV5 expression is independent of $1,25(OH)_2D_3$, since estrogen was still able to increase it in VDR and 1α (OH)ase knockout mice(504). Testosterone has the opposite effect on expression of transcellular pathway proteins as demonstrated by several observations in mice. First, male mice have higher urinary calcium excretion than female mice, associated with lower expression of TRPV5, Calbindin-d28K, NCX1 and PMCA1b (205). Orchiectomy increased the abundance of TRPV5 and Calbindin D28K at both the mRNA and protein level; testosterone replacement reversed this effect. No significant differences in serum estrogen, parathyroid hormone, or 1,25-dihydroxyvitamin D3 levels between control and orchidectomized mice with or without testosterone were observed, suggesting that testosterone is acting independently of these hormones.

d. Glucocorticoids: Stress hormone pathways may play a role in modulating renal Ca^{2+} transport through an effect on expression levels of the transcellular pathway machinery. Chronic glucocorticoid treatment has many systemic side-effects, including decreased calcium absorption by the duodenum (211) increased renal calcium excretion (486) (Weinstein *et al.* 1998), and osteoporosis (56, 380, 398). In rats, the synthetic glucocorticoid dexamethasone significantly enhanced renal TRPV5 and Calbindin-d28K mRNA and protein abundance, probably to compensate for reduced Ca^{2+} reabsorption along proximal

tubule and TAL (355).)Restraint stress was reported to increase expression of NCX (209), while chronic treatment of mice with ACTH, which stimulates glucocorticoid secretion, led to increase Calbindin expression, but reduced TRPV5 expression (110).

e. Acid-base status: Chronic metabolic acidosis results in hypercalciuria, whereas chronic metabolic alkalosis has the opposite effect. Some of these effects are likely related to the increased dissolution of bone in chronic metabolic acidosis, and therefore maybe independent of changes in kidney transport proteins; but this does not rule out important renal changes. Micropuncture studies in dogs showed that chronic (but not acute) metabolic acidosis increased urinary calcium excretion, whereas metabolic alkalosis (or bicarbonate infusion) led to calcium retention, independently of parathyroid hormone (485). In mice, chronic metabolic acidosis induced by NH_4Cl loading or administration of the carbonic anhydrase inhibitor acetazolamide increased urinary calcium excretion, associated with reduced expression of renal TRPV5 and calbindin-d28K at the mRNA and protein level (358). In contrast, chronic metabolic alkalosis induced by NaHCO3 administration induced the expression of Ca^{2+} transport proteins and caused hypocalciuria. The Cl^-/HCO_3-exchanger pendrin is expressed on the apical membrane of intercalated cells in the DCT/CNT and CCD, (245, 418, 541) and is the major transporter responsible for bicarbonate secretion along the distal nephron (10, 418). Recently, it was shown that pendrin knockout mice, display calcium wasting, most likely as a result of reduced expression of TRPV5, calbindin-d28K and NCX1 (21). Thus, bicarbonate and calcium handling by the distal nephron appear to be closely coupled.

4. Regulation of TRPV5 activity—TRPV5 activity is regulated by two mechanisms (i) plasma membrane abundance and (ii) open probability. Following irreversible blockade of TRPV5 at the plasma membrane, TRPV5 activity rapidly returns, suggesting insertion of new channels to the membrane (267). A pool of TRPV5-containing vesicles close to the plasma membrane is the likely source of these new channels. Plasma membrane abundance of TRPV5 is also regulated by endocytosis, with the majority of internalized TRPV5 entering the recycling pathway rather than the degradation pathway (511). Finally, extracellular mechanisms act to regulate the retention of TRPV5 channels at the plasma membrane.

Channel activity is determined by the combination of the probability of the channel being open (open probability, P_o), and the amount of current flowing through the channel during the open state (conductance). Several factors have been identified that regulate plasma membrane abundance or activity of TRPV5, described below.

4. Regulation of TRPV5

a. Plasma membrane abundance: intracellular mechanisms

i. S100A10/Annexin 2: *In vitro* yeast-two hybrid and immunoprecipitation studies identified S100A10 as a TRPV5-interacting protein (510). S100A10 typically exists as a heterodimer with annexin 2, and S100A10/annexin 2 were subsequently shown to form a complex with TRPV5 (510). All three proteins were also shown to co-localize along the DCT2/CNT *in vivo*. The S100A10/annexin 2 complex plays a role in several cellular processes including

endocytosis, exocytosis and membrane–cytoskeleton interactions (6, 155), suggesting that S100A10/annexin 2 might regulate plasma membrane expression of TRPV5. Downregulation of annexin 2 using annexin 2-specific siRNAs in HEK293 cells significantly inhibited the currents through TRPV5, indicating that the S100A10/annexin 2 plays a role in regulating TRPV5 activity (510). Mutation of amino acids in the C-terminus of TRPV5 involved in its binding to S100A10 significantly reduced TRPV5 plasma membrane abundance in *Xenopus laevis* oocytes, indicating that S100A10/annexin 2 may regulate TRPV5 activity through an effect on TRPV5 trafficking (510). Importantly, expression levels of both S100A10 (510) and annexin 2 (333) are increased by $1,25(OH)_2D_3$, suggesting a physiological role in Ca2+ homeostasis.

ii. Rab11a: Similar to S100A10, the ubiquitously expressed small GTPase Rab11a was identified as a TRPV5-binding partner using a yeast two-hybrid approach (509). Rab11a is associated with recycling endosomes, which return internalized TRPV5 to the plasma membrane. Immunofluorescence revealed that Rab11a is expressed along the DCT2/CNT, and within cells, is localized with TRPV5 in vesicles lying close to the apical membrane. In *Xenopus laevis* oocytes, coexpression of a Rab11a mutant unable to bind GTP with TRPV5 significantly decreased TRPV5 plasma membrane abundance (possibly through an effect on channel recycling to the plasma membrane) and hence activity (509). A more recent study showed that TRPV5 is constitutively internalized in a dynamin- and clathrin-dependent manner in HEK293 cells (511); histidine 712 of TRPV5 is critical for this process (98). Internalized TRPV5 initially appeared in small vesicular structures and then localizes to perinuclear structures positive for Rab11a. Treatment of cells with brefeldin A, which disrupts delivery of newly synthesized channels to the plasma membrane did not inhibit TRPV5 activity, suggesting that TRPV5 exists in a vesicles capable of recycling back to the surface (511). Recycling of TRPV5 was inhibited by BAPTA-AM, suggesting that channel recycling is regulated by intracellular Ca^{2+}.

iii. WNK4: As described in **section IV.C**, patients with the Q565E mutation in WNK4 display hypercalciuria, in contrast to patients with mutations in *WNK1* (321). There is conflicting data regarding the effect of WNK4 on TRPV5 activity. WNK4 was first reported to increase TRPV5 activity in a *Xenopus laevis* oocyte overexpression system by increasing TRPV5 membrane abundance (222). WNK4 had no effect on open probability in this study. In contrast, studies performed using the mammalian HEK293 cell line found that WNK4 reduced TRPV5 activity and cell surface expression by stimulating caveolin-mediated endocytosis (64).

iv. Intracellular Mg^{2+} and PIP2: Intracellular Mg^{2+} reversibly inhibits TRPV5 activity through a conformational change induced by direct binding of Mg^{2+} to aspartate 542 (276). This inhibition is reversed by PIP2, an activator of phospholipase C, without impairing Mg^{2+} binding to TRPV5, which could also stimulate the channel independently of intracellular Mg^{2+} levels. *In vivo*, intracellular Mg^{2+} levels are high, and PIP2 may serve to prevent Mg^{2+}-induced TRPV5 inhibition by stabilization the channel in the open state. Activators of phospholipase C such as TK may therefore act through PIP2 to stimulate TRPV5.

v. Adenylyl cyclase signaling and channel phosphorylation: In addition to the chronic effects of PTH on regulating expression levels of the transcellular pathway machinery described above, PTH also acutely stimulates Ca^{2+} reabsorption along the distal nephron (264, 453). In purified luminal membranes from the distal nephron (264) and in primary cultures of rabbit DCT and CNT cells (269), PTH stimulates Ca^{2+} uptake. Inhibitors of cAMP prevented PTH stimulation of Ca^{2+} uptake along rabbit connecting tubules (269), while the adenylyl cyclase activator forskolin and cell-permeable cAMP analogues stimulated it. PTH also stimulated an accumulation of cAMP in isolated rabbit cells (174). These effects are now known to involve effects on TRPV5 (97). The precise mechanism by which adenylyl cyclase-mediated activation of PKA leads to activation of TRPV5 has recently been elucidated. In HEK293 cells, forskolin did not affect TRPV5 plasma membrane abundance, but did alter single-channel activity (97). Cotransfection of the catalytic subunit of PKA, increased phosphorylation of TRPV5 and directly stimulated channel open probability. Mutagenesis identified threonine 709 as the residue phosphorylated following PTH stimulation. This residue lies in the CaSR-binding region important for feedback inhibition of TRPV5 activity (96). In functional studies, TRPV5-W702A, which was predicted be unable to bind the CaSR but retained an intact PKA phosphorylation site, displayed a significantly increased open probability and was not further stimulated by PTH. These data suggest that PTH-induced phosphorylation of threonine 709 induces dissociation of TRPV5 and CaSR, leading to increased TRPV5 activity. PTH-mediated channel phosphorylation therefore reverses CaSR feedback inhibition of TRPV5.

vi. 80k-h: 25-hydroxyvitamin D3-1α-hydroxylase knockout mice display up-regulation of TRPV5 mRNA levels. To identify other genes transcriptionally altered in these from 25-hydroxyvitamin D3-1α-hydroxylase knockout mice, microarray analysis of kidney mRNA was performed, and revealed that expression of the protein kinase C substrate, 80k-h was downregulated; dietary Ca^{2+} supplementation was then shown to stimulate renal expression of 80k-h (161). 80k-h colocalizes withα TRPV5 in the DCT/CNT, and was shown to interact with TRPV5 *in vitro*. 80k-h binds Ca^{2+} through two EF-hand structures, and mutating them reduced TRPV5 activity and increased its sensitivity to intracellular Ca^{2+}, enhancing Ca^{2+}-mediated feedback inhibition of the channel (161). These mutations did not disrupt binding of 80k-h to TRPV5, or alter the plasma membrane abundance of TRPV5, suggesting that 80k-h directly modulates activity of the channel.

vii. Non-genomic effects of steroid hormones: In addition to long-term effects on expression levels of the transcellular pathway machinery, steroid hormones may exert acute regulatory effects on TRPV5. Late distal convoluted tubules and connecting tubules isolated from mice displayed a rapid dose-dependent uptake of Ca^{2+} in response to $1,25(OH)_2D_3$ treatment, suggesting that $1,25(OH)_2D_3$ may act through non-genomic effects (196). Similar rapid effects of 17beta-estradiol on TRPV5 activity have been observed in a rat cell line, with the caveat that the cell line used was derived from CCD rather than DCT/CNT (218).

b. Plasma membrane abundance: Extracellular factors

i. Klotho: A possible role for klotho in regulating renal Ca^{2+} reabsorption was revealed by the finding that mice lacking klotho display an increased fractional excretion of Ca^{2+} (500). In primary cultures of CNT and CCD cells, klotho stimulated TRPV5 activity, an effect that was mimicked by treatment of the cells with purified β-glucuronidase (72). Since klotho is detected in urine, it is likely that it exerts its effect along the lumen of the nephron by modifying TRPV5 glycosylation. Mutation of a conserved extracellular N-glycosylation site (N358) in TRPV5, which is a target of β-glucuronidase, prevented activation of TRPV5 by klotho (72), and removal of a specific sialic acid is involved (65). Cell surface biotinylation experiments revealed that klotho increases plasma membrane abundance of TRPV5 (72). The precise mechanism involves a reduction in TRPV5 endocytosis by increasing its interaction with galectin-1 at the membrane following sialic acid removal from TRPV5 (65). It is not known if klotho regulates open probability.

ii. Tissue Kallirein: A possible role for the serine protease tissue kallikrein (TK) in the regulation of TRPV5 was proposed following the observation that TK knockout mice display significant hypercalciuria (387). Studies in TRPV5 knockout mice suggest that TK plays a role in Ca^{2+} homeostasis since these mice display increased TK excretion that is abolished by Ca^{2+} supplementation (162). Activated TK is secreted from the CNT into the lumen of the nephron and can act directly or indirectly (by converting kinogens to kinins) on bradykinin 2 receptors (162). Thus, the effect of TK to increase plasma membrane expression of TRPV5 and stimulate transcellular Ca^{2+} transport is likely to involve signaling through the bradykinin pathway (162). This pathway involves activation of phospholipase C through $G_{q/11}$; the subsequent production of diacycglycerol activates protein kinase C. Treatment of cells with the phospholipase C inhibitor U73122 prevented TK activation of TRPV5, whereas treatment of cells with a cell-permeable diacylglycerol (a product of phospholipase C activity) analogue activated TRPV5 (162). Finally, mutagenesis studies revealed that phosphorylation of TRPV5 by protein kinase C, which is activated by diacylglycerol, is required for TK stimulation of TRPV5. Cell surface biotinylation studies showed that the effect of protein kinase C phosphorylation on TRPV5 is to increase its plasma membrane abundance (162), an effect that involves caveolin-1 (66). In summary, TK appears to act locally in the CNT to stimulate transcellular Ca^{2+} reabsorption by increasing TRPV5 plasma membrane abundance; it is not known if it regulates open probability.

iii. Tissue transglutaminase: Recently, a role for the Ca^{2+}-dependent protein crosslinking enzyme tissue transglutaminase (tTG) in regulating TRPV5 activity has been described. tTG was detected in mouse urine and in the apical medium of polarized cultures of rabbit CNT/CCD cells (42). Application of purified tTG to both HEK293 and polarized rabbit CNT/CCD cells inhibited TRPV5 activity. The mechanism of inhibition was proposed to involve crosslinking of TRPV5 by tTG, which may increases rigidity of the channel and lead to a reduction in channel pore diameter (42). Changes in pH may inhibit TRPV5 activity by a similar effect on channel rigidity (see below). Furthermore, in the absence of N-linked glycosylation, TRPV5 was insensitive to tTG, indicating that N-glycosylation is essential for tTG inhibition. This raises the possibility that there is crosstalk between tTG, which inhibits TRPV5, and klotho, which stimulates TRPV5.

iv. Ca^{2+}: High intracellular Ca^{2+} exerts feedback inhibition of TRPV5 directly. Studies with HEK293 cells showed that in the absence of divalent cations, TRPV5 can act as a Na^{+} channel (361). Ca^{2+} currents were induced by addition of Ca^{2+} to the culture medium, but increasing intracellular Ca^{2+} eventually inhibited Ca^{2+} flux into the cells. Mutational analysis of TRPV5 subsequently identified two C-terminal intracellular Ca^{2+}-sensing regions required for Ca^{2+}-dependent inhibition of channel activity (362). The mechanism by which the Ca^{2+}-sensing regions modulate TRPV5 activity has recently been elucidated. The CaSR has been shown to directly interact with the C-terminus of TRPV5 to reduce its activity (96). When the TRPV5 residues involved in calmodulin binding were mutated, the mutant channels TRPV5-W702A and TRPV5-R706E, displayed a significant reduction in Ca^{2+}-dependent inactivation (open probability was increased) compared to the wild-type channel. CaSR-mediated feedback inhibition through binding to TRPV5 is reversed by PTH **(see below)**. Feedback inhibition is also reduced by the actions of calbindin D28K. In cells, when intracellular Ca^{2+} is reduced, calbindin-D28k, which translocates towards the plasma membrane, and directly interacts with the N- and C-termini of TRPV5, as noted above (266). This interaction is disrupted by increasing intracellular Ca^{2+} levels. Calbindin 28K overexpression stimulated TRPV5 activity, an effect prevented by disruption of the six calcium-binding EF-hand motifs present in calbindin 28K. Therefore, calbindin does not simply shuttle Ca^{2+} from the apical to basolateral membranes within the cell, but may actively suppress feedback inhibition, possibly by competing with the CaSR for binding to the C-terminus of TRPV5.

Finally, in HEK293 cells, channel recycling has been shown to be inhibited by treatment with the Ca^{2+} chelator BAPTA-AM (511). BAPTA-AM did not reduce TRPV5 endocytosis, but rather reduced the reappearance of internalized TRPV5 at the plasma membrane. These data suggest that in addition to direct effects on open probability mediated through calmodulin, or calbindin D28K association with the channel, Ca^{2+} stimulates TRPV5 recycling, allowing the cell to rapidly replace inactivated cell surface TRPV5 with the active channel from a recycling compartment to restore Ca^{2+} influx.

v. pH: As described above, acid-base status is likely to regulate Ca^{2+} balance through effects of the expression levels of the components of the transcellular pathway machinery. In addition to these more chronic effects, pH has a direct effect on Ca^{2+} transcellular transport in primary cultures of rabbit CNT and CCD, with lower pH inhibiting transport relative to higher pH (30). The possible role of modulation of TRPV5 activity in mediating this effect was demonstrated by the observation that lowering extracellular pH reduced $^{45}Ca^{2+}$ influx at the apical membrane of these cells. Changes in pH are known to directly affect TRPV5 activity by two mechanisms. Firstly, in a mammalian cell expression system, eGFP-TRPV5 was detected in a pool of vesicles lying close to the plasma membrane (267). Increasing extracellular pH stimulated TRPV5 activity by causing the eGFP-TRPV5-containing vesicles to fuse with, but not merge with, the plasma membrane. Reducing the extracellular pH caused these vesicles to rapidly internalize, resulting in lower TRPV5 activity. This phenomenon, whereby exocytic vesicles transiently fuse with the plasma membrane, without escape of vesicular contents, has been termed “kiss-and-run” (472). Thus TRPV5 can be rapidly shuttled to and from the plasma membrane by changes in extracellular pH. Secondly,

lowering pH either inside and outside the cell reduce activity of single TRPV5 channels by reducing open probability and single-channel conductance (587). TRPV5 contains two proton-binding amino acids, the extracellular glutamate 522, and the intracellular lysine 607. On acidification, binding of protons to these residues is proposed to induce a conformational change in the channel pore. Patch-clamp studies in which these amino acid residues are mutated revealed that the major role of this mechanism is to reduce open probability(587), possibly resulting from a reduction in pore diameter (65).

5. Regulation of basolateral Ca^{2+} extrusion—As noted above, ~70% of active Ca^{2+} transport is due to activity of NCX1, with the remaining 30% arising from PMCA1b activity. Functional studies have shown that the acute administration of physiological doses of PTH significantly increased NCX1 activity in renal basolateral membrane vesicles from rats (221), rabbits (45), and dogs (443). This effect was mimicked by dibutyryl cAMP in the rabbit (45), but not in the dog (443). The signal transduction pathways that mediate PTH effects on NCX1 are still unknown.

6. Regulation of Ca^{2+} transport by diuretics and disease—Thiazide diuretics have long been known to reduce urinary Ca^{2+} excretion, an effect that resembles one of the cardinal manifestations of Gitelman syndrome. Although the molecular biology of Ca^{2+} transport along the DCT is now well understood, as is the genetic basis of Gitelman syndrome, the mechanisms resulting in hypocalciuria remain surprisingly controversial (for a review, see (401)). One mechanism clearly results from enhanced NaCl reabsorption along the proximal tubule, owing to ECF volume contraction. Along the proximal tubule, Ca^{2+} reabsorption is coupled tightly to NaCl and fluid reabsorption (39, 567). ECF volume depletion stimulates both, thereby favoring passive proximal Ca^{2+} reabsorption. Evidence in support of a role for ECF volume contraction includes temporal aspects of thiazide effects. Acute thiazide administration often increases calcium excretion (116); while this effect is likely related to the carbonic anhydrase inhibiting effects of these drugs, it suggests that these drugs are not profoundly hypocalciuric in the setting of euvolemia. Yet even in the short term, the rise in calcium excretion is less than that caused by other diuretics (49), raising the possibility of an ECF volume-independent effect. Several human studies showed that the development of frank hypocalciuria during thiazide treatment does depend on a reduction in ECF volume (48, 49). Yet there are countervailing data, as well.

Costanzo and Weiner reported that ECF volume depletion is not necessary for acute thiazide-induced hypocalciuria in dogs (88), as hypocalciuria could be generated by unilateral chlorothiazide infusion into a renal artery. In individuals with Gitelman syndrome, saline infusion, to increase urinary NaCl excretion, did not increase Ca^{2+} excretion substantially (76). Similar findings have been obtained in models of impaired DCT function. Yang and colleagues (584) generated an NCC S707X knockin mouse, to mimic patients with Gitelman syndrome. In these mice, hypocalciuria could not be reversed by NaCl infusion. McCormick and colleagues (326) found that dietary NaCl loading did not reverse the hypocalciuria that resulted from disruption of SPAK, an important activator of NCC in the distal nephron.

While enhanced proximal Ca^{2+} reabsorption certainly contributes to hypocalciuria in individuals with Gitelman syndrome and probably in patients taking thiazide diuretics chronically, recent studies suggest that enhanced Ca^{2+} reabsorption along the TAL may also contribute (118). Favre and colleagues (138) used clearance techniques to demonstrate that loop segment NaCl transport is increased in individuals with Gitelman syndrome. As transport related to NKCC2 activity generates the transepithelial voltage along the TAL, activation would be expected to increase the magnitude of the lumen positive voltage that drives Ca^{2+} reabsorption there. This would be expected to result in reduce Ca^{2+} delivery to the DCT (the opposite of a furosemide effect). Our group reported that SPAK deletion in mice increases the abundance of pNKCC2 and enhanced the furosemide effect, both findings consistent with loop segment activation when DCT function is disrupted. Together, these findings suggest a role for the TAL in thiazide-induced hypocalciuria.

Despite evidence for effects of thiazides/NCC knockout to enhance Ca^{2+} reabsorption along more proximal segments, there is also strong evidence that thiazides stimulate Ca^{2+} reabsorption directly along the distal nephron. Costanzo and Windhager (89) used micropuncture and microperfusion to show that chlorothiazide perfusion increased Ca^{2+} reabsorption along the DCT. Coupled with evidence, cited above, for a ECF volume-independent component of Ca^{2+} reabsorption, most investigators viewed an effect along the distal tubule as proven. Controversy was raised, however, when Nijenhuis and colleagues (356, 360) reported that thiazide-induced hypocalciuria was associated with decreased, rather than increased, abundance of Trpv5, calbindin-D_{28K}, and NCX1. They also found that urinary calcium excretion was reduced by hydrochlorothiazide treatment, but not in sodium-repleted rats treated with hydrochlorothiazide (356, 360). The authors concluded that ECF volume contraction was a critical component of thiazide-induced hypocalciuria. In the second study, the same group compared the effect of thiazide diuretics on renal Ca^{2+} handling in *Trpv5* -knockout mice and their wild-type littermates (356, 360). Here, they reported that the decrease in fractional Ca^{2+} delivery along the length of accessible distal tubule was similar in the control and thiazide-treated animals. As the hypocalciuric effect persisted in *Trpv5*-knockout mice, the authors concluded that increased passive Ca^{2+} reabsorption in the proximal tubule rather than Trpv5-mediated Ca^{2+} reabsorption distally explained the chronic thiazide-induced hypocalciuria.

While these results clearly support a volume-dependent component to thiazide (and Gitelman)-related hypocalciuria, the very high urinary Ca^{2+} excretion in the basal state makes interpretation of the Trpv5 knockout mice experiments more difficult. Furthermore, distal Ca^{2+} reabsorption is load-dependent. The decrease in the fractional Ca^{2+} delivery to the distal tubule during thiazide treatment in the free-flow micropuncture study precludes accurate assessment of maximal reabsorptive capacity. Furthermore, the data concerning abundance of Ca^{2+} transport proteins along the DCT is somewhat contradictory. In the NCC S707X knockin mice, noted above, TrpV5 abundance was increased. Furthermore, Lee and colleagues (273) used a lower dose of thiazide than that used by Nijenhuis and colleagues. Acute treatment with chlorothiazide reduced the urinary calcium-to-creatinine ratio and increased Trpv5 expression. During chronic treatment, Trpv5 mRNA abundance increased, but only when ECF volume depletion was prevented. They concluded that the proximal tubule plays a major role during volume contraction, but when volume contraction is absent,

thiazide-induced hypocalciuria is the result of increased calcium reabsorption in the distal tubule and upregulation of Trpv5 and calbindins. A final model supporting a volume-independent effect of thiazides on Ca^{2+} excretion involves parvalbumin knockout mice (26). Parvalbumin in the kidney is selectively expressed in the DCT1 and colocalizes with the NCC; it plays a variety of cellular roles. Interestingly, *Pvalb*-knockout mice have modestly reduced abundance of NCC, and do not exhibit a natriuretic response to thiazides; despite this, these mice exhibited the typical (though slightly blunted) reduction in urinary Ca^{2+} excretion following thiazide administration. The reasons between differences in NCC and parvalbumin knockout mice are not entirely clear.

Of course, transport protein abundance and transport activity or capacity may not be equivalent. There are a number of other potential mechanisms by which thiazides/NCC knockout might affect Ca^{2+} reabsorption, independent of transport protein abundance. When Na^+ and Cl^- cannot enter the cell across the apical membrane, intracellular concentrations decline. As NCX1 exchanges Na^+ for Ca^{2+}, this will favor Ca^{2+} reabsorption across the basolateral membrane. Additionally, as noted above, Cl^- channels at the basolateral membrane participate in setting the membrane voltage. When intracellular Cl^- activity declines, this will hyperpolarize the basolateral membrane. As the NCX1 is also electrogenic, this will also favor basolateral Ca^{2+} reabsorption.

To summarize current information about thiazide and Gitelman syndrome associated hypocalciuria, it appears that ECF volume-dependent and independent mechanisms are both involved. The ECF volume-dependent processes involve enhanced Ca^{2+} reabsorption, primarily along the proximal tubule, but probably also along the TAL. In addition, however, there are clearly other effects of thiazides/NCC deletion that do not require ECF volume depletion. Some of these involve the distal tubule, although this does not mean that the increased Ca^{2+} uptake occurs in the cells that express NCC. As the majority of NCC is expressed along the DCT1, while the majority of Ca^{2+} reabsorption occurs along the CNT, the two processes may be sequential. The cellular processes involve likely include changes in transport protein abundance, but changes in activity may also occur.

F. Magnesium transport

1. Rates of magnesium transport—Magnesium has many cellular functions including acting as a cofactor in energy metabolism, nucleotide and protein synthesis pathways, and regulating Na^+, K^+ and Ca^{2+}. The normal physiological range of Mg^{2+} in the plasma is 0.7–1.1 mmol/l. In the kidney, 90–97% of the filtered Mg^{2+} (approximately 2500mg) is reabsorbed. Unlike many solutes, such as Na^+ and Ca^{2+}, relatively little Mg^{2+} is reabsorbed along the proximal tubule (10–30% of reabsorption). In contrast, the majority of Mg^{2+} is reabsorbed paracellularly, along the TAL (40–70% of reabsorption). The remaining 3–7% is reabsorbed along the DCT by a transcellular pathway. Basal rates of magnesium reabsorption along the DCT are approximately 0.5 $pmol \cdot min^{-1} \cdot mm^{-1}$ (1 $pEq \cdot min^{-1} \cdot mm^{-1}$) (392, 394), approximately half the rate of Ca^{2+} transport along the same segment. As the fraction of filtered Mg^{2+} reabsorbed along the distal tubule is relatively small, the DCT was assumed for many years to play a relatively modest role in systemic magnesium balance (395). It was only the identification of the molecular basis of monogenic Mg^{2+} wasting

disorders that changed this view. The DCT is now believed to play a crucial role in mammalian Mg^{2+} homeostasis (103).

Magnesium is reabsorbed throughout the DCT. This includes both the DCT1 and the DCT2, in contrast with Ca^{2+}, which is reabsorbed primarily along DCT2 and CNT (103). This spatial separation may have physiological consequences, and it clearly has pathophysiological one; in Gitelman syndrome, the DCT1 segment is atrophic (303). As DCT1 is the primary site for magnesium reabsorption along the DCT, this leads to profound Mg^{2+} wasting. Yet, as Ca^{2+} is reabsorbed primarily along the DCT2 and CNT (33), which remain intact, calcium reabsorption is not impaired. Also unlike the case for Ca^{2+}, the Mg^{2+} chemical gradient across the apical membrane is small, meaning that the driving force for Mg^{2+} entry is much smaller than for Ca^{2+}, and largely driven by the apical membrane voltage.

2. Mechanisms of magnesium transport—Most transport along the DCT appears to be transcellular, although an initial report suggested the claudin 16 (paracellin) is expressed along the DCT, as it is along TAL (456). That this pathway does not play an important role along the DCT is consistent with microperfusion studies by Quamme and colleagues showing little Mg^{2+} secretion when DCT segments were perfused with Mg^{2+}-free solution (394). It should be noted, however, that the same study concluded that loop segments also exhibit little permeability, although it is now believed that paracellular Mg^{2+} permeability is important along the thick ascending limb (201).

The pathways involved in transcellular Mg^{2+} reabsorption along the DCT are not as well delineated as those for Ca^{2+}, but progress has been made. The transient receptor potential melastatin member 6 (TRPM6) appears to be the major apical entry pathway. Unfortunately, although the major basolateral exit pathway has not yet been identified, other proteins involved in transcellular Mg^{2+} transport and its regulation have been. These include the potassium channel, Kv1.1, the γ subunit of the Na^+-K^+-ATPase, and several other more recently identified proteins. These will be discussed below. Although intracellular Mg^{2+} buffers may exist, their role is not as clear as it is for calbindins, because the intracellular Mg^{2+} concentration is not maintained in the nanomolar range, as it is for Ca^{2+}.

TRPM6 was identified as playing an important role in renal reabsorption of Mg^{2+} through genetic analysis of individuals presenting with hypomagnesemia and secondary hypocalcemia (432, 539, 540). TRPM6 is expressed in both intestine and in kidney, where it localizes to the apical membrane of the DCT (DCT1 and DCT2 (534)). TRPM6 disruption is embryonic lethal in mice, but mice heterozygous for the channel are viable and display hypomagnesemia. Mg^{2+} supplementation does not prevent either embryonic lethality or hypomagnesemia in these mice (563), indicating the crucial role of TRPM6 in regulating Mg^{2+} homeostasis. Patch-clamp analysis showed that TRPM6 is permeable to both Mg^{2+} and Ca^{2+}, but permeability to Ca^{2+} is substantially lower (534).

TRPM6 contains six putative TM domains with a pore region between the fifth and sixth segments, and large intracellular amino and carboxyl termini. TRPM6 displays strong outward rectification and is tightly regulated by intracellular magnesium. TRPM6 may form

a functional homotetrameric channel or a heteroteramer with TRPM7, but this remains to be clarified. TRPM6 exhibits a conductance two-fold greater than that of TRPM7 and the TRPM6/7 heterotetramer (283). TRPM6 has an approximately five-fold higher affinity for magnesium than for calcium, while other calcium permeable channels display a much lower affinities for Mg^{2+} than for Ca^{2+}. One striking feature of TRPM6, and TRPM7, is the presence at the C-terminus of the α-kinase domain; these two channels are unique in possessing intrinsic kinase activity. The α-kinase domain has been proposed to act as an intracellular Mg^{2+}-sensor, and is thus likely to be involved in regulation of channel activity (206).

The pathway followed by Mg^{2+} following entry through TRPM6 is unknown. In contrast to Ca^{2+} **(see section III.d.)**, there is little difference between the intra- and extracellular concentrations of Mg^{2+}, which are both in the submillimolar range, so a specific Mg^{2+}-binding protein for the shuttling of Mg^{2+} to the basolateral membrane may not be required. The lack of an Mg^{2+} gradient does not preclude a role for regulation of TRPM6 activity by Mg^{2+}, since increasing intracellular Mg^{2+} has been shown to inhibit channel activity (534). While there are many intracellular proteins that bind Mg^{2+} in all tissues, parvalbumin and calbindin D28K are relatively highly expressed along the DCT (32). However, these proteins also bind Ca^{2+}, and no protein that specifically binds Mg^{2+} has been identified. Since parvalbumin is highly expressed along DCT1 (where TRPM6 expression is highest), but relatively weakly expressed along the DCT2 and CNT, it may fulfill the role of the Mg^{2+} shuttle. However, parvalbumin knockout mice do not display any defect in Mg^{2+} homeostasis (26). Regarding Mg^{2+} extrusion at the basolateral membrane, while there is some evidence of the existence of a Na^{+}/Mg^{2+} exchanger in epithelial cells and in rat kidney (442, 498), its identity Is unknown. Similarly, there is evidence for the existence of a Mg^{2+} pump, similar to PMCA1b (441). A recent association study found that variants in the PMCA1 gene are associated with serum Mg^{2+} concentrations (337). One previous study reported that the phosphatase activity of PMCA1 is dependent on magnesium ions (323), suggesting it might fulfill the role of a basolateral Mg^{2+} pump.

3. Regulation of magnesium transport

a. General: Since the transcellular pathway machinery is largely unknown, little is known about its regulation. Some information has been gleaned regarding regulation of TRPM6 activity and includes (i) regulation of TRPM6 expression, (ii) regulation of TRPM6 plasma membrane abundance and (iii) alteration of TRPM6 open probability (P_o).

b. Regulation of TRPM6 expression: In contrast to TRPV5 **(see section III.d.iii.)**, expression of TRPM6 does not appear to be regulated by PTH or $1,25(OH)_2D_3$ in mice (160). However, several factors stimulating its expression have been identified.

i. Dietary Mg^{2+}: Dietary Mg^{2+} increased expression of renal TRPM6 both at the mRNA and protein level, without effects on TRPM7 expression (160). The increased TRPM6 expression was still restricted to the apical membrane of the DCT. Supplementation of Mg^{2+} had no significant effects on TRPM6 mRNA or protein expression.

ii. Hormonal and growth factor regulation: 1α (OH)ase knockout mice, which lack $1,25(OH)_2D_3$, displayed no differences in renal TRPM6 expression compared with wild-type mice, and $1,25(OH)_2D_3$ supplementation did not induce any effects in these mice (160). The same observation was made in rats that had undergone parathyroidectomy, or parathyroidectomy with PTH replacement. Ovariectomy of rats reduced renal TRPM6 expression, an effect reversed by estrogen replacement (160). None of these manipulations affected TRPM7 expression levels. The effects of testosterone on TRPM6 expression have not been determined.

Hyperaldosteronism can lead to hypomagnesemia and decreased intracellular Mg^{2+} (5, 420), and the associated urinary Mg^{2+} wasting is ameliorated by the mineralocorticoid receptor blockers spironolactone and eplerenone, and by Mg^{2+} supplementation (170, 389, 558). Chronic aldosterone administration in mice had no effect on renal TRPM6 mRNA levels, but significantly reduced TRPM7 mRNA and protein expression (463). Mg^{2+} supplementation increased expression of both TRPM6 and TRPM7 mRNA in aldosterone-infused mice. A subsequent study revealed that while aldosterone did not affect TRPM6 mRNA expression, it had a clear effect on TRPM6 membrane expression that was dependent on Mg^{2+} status **(see below)**.

In addition to direct effects on TRPM6 activity **(see below)**, EGF has been reported to stimulate its expression in cultured cells through both ERK- and PI3-kinase-dependent pathway (212–214). The effects mediated through the PI3-kinase pathway appear to be an effect on TRPM6 mRNA stability rather than an effect on gene transcription (214). *In vivo*, rats treated with EGF for 28 days, displayed reduced fractional excretion of Mg^{2+}, accompanied by increased renal expression of TRPM6, but no change in TRPM7 expression (272). It is unclear, however, if the chronic of EGF on TRPM6 expression is secondary to other changes along the distal nephron.

iii. Acid-base status: Systemic acidosis is associated with renal Mg^{2+} wasting (36, 279, 316), and acute metabolic acidosis produced by infusion of NH_4Cl or HCl stimulates Mg2+ excretion (316). Chronic acidosis also leads to urinary magnesium wasting which, as with acute acidosis, may be partially corrected by the administration of bicarbonate (447). In contrast, acute and chronic metabolic alkalosis reduces urinary Mg^{2+} excretion (357, 562). Studies in mice have shown that changes in Mg^{2+} excretion induced by manipulation of acid-base status are associated with changes in renal TRPM6 expression levels (358). Consistent with the observed effects on urinary Mg^{2+} excretion, TRPM6 mRNA and protein expression levels were significantly reduced by NH_4Cl loading (which increased Mg^{2+} excretion), whereas $NaHCO_3$ treatment (which decreased Mg^{2+} excretion) increased TRPM6 expression. These correlative findings do not confirm that the changes in TRPM6 expression are the primary cause of altered urinary Mg^{2+} excretion, but micropuncture studies in dogs showed that Mg^{2+} uptake along the distal nephron varied with acid-base status (447, 562). Consistent with these data, in isolated mouse DCT cells, increasing extracellular pH increased Mg^{2+} uptake, and low pH had the opposite effect (93).

iv. Pharmacological regulation: In humans, usage of thiazide diuretics, which block NCC, or immunosuppressants such as the calcineurin inhibitors cyclosporin A and tacrolimus

(FK506) leads to hypomagnesemia (186), so may act through regulation of TRPM6. Administration of thiazide diuretics to mice increases urinary Mg^{2+} excretion, an effect accompanied by a reduction in TRPM6 expression (359). NCC knockout mice also display hypomagnesemia (440), but it is possible that this is related to the significant atrophy of the DCT1 observed in these animals causing an indirect reduction in TRPM6 expression. A similar effect on DCT1 structure has been observed following chronic thiazide treatment (300, 356), but DCT atrophy was not observed in the study that showed reduced renal TRPM6 expression (359). In fact, NCC expression levels were *increased* following thiazide administration in this study. Therefore, the effect of thiazides to reduce TRPM6 may be specific, rather than secondary to DCT remodeling. Similarly, chronic treatment of rats with tacrolimus or cyclosporine A have the same effects on urinary Mg^{2+} excretion and TRPM6 expression (272, 355).

c. Regulation of TRPM6 activity: Microperfusion and experiments in cultured DCT cells showed that both PTH and $1,25(OH)_2D_3$ stimulate Mg^{2+} reabsorption (178, 393). However, as described above these effects are not mediated through expression of TRPM6, and the pathways involved remain unknown. Several other mediators of TRPM6 activity, some of which indirectly affect its activity through their effects on voltage, have been described, and will now be outlined.

i. Role of the α-kinase domain: The α-kinase domain of TRPM6 plays a critical role in modulating channel activity, and its activity results in autophosporylation of the channel at several sites (83). Incubation of the C-terminus of TRPM6 with ATP led to a noticeable shift in electrophoretic mobility on SDS-PAGE gels. Pre-incubation of this fragment with ATP increased its subsequent kinase activity, indicating that TRPM6 is activated by autophosphorylation (83). In HEK293 cells, a role for the α-kinase domain in channel activation is illustrated following its deletion, which significantly reduces, but does not abolish TRPM6 activity (497). However, activity of the α-kinase domain is not necessary for channel activation since kinase-dead (K1804R) and autophosphorylation-deficient (T1851A) TRPM6 mutants have similar activity to wild type channels (497). Thus the presence, but not the activity of the α-kinase domain is required for TRPM6 activity. ATP binding to a conserved ATP-binding pocket in the α-kinase domain also inhibits channel activity. Upon deletion of the α-kinase domain, the inhibitory effect of ATP is lost (497). Structural and mutation analysis of TRPM6 identified a conserved G*X*G(A)*XX*G loop involved in transferring the signal generated by ATP binding to the rest of TRPM6. Mutations of this loop result in reduced mobility of this loop rather than diminished ATP binding.

Yeast two-hybrid screening identified the receptor of activated protein kinase 1(RACK1) as interacting with TRPM6, and immunofluorescence studies confirmed the two proteins co-localize along the DCT in rat (58). Overexpression of RACK1 in HEK293 cells inhibited TRPM6 activity, while knockdown of RACK1 using siRNA stimulated activity (58). Intracellular Mg^{2+} levels have also been shown to inhibit TRPM6 activity (534), and RACK1 knockdown reduced Mg^{2+}-dependent channel inhibition (58). Inhibition of TRPM6 by RACK1 required kinase activity of the α-kinase domain since the kinase-dead K1804R TRPM6 mutant was not inhibited by RACK1, despite still being able to interact with it.

Further mutagenesis studies revealed that autophosphorylation at T1851 is required for the inhibitory effect of RACK1. The effect of RACK1 on TRPM6 does not involve regulation of channel membrane expression, but is mediated through protein kinase C.

ii. Epidermal Growth Factor: Groenestege and colleagues identified a mutation in the gene encoding pro-EGF as causing isolated recessive renal hypomagnesemia (IRH), a disorder characterized by low serum Mg^{2+} levels and mental retardation (179). The mutation resulted in the substitution of a highly conserved proline 1070 within the cytoplasmic tail with leucine (EGF P1070L). Patch-clamping studies showed that EGF stimulates TRPM6 activity (179). Analysis of the signaling pathways involved downstream of EGFR using specific inhibitors revealed that both Src-Family Kinases and MAPK are involved in mediating the effects of EGF, and that the downstream mediators of Src activation is likely to be PI3-kinase (496). Expression of a dominant-negative mutant of the PI3-kinase effector Rac1, which plays a role in cytoskeletal remodeling and membrane trafficking, led to inhibition of TRMP6 whereas a constitutively-active Rac1 mutant activated it (496). EGF was shown to promote insertion of TRPM6 into the plasma membrane from an intracellular pool, through a Rac1-dependent process. The IRH-causing disease mutation leads to incorrect processing of pro-EGF, reducing secretion and activation of basolateral EGF receptors, thus preventing EGF-mediated stimulation of apical TRPM6 (179).

iii. Na^+-K^+-ATPase γ-subunit: Isolated Dominant Hypomagnesemia (IDH) presents with hypocalciuria in addition to renal Mg^{2+} wasting, and is caused by mutations in the *FXYD2* gene (331). This gene encodes the γ-subunit of the Na^+-K^+-ATPase, which alters the affinity of the pump for Na^+ and K^+, thereby modulating its activity (15, 25). The mutation results in a FXYD2 protein with glycine 41 replaced by arginine (FXYD2-G41R) which is unable to interact with the Na^+-K^+-ATPase (54). Since wild type FXYD2 and FXYD2-G41R oligmerize, regulation of the Na^+-K^+-ATPase may be abrogated by mislocalization of the regulatory FXYD2 subunit (54). This would explain the dominant nature of IDH. While the connection between dysregulation of the Na^+-K^+-ATPase and Mg^{2+} transport has not been determined, reduced Na^+-K^+-ATPase activity may lead to depolarization of the apical membrane, leading to lower Mg^{2+} reabsorption.

The transcription factor HNF1B has been reported to stimulate transcription of the FXYD2 gene, whose promoter contains several HNF1-binding sites (4). Two studies have identified an association of hypomagnesemia with mutations in the *HNF1B* gene. In the first, mutations in *HNF1B* have been linked with maturity-onset diabetes of the young, and around half of the patients with these mutations also present with hypomagnesemia (4). Consistent with a possible defect in FYXD2 function, these patients also present with hypocalciuria. A second study also identified association of HNF1B mutations with hypomagnesemia (188), providing further evidence that reduced FXYD2 expression/function reduced renal Mg^{2+} reabsorption.

iv. Shaker-related voltage-gated K+ channel (Kv1.1): Mutation of the *KCNA1 gene*, which encodes the voltage-gated K^+ channel KV1.1, causes an autosomal dominant form of hypomagnesemia characterized by muscular defects including tetany and weakness, cerebellar atrophy and hypomagnesemia (164). Kv1.1 is coexpressed with TRPM6 along the

DCT. The wild type channel hyperpolarizes cells (164), whereas the disease-causing N255D mutation renders the channel nonfunctional as a result of loss of normal voltage dependence and channel gating, rather than an effect on channel membrane localization (515). Depolarization of the cell in the absence of functional Kv1.1 is the likely cause of reduced Mg^{2+} transport in this disease.

v. Kir4.1: Patients with the tubulopathy EAST/SeSAME **(see section IV.b.)** also present with hypomagnesemia. As discussed above **(section III.c.iii)**, disruption of the *KCNJ10* gene (which encodes Kir4.1) may result in reduced recycling of K^+ across the basolateral membrane of DCT cells, reducing membrane potential, and hence impairing activity of the Na^+-K^+-ATPase. As with mutations in FXYD2 and Kv1.1, the subsequent depolarization of the cell would thus lead to reduced transport of Mg^{2+} across apical TRPM6.

vi. Oxidative stress: Along the nephron, the DCT is the most metabolically active segment, as reflected by the large number of mitochondria present in DCT cells (231). Several studies have implicated TRPM channels in ischemia (328, 402). Reduced TRPM7 channel expression ameliorated neuronal cell death after global ischemia (481), and the role of TRPM2 in responses to oxidative stress is well-established (144, 352). Accumulating evidence suggests that reactive oxygen species are not only harmful side products of cellular metabolism but also central players in cell signaling and regulation (20, 115, 494). A possible role for oxidative stress in regulating TRPM6 was uncovered by the identification of methionine sulfoxide reductase B1 (MsrB1) as a binding partner for the TRPM6 α-kinase domain (57). Hydrogen peroxide was shown to inhibit TRPM6 activity without altering plasma membrane expression, and this inhibition was prevented by overexpression of MsrB1. Mutagenesis studies of exposed methionine residues in the α-kinase domain revealed that methionine 1755 displays hydrogen peroxide sensitivity, and MsrB1 may reduce oxidation of this residue (57). The high metabolic activity of DCT cells due to their high abundance of mitochondria results in a high intracellular level of hydrogen peroxide. Thus, MsrB1 acts to maintain TRPM6 activity in this inhibitory environment.

vii. Estrogen: In addition to effects on TRPM6 gene transcription **(see above)**, estrogen has been reported to exert an acute effect on TRPM6 channel activity. Immunoprecipitation studies using HEK293 cells identified the repressor of estrogen receptor activity (REA) as an TRPM6 binding partner, and co-expression was TRPM6 was demonstrated in DCT *in vivo* (59). Co-expression of REA with TRPM6 led to inhibition of TRPM6 activity, and this inhibition required α-kinase domain activity, since the kinase-dead mutant K1804R was not inhibited by REA. Treatment with 17β-estradiol reduced the interaction between REA and TRPM6, and stimulated TRPM6 activity (59). Together, these data show that estrogen has both acute effects on TRPM6 activity and a chronic effect on channel expression.

viii. Extracellular cations: The luminal concentration of free Mg^{2+} along the DCT is in the range of 0.2–0.7 mM (1). To preferentially conduct Mg^{2+} in the presence of Ca^{2+}, which is present at a concentration of ~1mM, TRPM6 displays a higher affinity for Mg^{2+} than for Ca^{2+} (534). In the absence of divalent cations, TRPM6 becomes highly permeable to Na^+, and the effects of altering extracellular Mg^{2+} and Ca^{2+} on TRPM6 Na^+-permeability were

determined in HEK293 cells. Inward Na^+ currents were blocked in a voltage-dependent manner by low micromolar concentrations of both Mg^{2+} and Ca^{2+}, with Mg^{2+} blocking at lower concentrations than Ca^{2+} (534). These data suggest that these cations inhibit Na^+ permeability by binding to a site in the channel pore, with Mg^{2+} displaying higher affinity. Precisely how this inhibitory effect relates to Mg^{2+}-dependent currents, rather than Na^+ currents, is unclear.

Studies in CHOK1 cells have revealed that lowering extracellular pH stimulates TRPM6 activity (282). Similar effects were seen in TRPM7, and the residues responsible for conferring pH sensitivity in both channels were identified by mutagenesis studies. In TRPM6, residues glutamates 1024 and 1029 are the key residues for determining Ca^{2+}/Mg^{2+} permeability and pH sensitivity. The TRPM6 mutant E1029Q mutant displayed increased activity in response to lowering pH, but to a smaller degree than wild-type TRPM6. In contrast, lowering pH actually blocked activity of the E1024Q TRPM6 mutant.

ix. Aldosterone: Although aldosterone does not appear to affect TRPM6 gene transcription (463), studies in mice selectively bred for either low (MgL) or high intracellular Mg^{2+} (MgH) levels suggest it does regulate TRPM6 activity through an effect on membrane protein abundance (588). MgL mice display decreased Mg^{2+} reabsorption, increased urinary Mg^{2+} loss and consequent hypomagnesemia. In MgL mice, the ratio of membrane:cytosloic TRPM6 protein is reduced compared with MgH mice. Aldosterone induced a significant increase in TRPM6 activity in MgH mice and increased urinary Mg^{2+} excretion, but decreased TRPM6 activity in MgL mice (588). Mg^{2+} supplementation increased TRPM6 membrane:cytosol expression without a significant effect on TRPM7 in aldosterone-infused MgL mice when compared to vehicle-treated MgL mice. It should be noted that the authors of this studies concluded that there was a discrepancy between these data and the lack of aldosterone effects on TRPM6 mRNA they reported previously (463). However, in the present studies total only the membrane:cytolosolic ratio of TRPM6 expression was determined, and not total TRPM6 expression. With regards to pathophysiology, dietary Mg^{2+} supplementation of MgL mice attenuated aldosterone-induced blood pressure increase, renal fibrosis and oxidative stress, processes associated with increased TRPM6 activity. Thus, low Mg^{2+} states seem to amplify the deleterious effects of aldosterone, which itself promotes Mg^{2+} excretion, possibly through inhibition of renal TRPM6 activity, suggesting a feed-forward system that can be interrupted by Mg^{2+} supplementation (588).

VI. Genetic Diseases

Many genetic diseases have informed our knowledge of DCT physiology. While much of the information derived from these disease processes, we will briefly review important genetic diseases of the DCT. These disease states are summarized in Table 2.

A. Gitelman syndrome

Shortly after the initial cloning of NCC, it was recognized that a subtype of Bartter syndrome of normotensive hypokalemic alkalosis mimics many of the effects of thiazide diuretic treatment. This subtype has come to be known as Gitelman syndrome, and includes hypomagnesemia and hypocalciuria. It is now recognized as an autosomal recessive disease,

with the vast majority of cases resulting from mutations in the gene encoding NCC, *SLC12a3* (248, 457). Gitelman syndrome is the most common of the hypokalemic tubulopathies, with an estimated gene frequency of approximately 1% (disease 1:10,000) (444). Soon thereafter, it was shown that many Gitelman causing mutations generate proteins that are misfolded and degraded, presumably by endoplasmic reticulum associated degradation (ERAD) (99, 259, 353, 421, 584).

While most of the clinical features of Gitelman syndrome are easily explained by the disease mechanisms involved, two have been more confusing. First, the hypocalciuria is likely to be the result of both proximal and distal effects, as discussed above; hypocalciuria from thiazide diuretics is commonly employed therapeutically to prevent the recurrence of kidney stones. In contrast, the profound and often unrelenting hypomagnesemia of Gitelman syndrome is not similar to common side effects of thiazide treatment. Although thiazides can predispose to magnesium-wasting, this is almost always mild (119). The most likely reason for the profound magnesium wasting in Gitelman syndrome is that disruption of NCC leads to the developmental loss of nearly all DCT1 cells (300, 303); this leads to loss of most TRPM6 and the resulting magnesium wasting (360). Although intensive thiazide treatment of rats with thiazides generates many of the same structural effects, this does not appear to occur when humans take this drug in typical therapeutic doses (124).

B. SeSAME/East syndrome

The autosomal recessive EAST Syndrome (37) (independently described as SeSAME syndrome (436)), is characterized by a combination of symptoms including epilepsy, ataxia, sensorineural deafness and a salt-wasting renal tubulopathy; mental retardation is observed in some patients (37, 436). Genetic analysis of patients with EAST/SeSAME syndrome identified inactivating mutations in *KCNJ10* as the underlying cause of the disease. To date, eight different mutations in KCNJ10 causing the syndrome have been described (37, 397, 422, 436, 488). The renal salt-wasting observed in EAST/SeSAME syndrome is very similar to Gitelman Syndrome (discussed above), and similar morphological changes in the DCT are also observed i.e. atrophy of the DCT (397).

The role of KCNJ10 (and 15) in transepithelial NaCl transport is just now being examined. Extrusion of K^+ through KCNJ10/15 channels may provide a mechanism to keep basolateral K^+ concentrations in a range compatible with continued operation of the Na^+-K^+-ATPase pump. Secondly, KCNJ10 activity hyperpolarizes the basolateral membrane (594), generating the electrochemical gradient to favoring Na^+/Ca^{2+} exchange and favoring Cl^- exit (through CLCKB).

C. Familial Hyperkalemic Hypertension/Gordon Syndrome/pseudohypaldosteronism type 2

FHHt is a disease of hyperkalemia and hypertension originally identified by Paver and (381). Most cases appear to be inherited in an autosomal dominant manner, but a few follow a recessive mode of inheritance (46). The disease is often deemed to be a mirror image of Gitelman syndrome. Hyperkalemia is the cardinal feature, present in nearly all affected individuals, and occurring at a young age. Hypertension is common, but typically develops more gradually; recent genetic studies suggest that the severity of both the hypertension and

the hyperkalemia depends upon the mutated gene. Many individuals have mild hyperchloremic acidosis, and some have hypercalciuria (2, 322).

As discussed above, mutations in WNK1 and WNK4 were the first mutations shown to cause the disease; these mutations appear to have effects on several transport proteins along several nephron segments, but an important one is to stimulate NCC along the distal tubule (379). More recently, mutations in two additional genes were shown to cause the disease (46, 305). These genes, cullin 3 and KLHL3, are members of a cullin ring ligase pathway that participates in targeting proteins for destruction by tagging them with the protein ubiquitin. Some KLHL3 mutations cause recessive disease. The interested reader is referred to other reviews for additional details about this interesting syndrome pseudohypoaldosteronism (67, 148, 325, 379).

D. Hereditary hypomagnesemia

Magnesium wasting and resulting hypomagnesemia are important components of several genetic diseases. Some of these affect primarily segments of the nephron other than the DCT, but others have helped identify the essential role of the DCT in systemic magnesium balance. Gitelman syndrome, which is characterized by magnesium wasting and hypomagnesemia has been discussed above, as has the similar renal phenotype of EAST/SeSAME syndrome. Here, we will describe briefly a number of other magnesium wasting syndromes associated with dysfunction is the DCT. Walder et al. (540) described kindreds suffering from hypomagnesemia and secondary hypocalcemia (HSH; OMIM 602014). The phenotype consisted of neurological symptoms such as tetany, muscle spasms, and seizures, and the patients display low plasma Mg^{2+} levels caused by defective intestinal and renal absorption of Mg^{2+}. The low plasma Ca^{2+} levels are secondary, likely due to parathyroid failure caused by hypomagnesemia. The disease was subsequently shown to result from mutations in TRPM6 (432, 539), which plays a central role in reabsorbing Mg^{2+}, as discussed above.

As discussed briefly below, antagonists of epidermal growth factor (EGF), used commonly for their antineoplastic properties, were observed to cause hypomagnesemia commonly, when used therapeutically. This suggested an interaction between EGF receptors and renal magnesium balance. Geven et al. (156) first described autosomal recessive isolated renal hypomagnesemia (HOMG4; OMIM 611718), with effects including seizures and mild mental retardation. The disease is now known to be caused by mutations in EGF (179). In rat kidney, pro-EGF was shown to localize primarily in DCT. Although the specific role of EGF in mediating the disease is still not clear, it appears to play an important role in trafficking TRPM6 to the luminal membrane. This trafficking effect is disrupted in the patients with the disease.

Mutations in Kv1.1 were shown to cause autosomal-dominant hypomagnesemia (164). The patients presented in infancy with recurrent muscle cramps, tetany, tremor, muscle weakness, cerebellar atrophy, and myokymia. Although Kv1.1 is expressed together with TRPM6 along the luminal membrane of the DCT and expression studies showed that the mutation resulted in a non-functional channel, the exact mechanism involved in the TRPM6 dysfunction remains somewhat unclear (121).

Another identified gene proposed to have a role in Mg^{2+} homeostasis is FXYD2, which encodes the γ-subunit of the basolateral Na^+-K^+-ATPase. This gene is mutated in patients with autosomal-dominant renal hypomagnesemia associated with hypocalciuria. The hypomagnesemia in these patients can be very low resulting in convulsions. The FXYD2 gene encodes two splice variants. Splice variant gb localizes to the basolateral membrane of the DCT and the connecting tubule region (16). The exact molecular mechanism by which γ regulates Mg^{2+} handling in the DCT remains to be determined.

VII. Drugs and the DCT

A. Uses of DCT diuretics

The thiazide and thiazide-like diuretics act predominantly along the DCT to inhibit NaCl cotransport. These drugs have many uses, but most commonly are employed to treat essential hypertension. They have in use continuously for more than 60 years, and yet still are viewed as one of the most essential components of antihypertensive drug treatment (220). The drugs are also used commonly to reduce the likelihood of recurrence for nephrolithiasis. The interested reader is referred elsewhere for a discussion of the uses and side effects of these drugs (123, 373).

B. Cisplatin and carboplatin

The platins are used to treat a variety of malignancies. One of their predominant side effects, however, is a salt wasting syndrome that resembles Gitelman syndrome (34, 204, 260, 319, 378). Recently, it was shown that cisplatin treatment of animals leads to salt and magnesium wasting, with hypomagnesemia. This effect was associated with decreases in both TRPM6 and NCC (506). This suggests that the platins cause an acquired form of Gitelman syndrome by damaging DCT specifically (120).

C. Amphotericin

The antifungal amphotericin has also long been known to cause a salt wasting syndrome, as well as acute kidney injury (23, 182, 187). This syndrome can include both hypokalemia and hypomagnesemia, making it resemble Gitelman syndrome and suggesting a central pathological effect along the DCT.

D. Calcineurin inhibitors

Calcineurin inhibitors (CNIs) are immunosuppressive drugs that are used frequently to prevent rejection of transplantated organs and treat immune diseases. Their use, however, is often complicated by hypertension and renal tubular dysfunction, which can lead to hyperkalemia, hypercalciuria, and acidosis (191, 315). In mice, the CNI tracrolimus caused hypertension by increasing the abundance of phosphorylated NCC (199). It also activated WNK3, WNK4, and SPAK. As the ability of tacrolimus to cause hypertension and K^+ retention was absent from mice lacking NCC, it was suggested that NCC plays a central and non-redundant role in this process. Mice overexpressing NCC exhibited an increased hypertensive response to tacrolimus. These observations were extended to patients treated with tacrolimus, who exhibited a more robust response to the bendroflumethiazide than did controls, and renal NCC abundance was greater. Together the results indicate that CNI-

induced hypertension is mediated by NCC activation. They suggest that thiazides, inexpensive and well-tolerated agents, may be especially effective drugs to prevent complications of CNI treatment.

Calcineurin inhibitors also cause magnesium wasting. In mice, the CNI cyclosporine was found to reduce the abundance of TRPM6, EGF, and NCC (272). They suggested that the effect on TRPM6 was the likely cause of magnesium wasting in patients treated with this drug.

E. EGF antagonists

Cetuximab, a monoclonal EGFR antagonist, commonly causes hypomagnesemia, which may be severe. This prompted the Food and Drug Administration to issue a warning concerning the relationship between severe hypomagnesaemia and cetuximab treatment. The serum Mg^{2+} concentration decreases during cetuximab treatment in most patients (491). In total, 54 % of the treated patients developed hypomagnesaemia, and in 6%, it was severe. Clinically significant hypocalcaemia was rare and not progressive upon treatment. Careful monitoring of serum Mg^{2+} levels is, therefore, essential during treatment.

V. Adaptation of the DCT

The nephron comprises various segments arranged in sequence. This means that when transport by one segment is modified, other segments can be affected secondarily. When NaCl reabsorption along the TAL is inhibited by loop diuretics, the NaCl concentration in fluid that enters the distal tubule is greatly increased. In one study, the Na^+ concentration in fluid entering the distal tubule of rats rose from 42 to 140 mM during acute loop diuretic infusion (203). The increased luminal NaCl concentration drives increased Na^+ absorption along the distal tubule (from 148 to 361 pmol/min) (203) because NaCl transport by the distal tubule is load dependent (as discussed above). This increase insolute reabsorption by segments that lie distal to the site of diuretic action is the first form of diuretic adaptation and limits the intrinsic potency of the diuretic drug. The net effect of acute diuretic administration on urinary Na^+ and Cl^- excretion, therefore, reflects the sum of effects in the diuretic-sensitive segment (inhibition of NaCl reabsorption) and in diuretic-insensitive segments (secondary stimulation of NaCl reabsorption). As the acute effect of a diuretic declines, a period of NaCl retention usually commences. This phenomenon is often termed *postdiuretic NaCl retention*. One mechanism by which diuretic drugs may increase the tendency for NaCl retention directly, without changes in extracellular fluid volume, involves diuretic-induced activation of ion transporters within the diuretic-sensitive nephron segment. Within 60 min of thiazide administration, the number of [^{3}H]metolazone binding sites increases substantially (75). An increase in the number of activated ion transporters at the apical membrane would be expected to increase the transport capacity so that when diuretic concentrations decline, increased Na^+ and Cl^- transport would result. Another mechanism by which diuretic drugs may enhance the tendency to NaCl retention directly involves stimulation of transport pathways in nephron segments that lie distal to the target of diuretic action (segments that are insensitive to the diuretic drug). For example, the number of thiazide-sensitive Na-Cl^+ transporters in the kidney (and presumably in the DCT) increases

within 60 minutes after a loop diuretic has been administered (75). Because thiazide-sensitive transporters are expressed only by nephron segments that do not express loop diuretic- sensitive pathways, the increased number of thiazide- sensitive NCC is believed to result from increases in salt and water delivery to DCT cells.

When delivery to the DCT is increased chronically, DCT cells undergo both hypertrophy and hyperplasia. Infusion of furosemide into rats continuously for 7 days nearly doubled the percentage of the renal cortex occupied by DCT cells (127, 227, 228, 230, 234). Chronic loop diuretic administration increases the Na^+-K+-ATPase activity in the distal convoluted and CCT (429, 538). In one study, chronic furosemide treatment also increased expression of mRNA encoding the thiazide-sensitive NCC, as detected by in situ hybridization (366). In another study, however, mRNA expression of the thiazide-sensitive NCC as well as the ouabain-sensitive Na^+-K^+-ATPase was not affected by chronic furosemide infusion, when detected by Northern analysis merino (336). Distal tubule cells that express high levels of transport proteins and are hypertrophic have a higher Na^+ and Cl^- transport capacity than normal tubules; compared with tubules from normal animals, tubules of animals treated chronically with loop diuretics can absorb Na^+ and Cl^- up to three times more rapidly than control animals (127). It has also been observed that chronic treatment of rats with loop diuretics also results in significant hyperplasia of cells along the distal nephron (299).

The diuretic-induced signals that initiate changes in distal nephron structure and function are poorly understood. Several factors, acting in concert, may contribute, including diuretic-induced increases in Na^+ and Cl^- delivery to distal segments, effects of ECF volume depletion on systemic hormone secretion and renal nerve activity, and local effects on autocrine and paracrine secretion. Increased production of angiotensin II or increased secretion of aldosterone resulting from increases in renin activity may contribute to hypertrophy and hyperplasia. Angiotensin II is a potent mitogen and stimulates NCC activity, as discussed above (423, 426). Aldosterone also promotes growth of responsive tissues under some circumstances kaissling (235); when salt delivery to the collecting duct is increased in the presence of high levels of circulating aldosterone, principal cell hypertrophy develops; when salt delivery is high in the absence of aldosterone secretion, hypertrophy is absent. This indicates that aldosterone plays a permissive role in the development of cellular hypertrophy in this aldosterone- responsive renal epithelium. Although recent experiments suggest that aldosterone does affect ion transport by cells of the DCT, and aldosterone almost certainly contributes to adaptations along the CCT, hypertrophy of DCT cells has been shown to occur during chronic loop diuretic infusion even when changes in circulating mineralocorticoid, glucocorticoid, and vasopressin levels are prevented (234, 469).

One possibility is that cellular ion concentrations regulate epithelial cell growth directly (470). Increases in Na^+ uptake across the apical plasma membrane precede cell growth in the TAL during treatment with antidiuretic hormone (44), in principal cells of the CCT during treatment with mineralocorticoid hormones (227, 386), and in the DCT during treatment with loop diuretics (127, 234). Although the cause of the increased Na^+ uptake varies, changes in the intracellular Na^+ concentration appear to precede growth in each example beck (24). If increased Na^+ entry causes cell growth, then one would expect that blockade of apical Na^+ entry would lead to atrophy of epithelial cells, a prediction supported

by the effects of thiazide treatment of rats to reduce Na^+-K^+-ATPase and Na^+ transport capacity of DCT segments (153, 346). Treatment with thiazide diuretics also causes apotosis and atrophy of DCT1 segments, consistent with an important role for Na^+ entry in regulating DCT cells (300). Regardless of the proximate stimulus for DCT cell growth, DCT cells express insulin-like growth factor 1 IGF-1 and insulin-like receptor binding protein (IGFBP-1), both of which increase during chronic treatment of rats with loop diuretics (249). Although experimental data concerning structural and functional responses of the distal nephron to chronic treatment with diuretic drugs come predominantly from studies employing experimental animals, Loon et al. (304) reported that chronic treatment with loop diuretics in humans enhanced the thiazide-sensitive component of salt transport. The extracellular fluid volume-independent component of NaCl retention that occurs after loop diuretic administration (8) may also reflect changes in distal nephron structure and function. Hypertrophy of the DCT also occurs when NaCl transport is stimulated directly, in the absence of substantial increases in NaCl delivery. Mice in which activation of NCC has been induced by transgenic or knockin expression of mutant WNK4 exhibit signs of NCC overactivity, but also show hypertrophy of DCT cells (265).

Another indication that solute transport is essential for DCT structure and function is the effect of NCC deletion or deficiency. NCC knockout mice exhibit atrophy and underdevelopment of the DCT1 segment (303); the same appearance of atrophic DCT cells was observed in a patient with EAST syndrome, in which DCT function is reduced (37). Similar findings have been reported in mice in which SPAK is disrupted, a situation in which NCC activity is strikingly reduced (177, 326). Together, these data suggest that DCT cells require NaCl throughput to maintain their structure and function, and the induction of such transport is also essential for the development of the DCT1.

Conclusion

The DCT is a relatively short nephron segment that serves several essential and non redundant functions. It transports Na^+ and Cl^- in an electroneurtral manner. This is important during states of ECF volume depletion. Yet NaCl transport along this segment also plays a key role in adjusting the Na^+ delivery to K^+ secretory segments downstream. In this way, the DCT contributes importantly to K^+ homeostasis. This role is reflected in the human diseases that result from DCT dysfunction in which abnormal K^+ homeostasis is often a key manifestation. These include diseases of increased NCC activity, primarily FHHt, and diseases of NCC hypofunction, including Gitelman and EAST syndrome. The DCT also plays a crucial and non redundant role in reabsorbing magnesium, with DCT dysfunction also manifesting at disordered magnesium homeostasis. The DCT2 is a transitional segment, sharing properties of both the DCT1 and the CNT. This segment plays a crucial role in calcium transport; it also includes both electrogenic and electroneurtral Na^+ transport pathways, enabling it to mediate either Na^+/K^+ exchange or NaCl cotransport, depending on physiological need. This segment is regulated by a number of hormones, many of which appear to act via WNK kinases and SPAK/OSR1. Mutations of these signaling molecules also leads to dysfunction of the DCT and to human disease.

References

1. Abdallah JG, Schrier RW, Edelstein C, Jennings SD, Wyse B, Ellison DH. Loop diuretic infusion increases thiazide-sensitive Na(+)/Cl(−)-cotransporter abundance: role of aldosterone. Journal the American Society of Nephrology: JASN. 2001; 12:1335–1341.
2. Achard JM, Warnock DG, Disse-Nicodeme S, Fiquet-Kempf B, Corvol P, Fournier A, Jeunemaitre X. Familial hyperkalemic hypertension: phenotypic analysis in a large family with the WNK1 deletion mutation. AmJMed. 2003; 114:495–498.
3. Ackermann D, Gresko N, Carrel M, Loffing-Cueni D, Habermehl D, Gomez-Sanchez C, Rossier BC, Loffing J. In vivo nuclear translocation of mineralocorticoid and glucocorticoid receptors in rat kidney: differential effect of corticosteroids along the distal tubule. Am J Physiol Renal Physiol. 2010; 299:F1473–1485. [PubMed: 20861076]
4. Adalat S, Woolf AS, Johnstone KA, Wirsing A, Harries LW, Long DA, Hennekam RC, Ledermann SE, Rees L, van't Hoff W, Marks SD, Trompeter RS, Tullus K, Winyard PJ, Cansick J, Mushtaq I, Dhillon HK, Bingham C, Edghill EL, Shroff R, Stanescu H, Ryffel GU, Ellard S, Bockenhauer D. HNF1B mutations associate with hypomagnesemia and renal magnesium wasting. Journal of the American Society of Nephrology: JASN. 2009; 20:1123–1131. [PubMed: 19389850]
5. Ahokas RA, Sun Y, Bhattacharya SK, Gerling IC, Weber KT. Aldosteronism and a proinflammatory vascular phenotype: role of Mg2+, Ca2+, and H2O2 in peripheral blood mononuclear cells. Circulation. 2005; 111:51–57. [PubMed: 15611366]
6. Ali SM, Geisow MJ, Burgoyne RD. A role for calpactin in calcium-dependent exocytosis in adrenal chromaffin cells. Nature. 1989; 340:313–315. [PubMed: 2526299]
7. Almeida AJ, Burg MB. Sodium transport in the rabbit connecting tubule. AmJPhysiol. 1982; 243:F330–F334.
8. Almeshari K, Ahlstrom NG, Capraro FE, Wilcox CS. A volume-independent component to postdiuretic sodium retention in humans. JAmSocNephrol. 1993; 3:1878–1883.
9. Amemiya M, Loffing J, Lotscher M, Kaissling B, Alpern RJ, Moe OW. Expression of NHE-3 the apical membrane of rat renal proximal tubule and thick ascending limb. Kidney international. 1995 Oct.48:1206–1215. [PubMed: 8569082]
10. Amlal H, Petrovic S, Xu J, Wang Z, Sun X, Barone S, Soleimani M. Deletion of the anion exchanger Slc26a4 (pendrin) decreases apical Cl(−)/HCO3(−) exchanger activity and impairs bicarbonate secretion in kidney collecting duct. American journal of physiology Cell physiology. 2010; 299:C33–41. [PubMed: 20375274]
11. Amlal H, Soleimani M. Pendrin as a novel target for diuretic therapy. Cellular physiology and biochemistry: international journal of experimental cellular physiology, biochemistry, and pharmacology. 2011; 28:521–526.
12. Ankorina-Stark I, Haxelmans S, Schlatter E. Receptors for bradykinin and prostaglandin E2 coupled to Ca2+ signalling in rat cortical collecting duct. Cell calcium. 1997; 22:269–275. [PubMed: 9481477]
13. Arroyo JP, Lagnaz D, Ronzaud C, Vazquez N, Ko BS, Moddes L, Ruffieux-Daidie D, Hausel P, Koesters R, Yang B, Stokes JB, Hoover RS, Gamba G, Staub O. Nedd4-2 modulates renal Na+-Cl-cotransporter via the aldosterone-SGK1-Nedd4-2 pathway. Journal of the American Society of Nephrology: JASN. 2011; 22:1707–1719. [PubMed: 21852580]
14. Arroyo JP, Ronzaud C, Lagnaz D, Staub O, Gamba G. Aldosterone paradox: differential regulation of ion transport in distal nephron. Physiology. 2011; 26:115–123. [PubMed: 21487030]
15. Arystarkhova E, Wetzel RK, Asinovski NK, Sweadner KJ. The gamma subunit modulates Na(+) and K(+) affinity of the renal Na, K-ATPase. J Biol Chem. 1999; 274:33183–33185. [PubMed: 10559186]
16. Arystarkhova E, Wetzel RK, Sweadner KJ. Distribution and oligomeric association of splice forms of Na(+)-K(+)-ATPase regulatory gamma-subunit in rat kidney. American journal of physiology Renal physiology. 2002; 282:F393–407. [PubMed: 11832419]
17. Bachmann S, Bostanjoglo M, Schmitt R, Ellison DH. Sodium transport-related proteins in the mammalian distal nephron - distribution, ontogeny and functional aspects. Anatomy and Embryology. 1999; 200:447–468. [PubMed: 10526014]

18. Bachmann S, Velazquez H, Obermuller N, Reilly RF, Moser D, Ellison DH. Expression of the thiazide-sensitive Na-Cl cotransporter by rabbit distal convoluted tubule cells. J Clin Invest. 1995; 96:2510–2514. [PubMed: 7593642]
19. Bailey MA, Giebisch G, Abbiati T, Aronson PS, Gawenis LR, Shull GE, Wang T. NHE2- mediated bicarbonate reabsorption in the distal tubule of NHE3 null mice. The Journal of physiology. 2004; 561:765–775. [PubMed: 15604231]
20. Bandulik S, Schmidt K, Bockenhauer D, Zdebik AA, Humberg E, Kleta R, Warth R, Reichold M. The salt-wasting phenotype of EAST syndrome, a disease with multifaceted symptoms linked to the KCNJ10 K+ channel. Pflugers Archiv: European journal of physiology. 2011; 461:423–435. [PubMed: 21221631]
21. Barone S, Amlal H, Xu J, Soleimani M. Deletion of the Cl-/HCO3- exchanger pendrin downregulates calcium-absorbing proteins in the kidney and causes calcium wasting. Nephrology, dialysis, transplantation: official publication of the European Dialysis and Transplant Association - European Renal Association. 2012; 27:1368–1379.
22. Barratt LJ. The effect of amiloride on the transepithelial potential difference of the distal tubule of the rat kidney. Pflügers Archives. 1976; 361:251–254. [PubMed: 943768]
23. Barton CH, Pahl M, Vaziri ND, Cesario T. Renal magnesium wasting associated with amphotericin B therapy. AmJMed. 1984; 77:471–474.
24. Beck F-X, Dörge A, Giebisch G, Thurau K. Effect of diuretics on cell potassium transport: An electron microprobe study. Kidney Int. 1990; 37:1423–1428. [PubMed: 2163464]
25. Beguin P, Wang X, Firsov D, Puoti A, Claeys D, Horisberger JD, Geering K. The gamma subunit is a specific component of the Na, K-ATPase and modulates its transport function. The EMBO journal. 1997; 16:4250–4260. [PubMed: 9250668]
26. Belge H, Gailly P, Schwaller B, Loffing J, Debaix H, Riveira-Munoz E, Beauwens R, Devogelaer JP, Hoenderop JG, Bindels RJ, Devuyst O. Renal expression of parvalbumin is critical for NaCl handling and response to diuretics. Proceedings of the National Academy of Sciences of the United States of America. 2007; 104:14849–14854. [PubMed: 17804801]
27. Beutler KT, Masilamani S, Turban S, Nielsen J, Brooks HL, Ageloff S, Fenton RA, Packer RK, Knepper MA. Long-term regulation of ENaC expression in kidney by angiotensin II. Hypertension. 2003; 41:1143–1150. [PubMed: 12682079]
28. Bickel CA, Verbalis JG, Knepper MA, Ecelbarger CA. Increased renal Na-K-ATPase, NCC, and beta-ENaC abundance in obese Zucker rats. American journal of physiology Renal physiology. 2001; 281:F639–648. [PubMed: 11553510]
29. Biemesderfer D, Reilly RF, Exner M, Igarashi P, Aronson PS. Immunocytochemical characterization of Na+-H+ exchanger isoform NHE-1 in the rabbit kidney. AmJPhysiol. 1992; 263:F833–F840.
30. Bindels RJ, Hartog A, Abrahamse SL, Van Os CH. Effects of pH on apical calcium entry and active calcium transport in rabbit cortical collecting system. The American journal of physiology. 1994; 266:F620–627. [PubMed: 8184895]
31. Bindels RJ, Ramakers PL, Dempster JA, Hartog A, van Os CH. Role of Na+/Ca2+ exchange in transcellular Ca2+ transport across primary cultures of rabbit kidney collecting system. Pflugers Archiv: European journal of physiology. 1992; 420:566–572. [PubMed: 1614831]
32. Bindels RJ, Timmermans JA, Hartog A, Coers W, van Os CH. Calbindin-D9k and parvalbumin are exclusively located along basolateral membranes in rat distal nephron [published erratum appears in J Am Soc Nephrol 1992 Mar;2(9):1461]. Journal of the American Society of Nephrology: JASN. 1991 Dec.2:1122–1129. [PubMed: 1777592]
33. Bindels RJM, van Os CH, Slegers JFG. Effects of chlorothiazide, furosemide and PTH on Na+ and Ca2+ handling in isolated perfused kidneys of the spontaneously hypertensive rat. ClinExpHypertension. 1987; A9:33–50.
34. Blachley JD, Hill JB. Renal and electrolyte disturbances associated with cisplatin. AnnInternMed. 1981; 95:628–632.
35. Blakely P, Vaughn DA, Fanestil DD. Amylin, calcitonin gene-related peptide and adrenomedullin: effects on renal thiazide receptor. AmJPhysio. 1997; 272:F410–F415.

36. Blumberg D, Bonetti A, Jacomella V, Capillo S, Truttmann AC, Luthy CM, Colombo JP, Bianchetti MG. Free circulating magnesium and renal magnesium handling during acute metabolic acidosis in humans. American journal of nephrology. 1998; 18:233–236. [PubMed: 9627040]
37. Bockenhauer D, Feather S, Stanescu HC, Bandulik S, Zdebik AA, Reichold M, Tobin J, Lieberer E, Sterner C, Landoure G, Arora R, Sirimanna T, Thompson D, Cross JH, van't Hoff W, Al Masri O, Tullus K, Yeung S, Anikster Y, Klootwijk E, Hubank M, Dillon MJ, Heitzmann D, Arcos-Burgos M, Knepper MA, Dobbie A, Gahl WA, Warth R, Sheridan E, Kleta R. Epilepsy, ataxia, sensorineural deafness, tubulopathy, and KCNJ10 mutations. The New England journal of medicine. 2009; 360:1960–1970. [PubMed: 19420365]
38. Boettger T, Hubner CA, Maier H, Rust MB, Beck FX, Jentsch TJ. Deafness and renal tubular acidosis in mice lacking the K-Cl co-transporter Kcc4. Nature. 2002; 416:874–878. [PubMed: 11976689]
39. Bomsztyk K, George JP, Wright FS. Effects of luminal fluid anions on calcium transport by proximal tubule. AmJPhysiol. 1984; 246:F600–F608.
40. Bonny O, Edwards A. Calcium reabsorption in the distal tubule: regulation by sodium, pH, and flow. American journal of physiology Renal physiology. 2013; 304:F585–600. [PubMed: 23152295]
41. Boros S, Bindels RJ, Hoenderop JG. Active Ca(2+) reabsorption in the connecting tubule. Pflugers Archiv: European journal of physiology. 2009; 458:99–109. [PubMed: 18989697]
42. Boros S, Xi Q, Dimke H, van der Kemp AW, Tudpor K, Verkaart S, Lee KP, Bindels RJ, Hoenderop JG. Tissue transglutaminase inhibits the TRPV5-dependent calcium transport in an N-glycosylation-dependent manner. Cellular and molecular life sciences: CMLS. 2012; 69:981–992. [PubMed: 21952826]
43. Bostanjoglo M, Reeves WB, Reilly RF, Velazquez H, Robertson N, Litwack G, Morsing P, Dorup J, Bachmann S, Ellison DH. 11Beta-hydroxysteroid dehydrogenase, mineralocorticoid receptor, and thiazide-sensitive Na-Cl cotransporter expression by distal tubules. Journal of the American Society of Nephrology: JASN. 1998; 9:1347–1358. [PubMed: 9697656]
44. Bouby N, Bankir L, Trinh-Trang-Tan MM, Minuth WW, Kriz W. Selective ADH-induced hypertrophy of the medullary thick ascending limb in Brattleboro rats. Kidney Int. 1985; 28:456–466. [PubMed: 4068480]
45. Bouhtiauy I, Lajeunesse D, Brunette MG. The mechanism of parathyroid hormone action on calcium reabsorption by the distal tubule. Endocrinology. 1991; 128:251–258. [PubMed: 1846100]
46. Boyden LM, Choi M, Choate KA, Nelson-Williams CJ, Farhi A, Toka HR, Tikhonova IR, Bjornson R, Mane SM, Colussi G, Lebel M, Gordon RD, Semmekrot BA, Poujol A, Valimaki MJ, De Ferrari ME, Sanjad SA, Gutkin M, Karet FE, Tucci JR, Stockigt JR, Keppler-Noreuil KM, Porter CC, Anand SK, Whiteford ML, Davis ID, Dewar SB, Bettinelli A, Fadrowski JJ, Belsha CW, Hunley TE, Nelson RD, Trachtman H, Cole TR, Pinsk M, Bockenhauer D, Shenoy M, Vaidyanathan P, Foreman JW, Rasoulpour M, Thameem F, Al-Shahrouri HZ, Radhakrishnan J, Gharavi AG, Goilav B, Lifton RP. Mutations in kelch-like 3 and cullin 3 cause hypertension and electrolyte abnormalities. Nature. 2012; 482:98–102. [PubMed: 22266938]
47. Brenner R, Chen QH, Vilaythong A, Toney GM, Noebels JL, Aldrich RW. BK channel beta4 subunit reduces dentate gyrus excitability and protects against temporal lobe seizures. Nature neuroscience. 2005; 8:1752–1759. [PubMed: 16261134]
48. Breslau N, Moses AM, Weiner IM. The role of volume contraction in the hypocalciuric action of chlorothiazide. Kidney international. 1976; 10:164–170. [PubMed: 966453]
49. Brickman AS, Massry SG, Coburn JW. changes in serum and urinary calcium during treatment with hydrochlorothiazide: studies on mechanisms. J Clin Invest. 1972; 51:945–954. [PubMed: 4552338]
50. Brini M, Cali T, Ottolini D, Carafoli E. The plasma membrane calcium pump in health and disease. FEBS J. 2013; 280:5385–5397. [PubMed: 23413890]
51. Brooks HL, Allred AJ, Beutler KT, Coffman TM, Knepper MA. Targeted proteomic profiling of renal Na(+) transporter and channel abundances in angiotensin II type 1a receptor knockout mice. Hypertension. 2002 Feb.39:470–473. [PubMed: 11882592]

52. Busch AE, Suessbrich H, Kunzelmann K, Hipper A, Greger R, Waldegger, Mutschler E, Lindemann B, Lang F. Blockade of epithelial Na+ channels by triamterene-underlying mechanisms and molecular basis. Pflügers Arch. 1996; 432:760–766. [PubMed: 8772124]

53. Cai H, Cebotaru V, Wang YH, Zhang XM, Cebotaru L, Guggino SE, Guggino WB. WNK4 kinase regulates surface expression of the human sodium chloride cotransporter in mammalian cells. Kidney Int. 2006; 69:2162–2170. [PubMed: 16688122]

54. Cairo ER, Friedrich T, Swarts HG, Knoers NV, Bindels RJ, Monnens LA, Willems PH, De Pont JJ, Koenderink JB. Impaired routing of wild type FXYD2 after oligomerisation with FXYD2-G41R might explain the dominant nature of renal hypomagnesemia. Biochimica et biophysica acta. 2008; 1778:398–404. [PubMed: 17980699]

55. Campean V, Kricke J, Ellison D, Luft FC, Bachmann S. Localization of thiazide-sensitive Na(+)-Cl(−) cotransport and associated gene products in mouse DCT. American journal of physiology Renal physiology. 2001; 281:F1028–1035. [PubMed: 11704553]

56. Canalis E, Mazziotti G, Giustina A, Bilezikian JP. Glucocorticoid-induced osteoporosis: pathophysiology and therapy. Osteoporosis international: a journal established as result of cooperation between the European Foundation for Osteoporosis and the National Osteoporosis Foundation of the USA. 2007; 18:1319–1328.

57. Cao G, Lee KP, van der Wijst J, de Graaf M, van der Kemp A, Bindels RJ, Hoenderop JG. Methionine sulfoxide reductase B1 (MsrB1) recovers TRPM6 channel activity during oxidative stress. J Biol Chem. 2010; 285:26081–26087. [PubMed: 20584906]

58. Cao G, Thebault S, van der Wijst J, van der Kemp A, Lasonder E, Bindels RJ, Hoenderop JG. RACK1 inhibits TRPM6 activity via phosphorylation of the fused alpha-kinase domain. Current biology: CB. 2008; 18:168–176. [PubMed: 18258429]

59. Cao G, van der Wijst J, van der Kemp A, van Zeeland F, Bindels RJ, Hoenderop JG. Regulation of the epithelial Mg2+ channel TRPM6 by estrogen and the associated repressor protein of estrogen receptor activity (REA). J Biol Chem. 2009; 284:14788–14795. [PubMed: 19329436]

60. Carrisoza R, Salvador C, Bobadilla NA, Trujillo J, Escobar LI. Expression and immunolocalization of ERG1 potassium channels in the rat kidney. Histochemistry and cell biology. 2010; 133:189–199. [PubMed: 19921238]

61. Cassola AC, Giebisch G, Wang W. Vasopressin increases density of apical low-conductance K+ channels in rat CCD. The American journal of physiology. 1993; 264:F502–509. [PubMed: 7681263]

62. Castaneda-Bueno M, Cervantes-Perez LG, Vazquez N, Uribe N, Kantesaria S, Morla L, Bobadilla NA, Doucet A, Alessi DR, Gamba G. Activation of the renal Na+:Cl- cotransporter by angiotensin II is a WNK4-dependent process. Proceedings of the National Academy of Sciences of the United States of America. 2012; 109:7929–7934. [PubMed: 22550170]

63. Cha SK, Hu MC, Kurosu H, Kuro-o M, Moe O, Huang CL. Regulation of renal outer medullary potassium channel and renal K(+) excretion by Klotho. Molecular pharmacology. 2009; 76:38–46. [PubMed: 19349416]

64. Cha SK, Huang CL. WNK4 kinase stimulates caveola-mediated endocytosis of TRPV5 amplifying the dynamic range of regulation of the channel by protein kinase C. J Biol Chem. 2010; 285:6604–6611. [PubMed: 20061383]

65. Cha SK, Ortega B, Kurosu H, Rosenblatt KP, Kuro OM, Huang CL. Removal of sialic acid involving Klotho causes cell-surface retention of TRPV5 channel via binding to galectin-1. Proceedings of the National Academy of Sciences of the United States of America. 2008; 105:9805–9810. [PubMed: 18606998]

66. Cha SK, Wu T, Huang CL. Protein kinase C inhibits caveolae-mediated endocytosis of TRPV5. Am J Physiol Renal Physiol. 2008; 294:F1212–1221. [PubMed: 18305097]

67. Chadha V, Alon US. Hereditary renal tubular disorders. Semin Nephrol. 2009; 29:399–411. [PubMed: 19615561]

68. Chambrey R, Warnock DG, Podevin RA, Bruneval P, Mandet C, Belair MF, Bariety J, Paillard M. Immunolocalization of the Na+/H+ exchanger isoform NHE2 in rat kidney. The American journal of physiology. 1998 Sep.275:F379–386. [PubMed: 9729510]

69. Chang H, Fujita T. A kinetic model of the thiazide-sensitive Na-Cl cotransporter. The American journal of physiology. 1999; 276:F952–959. [PubMed: 10362783]
70. Chang H, Fujita T. A kinetic model of the thiazide-sensitive Na-Cl cotransporter. AmJPhysiol. 1999; 276
71. Chang H, Fujita T. A numerical model of the renal distal tubule. The American journal of physiology. 1999; 276:F931–951. [PubMed: 10362782]
72. Chang Q, Hoefs S, van der Kemp AW, Topala CN, Bindels RJ, Hoenderop JG. The beta-glucuronidase klotho hydrolyzes and activates the TRPV5 channel. Science. 2005; 310:490–493. [PubMed: 16239475]
73. Chavez-Canales M, Arroyo JP, Ko B, Vazquez N, Bautista R, Castaneda-Bueno M, Bobadilla NA, Hoover RS, Gamba G. Insulin increases the functional activity of the renal NaCl cotransporter. Journal of hypertension. 2013; 31:303–311. [PubMed: 23303355]
74. Chen Z, Vaughn DA, Blakeley P, Fanestil DD. Adrenocortical steroids increase renal thiazide diuretic receptor density and response. JAmSocNephrol. 1994; 5:1361–1368.
75. Chen ZF, Vaughn DA, Beaumont K, Fanestil DD. Effects of diuretic treatment and of dietary sodium on renal binding of 3H-metolazone. JAmSocNephrol. 1990; 1:91–98.
76. Cheng CJ, Shiang JC, Hsu YJ, Yang SS, Lin SH. Hypocalciuria in patients with Gitelman syndrome: role of blood volume. American journal of kidney diseases: the official journal of the National Kidney Foundation. 2007; 49:693–700. [PubMed: 17472852]
77. Cheng CJ, Truong T, Baum M, Huang CL. Kidney-specific WNK1 inhibits sodium reabsorption in the cortical thick ascending limb. American journal of physiology Renal physiology. 2012; 303:F667–673. [PubMed: 22791335]
78. Chiga M, Rai T, Yang SS, Ohta A, Takizawa T, Sasaki S, Uchida S. Dietary salt regulates the phosphorylation of OSR1/SPAK kinases and the sodium chloride cotransporter through aldosterone. Kidney Int. 2008; 74:1403–1409. [PubMed: 18800028]
79. Choate KA, Kahle KT, Wilson FH, Nelson-Williams C, Lifton RP. WNK1, a kinase mutated in inherited hypertension with hyperkalemia, localizes to diverse Cl- -transporting epithelia. Proc Natl Acad Sci U S A. 2003; 100:663–668. [PubMed: 12522152]
80. Choi MJ, Fernandez PC, Coupaye-Gerard B, D'Andrea DD, Szerlip H, Kleyman TR. Brief Report: Trimethoprim-induced hyperkalemia in a patient with AIDS. NEnglJMed. 1993; 328:703–706.
81. Chowdhury JA, Liu CH, Zuber AM, O'Shaughnessy KM. An inducible transgenic mouse model for familial hypertension with hyperkalaemia (Gordon's syndrome or pseudohypoaldosteronism type II). Clinical science. 2013; 124:701–708. [PubMed: 23336180]
82. Clapp JR, Rector FC Jr, Seldin DW. Effect of unreabsorbed anions on proximal and distal transtubular potentials in rats. The American journal of physiology. 1962; 202:781–786. [PubMed: 13879653]
83. Clark K, Middelbeek J, Morrice NA, Figdor CG, Lasonder E, van Leeuwen FN. Massive autophosphorylation of the Ser/Thr-rich domain controls protein kinase activity of TRPM6 and TRPM7. PloS one. 2008; 3:e1876. [PubMed: 18365021]
84. Coleman RA, Knepper MA, Wade JB. Rat renal connecting cells express AQP2. JAmSocNephrol. 1997:16A.
85. Coleman RA, Wu DC, Liu J, Wade JB. Expression of aquaporins in the renal connecting tubule. Am J Physiol Renal Physiol. 2000; 279:F874–883. [PubMed: 11053048]
86. Cope G, Murthy M, Golbang AP, Hamad A, Liu CH, Cuthbert AW, O'Shaughnessy KM. WNK1 affects surface expression of the ROMK potassium channel independent of WNK4. Journal of the American Society of Nephrology: JASN. 2006; 17:1867–1874. [PubMed: 16775035]
87. Costanzo LS. Comparison of calcium and sodium transport in early and late rat distal tubules: effect of amiloride. The American journal of physiology. 1984; 246:F937–F945. [PubMed: 6742137]
88. Costanzo LS, Weiner IM. On the hypocalciuric action of chlorothiazide. J Clin Invest. 1974; 54:628–637. [PubMed: 4853451]
89. Costanzo LS, Windhager EE. Calcium and sodium transport by the distal convoluted tubule of the rat. The American journal of physiology. 1978; 235:F492–F506. [PubMed: 727266]

90. Costanzo, LS., Windhager, EE. Renal regulation of calcium balance. In: Seldin, DW., Giebisch, G., editors. The Kidney: Physiology and Pathophysiology. New York: Raven Press, Ltd; 1992. p. 2375-2393.

91. Crayen ML, Thoenes W. Architecture and cell structures in the distal nephron of the rat kidney. Cytobiologie. 1978; 17:197–211. [PubMed: 689251]

92. Cruz DN, Simon DB, Nelson-Williams C, Farhi A, Finberg K, Burleson L, Gill JR, Lifton RP. Mutations in the Na-Cl cotransporter reduce blood pressure in humans. Hypertension. 2001; 37:1458–1464. [PubMed: 11408395]

93. Dai LJ, Friedman PA, Quamme GA. Acid-base changes alter Mg2+ uptake in mouse distal convoluted tubule cells. The American journal of physiology. 1997; 272:F759–766. [PubMed: 9227637]

94. Davis RH, Morgan DB, Rivlin RS. The excretion of calcium in the urine and its relation to calcium intake, sex and age. Clin Sci. 1970; 39:1–12. [PubMed: 5448164]

95. De Bermudez L, Windhager EE. Osmotically induced changes in electrical resistance of distal tubules of rat kidney. AmJPhysiol. 1975; 229:1536–1546.

96. de Groot T, Kovalevskaya NV, Verkaart S, Schilderink N, Felici M, van der Hagen EA, Bindels RJ, Vuister GW, Hoenderop JG. Molecular mechanisms of calmodulin action on TRPV5 and modulation by parathyroid hormone. Molecular and cellular biology. 2011; 31:2845–2853. [PubMed: 21576356]

97. de Groot T, Lee K, Langeslag M, Xi Q, Jalink K, Bindels RJ, Hoenderop JG. Parathyroid hormone activates TRPV5 via PKA-dependent phosphorylation. J Am Soc Nephrol. 2009; 20:1693–1704. [PubMed: 19423690]

98. de Groot T, Verkaart S, Xi Q, Bindels RJ, Hoenderop JG. The identification of Histidine 712 as a critical residue for constitutive TRPV5 internalization. J Biol Chem. 2010; 285:28481–28487. [PubMed: 20628046]

99. De Jong JC, Van Der Vliet WA, Van Den Heuvel LP, Willems PH, Knoers NV, Bindels RJ. Functional Expression of Mutations in the Human NaCl Cotransporter: Evidence for Impaired Routing Mechanisms in Gitelman's Syndrome. Journal of the American Society of Nephrology: JASN. 2002 Jun.13:1442–1448. [PubMed: 12039972]

100. Delaloy C, Lu J, Houot AM, Disse-Nicodeme S, Gasc JM, Corvol P, Jeunemaitre X. Multiple promoters in the WNK1 gene: one controls expression of a kidney-specific kinase-defective isoform. Mol Cell Biol. 2003; 23:9208–9221. [PubMed: 14645531]

101. den Dekker E, Hoenderop JG, Nilius B, Bindels RJ. The epithelial calcium channels, TRPV5 & TRPV6: from identification towards regulation. Cell Calcium. 2003; 33:497–507. [PubMed: 12765695]

102. Diezi J, Nenniger M, Giebisch G. Distal Tubular function in superficial rat tubules during volume expansion. AmJPhysiol. 1980; 239:F228–F232.

103. Dimke H, Hoenderop JG, Bindels RJ. Molecular basis of epithelial Ca2+ and Mg2+ transport: insights from the TRP channel family. The Journal of physiology. 2011; 589:1535–1542. [PubMed: 21041532]

104. Dorup J. Ultrastructure of three-dimensionally localized distal nephron segments in superficial cortex of the rat kidney. Journal of ultrastructure and molecular structure research. 1988; 99:169–187. [PubMed: 3171250]

105. Dorup J. Ultrastructure of three-dimensionally localized distal nephron segments in superficial cortex of the rat kidney. Journal of ultrastructure and molecular structure research. 1988; 99:169–187. [PubMed: 3171250]

106. Dorup J, Morsing P, Rasch R. Tubule-tubule and tubule-arteriole contacts in rat kidney distal nephrons: A morphologic study based on computer-assisted three-dimensional reconstructions. LabInvest. 1992; 67:761–769.

107. Doucet A. Function and control of Na-K-ATPase in single nephron segments of the mammalian kidney. Kidney Int. 1988; 34:749–760. [PubMed: 2850394]

108. Doucet A, Katz AI. Mineralocorticoid receptors along the nephron: [3H]aldosterone binding in rabbit tubules. AmJPhysiol. 1981; 241:F605–F611.

109. Duc C, Farman N, Canessa CM, Bonvalet J-P, Rossier BC. Cell-specific expression of epithelial sodium channel a, b, and g subunits in aldosterone-responsive epithelia from the rat: Localization by in situ hybridization and immunocytochemistry. JCell Biol. 1994; 127:1907–1921. [PubMed: 7806569]
110. Dunbar DR, Khaled H, Evans LC, Al-Dujaili EA, Mullins LJ, Mullins JJ, Kenyon CJ, Bailey MA. Transcriptional and physiological responses to chronic ACTH treatment by the mouse kidney. Physiological genomics. 2010; 40:158–166. [PubMed: 19920212]
111. Dunbar LA, Caplan MJ. Ion pumps in polarized cells: sorting and regulation of the Na+, K+- and H+, K+-ATPases. The Journal of biological chemistry. 2001; 276:29617–29620. [PubMed: 11404365]
112. Earley LE, Martino JA. Influence of sodium balance on the ability of diuretics to inhibit tubular reabsorption: A study of factors that influence renal tubular sodium reabsorption in man. Circulation. 1970; 42:323–334. [PubMed: 5431928]
113. Ecelbarger CA, Kim GH, Terris J, Masilamani S, Mitchell C, Reyes I, Verbalis JG, Knepper MA. Vasopressin-mediated regulation of epithelial sodium channel abundance in rat kidney. Am J Physiol Renal Physiol. 2000; 279:F46–53. [PubMed: 10894786]
114. Ecelbarger CA, Knepper MA, Verbalis JG. Increased abundance of distal sodium transporters in rat kidney during vasopressin escape. J Am Soc Nephrol. 2001; 12:207–217. [PubMed: 11158210]
115. Eckers A, Klotz LO. Heavy metal ion-induced insulin-mimetic signaling. Redox report: communications in free radical research. 2009; 14:141–146. [PubMed: 19695120]
116. Eknoyan G, Suki WN, Martinez-Maldonado M. Effect of diuretics on urinary excretion of phosphate, calcium, and magnesium in thyroparathyroidectomized dogs. JLabClinMed. 1970; 76:257–266.
117. El Mernissi G, Doucet A. Specific activity of Na-K-ATPase after adrenalectomy and hormone replacement along the rabbit nephron. Pflügers Arch. 1984; 402:258–263. [PubMed: 6097867]
118. Ellison DH. Adaptation in Gitelman syndrome: “we just want to pump you up”. Clinical journal of the American Society of Nephrology: CJASN. 2012; 7:379–382. [PubMed: 22344514]
119. Ellison DH. Divalent cation transport by the distal nephron: insights from Bartter’s and Gitelman’s syndromes. American journal of physiology Renal physiology. 2000; 279:F616–625. [PubMed: 10997911]
120. Ellison DH. Renal magnification by EGF. Nephrology, dialysis, transplantation: official publication of the European Dialysis and Transplant Association - European Renal Association. 2008; 23:1497–1499.
121. Ellison DH. The voltage-gated K+ channel subunit Kv1.1 links kidney and brain. J Clin Invest. 2009; 119:763–766. [PubMed: 19348045]
122. Ellison DH, Bostonjoglo M, Bachmann S, Reilly RF. Expression of calcium transport proteins by mammalian distal tubule. FASEB J. 1998
123. Ellison, DH., Hoorn, EJ., Wilcox, CS. Diuretics. In: Taal, MW.Chertow, GM.Marsden, PA.Skorecki, K.Yu, AS., Brenner, BM., editors. Brenner and Rector’s The Kidney. Philadelphia: Elsevier; 2012. p. 1879-1916.
124. Ellison DH, Loffing J. Thiazide effects and adverse effects: insights from molecular genetics. Hypertension. 2009; 54:196–202. [PubMed: 19564550]
125. Ellison DH, Reilly RF, Obermüller N, Canessa C, Bachmann S. Molecular localization of Na and Ca transport pathways along the renal distal tubule. J Am Soc Nephrol. 1995:947.
126. Ellison DH, Velazquez H, Wright FS. Adaptation of the distal convoluted tubule of the rat. Structural and functional effects of dietary salt intake and chronic diuretic infusion. J Clin Invest. 1989; 83:113–126. [PubMed: 2910903]
127. Ellison DH, Velazquez H, Wright FS. Adaptation of the distal convoluted tubule of the rat. Structural and functional effects of dietary salt intake and chronic diuretic infusion. J Clin Invest. 1989; 83:113–126. [PubMed: 2910903]
128. Ellison DH, Velazquez H, Wright FS. Stimulation of distal potassium secretion by low lumen chloride in the presence of barium. The American journal of physiology. 1985; 248:F638–649. [PubMed: 3993787]

129. Ellison DH, Velazquez H, Wright FS. Thiazide-sensitive sodium chloride cotransport in early distal tubule. The American journal of physiology. 1987; 253:F546–554. [PubMed: 3631283]

130. Fanestil DD, Vaughn DA, Blakely P. Dietary NaCl and KCl do not regulate renal density of the thiazide diuretic receptor. AmJPhysiol. 1997; 273:R1241–R1245.

131. Fanestil DD, Vaughn DA, Blakely P. Metabolic acid-base influences on renal thiazide receptor density. The American journal of physiology. 1997 Jun.272:R2004–2008. [PubMed: 9227621]

132. Fang L, Garuti R, Kim BY, Wade JB, Welling PA. The ARH adaptor protein regulates endocytosis of the ROMK potassium secretory channel in mouse kidney. J Clin Invest. 2009; 119:3278–3289. [PubMed: 19841541]

133. Faresse N, Lagnaz D, Debonneville A, Ismailji A, Maillard M, Fejes-Toth G, Naray-Fejes-Toth A, Staub O. Inducible kidney-specific Sgk1 knockout mice show a salt-losing phenotype. Am J Physiol Renal Physiol. 2012; 302:F977–985. [PubMed: 22301619]

134. Faresse N, Lagnaz D, Debonneville A, Ismailji A, Maillard M, Fejes-Toth G, Naray-Fejes-Toth A, Staub O. Inducible kidney-specific Sgk1 knockout mice show a salt-losing phenotype. American journal of physiology Renal physiology. 2012; 302:F977–985. [PubMed: 22301619]

135. Farman N. Steroid receptors: distribution along the nephron. Seminars in Nephrology. 1992; 12:12–17. [PubMed: 1312740]

136. Farman N, Bonvalet JP. Aldosterone binding in isolated tubules. III. Autoradiography along the rat nephron. The American journal of physiology. 1983; 245:F606–614. [PubMed: 6227254]

137. Farman N, Pradelles P, Bonvalet JP. Binding of aldosterone metabolites in isolated tubular segments. AmJPhysiol. 1985; 249:F923–F932.

138. Favre GA, Nau V, Kolb I, Vargas-Poussou R, Hannedouche T, Moulin B. Localization of tubular adaptation to renal sodium loss in Gitelman syndrome. Clinical journal of the American Society of Nephrology: CJASN. 2012; 7:472–478. [PubMed: 22241817]

139. Fejes-Toth G, Frindt G, Naray-Fejes-Toth A, Palmer LG. Epithelial Na+ channel activation and processing in mice lacking SGK1. Am J Physiol Renal Physiol. 2008; 294:F1298–1305. [PubMed: 18385268]

140. Fernandez PC, Puschett JB. Proximal tubular actions of metolazone and chlorothiazide. AmJPhysiol. 1973; 225:954–961.

141. Field MJ, Stanton BA, Giebisch G. Differential acute effects of aldosterone, dexamethasone, and hyperkalemia on distal tubule potassium secretion in the rat kidney. JClinInvest. 1984; 74:1792–1802.

142. Field MJ, Stanton BA, Giebisch GH. Influence of ADH on renal potassium handling: a micropuncture and microperfusion study. Kidney international. 1984 Mar.25:502–511. [PubMed: 6737842]

143. Figueroa CD, Gonzalez CB, Grigoriev S, Abd Alla SA, Haasemann M, Jarnagin K, Muller-Esterl W. Probing for the bradykinin B2 receptor in rat kidney by anti-peptide and anti-ligand antibodies. The journal of histochemistry and cytochemistry: official journal of the Histochemistry Society. 1995; 43:137–148. [PubMed: 7822771]

144. Fonfria E, Marshall IC, Benham CD, Boyfield I, Brown JD, Hill K, Hughes JP, Skaper SD, McNulty S. TRPM2 channel opening in response to oxidative stress is dependent on activation of poly(ADP-ribose) polymerase. British journal of pharmacology. 2004; 143:186–192. [PubMed: 15302683]

145. Frindt G, Palmer LG. Effects of dietary K on cell-surface expression of renal ion channels and transporters. American journal of physiology Renal physiology. 2010; 299:F890–897. [PubMed: 20702602]

146. Frindt G, Palmer LG. Surface expression of sodium channels and transporters in rat kidney: effects of dietary sodium. Am J Physiol Renal Physiol. 2009; 297:F1249–1255. [PubMed: 19741015]

147. Fudge NJ, Kovacs CS. Physiological studies in heterozygous calcium sensing receptor (CaSR) gene-ablated mice confirm that the CaSR regulates calcitonin release in vivo. BMC physiology. 2004; 4:5. [PubMed: 15099400]

148. Furgeson SB, Linas S. Mechanisms of Type I and Type II Pseudohypoaldosteronism. Journal of the American Society of Nephrology: JASN. 2010

149. Gamba G. Molecular physiology and pathophysiology of electroneutral cation-chloride cotransporters. Physiol Rev. 2005; 85:423–493. [PubMed: 15788703]

150. Gamba G, Miyanoshita A, Lombardi M, Lytton J, Lee WS, Hediger MA, Hebert SC. Molecular cloning, primary structure, and characterization of two members of the mammalian electroneutral sodium-(potassium)-chloride cotransporter family expressed in kidney. The Journal of biological chemistry. 1994; 269:17713–17722. [PubMed: 8021284]

151. Gamba G, Saltzberg SN, Lombardi M, Miyanoshita A, Lytton J, Hediger MA, Brenner BM, Hebert SC. Primary structure and functional expression of a cDNA encoding the thiazide-sensitive, electroneutral sodium-chloride cotransporter. ProcNatlAcadSciU S A. 1993; 90:2749–2753.

152. Garg LC, Knepper MA, Burg MB. Mineralocorticoid effects on Na-K-ATPase in individual nephron segments. AmJPhysiol. 1981; 240:F536–F544.

153. Garg LC, Narang N. Effects of hydrochlorothiazide on Na-K-ATPase activity along the rat nephron. Kidney Int. 1987; 31:918–922. [PubMed: 3035268]

154. Garty H, Karlish SJ. Role of FXYD proteins in ion transport. Annual review of physiology. 2006; 68:431–459.

155. Gerke V, Moss SE. Annexins: from structure to function. Physiol Rev. 2002; 82:331–371. [PubMed: 11917092]

156. Geven W, Willems J, Monnens L. Primary hypomagnesemia with a probable double magnesium transport defect. Nephron. 1990; 55:91. [PubMed: 2352584]

157. Giebisch G, Wang W. Renal tubule potassium channels: function, regulation and structure. Acta physiologica Scandinavica. 2000; 170:153–173. [PubMed: 11114953]

158. Giebisch G, Wang WH. Potassium transport: From clearance to channels and pumps. Kidney Int. 1996; 49:1624–1631. [PubMed: 8743466]

159. Gimenez I, Forbush B. Short-term stimulation of the renal Na-K-Cl cotransporter (NKCC2) by vasopressin involves phosphorylation and membrane translocation of the protein. The Journal of biological chemistry. 2003; 278:26946–26951. [PubMed: 12732642]

160. Gkika D, Hsu YJ, van der Kemp AW, Christakos S, Bindels RJ, Hoenderop JG. Critical role of the epithelial Ca2+ channel TRPV5 in active Ca2+ reabsorption as revealed by TRPV5/calbindin-D28K knockout mice. J Am Soc Nephrol. 2006; 17:3020–3027. [PubMed: 17005931]

161. Gkika D, Mahieu F, Nilius B, Hoenderop JG, Bindels RJ. 80K-H as a new Ca2+ sensor regulating the activity of the epithelial Ca2+ channel transient receptor potential cation channel V5 (TRPV5). J Biol Chem. 2004; 279:26351–26357. [PubMed: 15100231]

162. Gkika D, Topala CN, Chang Q, Picard N, Thebault S, Houillier P, Hoenderop JG, Bindels RJ. Tissue kallikrein stimulates Ca(2+) reabsorption via PKC-dependent plasma membrane accumulation of TRPV5. The EMBO journal. 2006; 25:4707–4716. [PubMed: 17006539]

163. Glaudemans B, Knoers NV, Hoenderop JG, Bindels RJ. New molecular players facilitating Mg(2+) reabsorption in the distal convoluted tubule. Kidney international. 2010; 77:17–22. [PubMed: 19812536]

164. Glaudemans B, van der Wijst J, Scola RH, Lorenzoni PJ, Franke B, van der Kemp AW, Knoers NV, Hoenderop JG, Bindels RJ. A missense mutation in KCNA1 encoding the voltage-gated potassium channel Kv1.1 causes autosomal dominant hypomagnesemia. J Clin Invest. 2009; 119

165. Golbang AP, Cope G, Hamad A, Murthy M, Liu CH, Cuthbert AW, O'Shaughnessy KM. Regulation of the Expression of the Na/Cl cotransporter (NCCT) by WNK4 and WNK1: evidence that accelerated dynamin-dependent endocytosis is not involved. Am J Physiol Renal Physiol. 2006; 291:F1369–1376. [PubMed: 16788137]

166. Golbang AP, Murthy M, Hamad A, Liu CH, Cope G, Van't Hoff W, Cuthbert A, O'Shaughnessy KM. A new kindred with pseudohypoaldosteronism type II and a novel mutation (564D>H) in the acidic motif of the WNK4 gene. Hypertension. 2005; 46:295–300. [PubMed: 15998707]

167. Gonzalez-Villalobos RA, Janjoulia T, Fletcher NK, Giani JF, Nguyen MT, Riquier-Brison AD, Seth DM, Fuchs S, Eladari D, Picard N, Bachmann S, Delpire E, Peti-Peterdi J, Navar LG, Bernstein KE, McDonough AA. The absence of intrarenal ACE protects against hypertension. J Clin Invest. 2013; 123:2011–2023. [PubMed: 23619363]

168. Good DW, Velázquez H, Wright FS. Luminal influences on potassium secretion: low sodium concentration. AmJPhysiol. 1984; 246:F609–F619.

169. Good DW, Wright FS. Luminal influences on potassium secretion: sodium concentration and fluid flow rate. AmJPhysiol. 1979; 236:F192–F205.

170. Goodwin KD, Ahokas RA, Bhattacharya SK, Sun Y, Gerling IC, Weber KT. Preventing oxidative stress in rats with aldosteronism by calcitriol and dietary calcium and magnesium supplements. The American journal of the medical sciences. 2006; 332:73–78. [PubMed: 16909053]

171. Gottschalk CW, Mylle M. Micropuncture study of the mammalian urinary concentrating mechanism: evidence for the countercurrent hypothesis. AmJPhysiol. 1959; 196:927–936.

172. Greenberg S, Reiser IW, Chou S-Y, Porush JG. Trimethoprim-sulfamethoxazole induces reversible hyperkalemia. AnnInternMed. 1993; 119:291–295.

173. Greger R, Lang F, Oberleithner H. Distal site of calcium reabsorption in the rat nephron. Pflugers Archiv: European journal of physiology. 1978 May 18.374:153–157. [PubMed: 566424]

174. Griffiths NM, Brick-Ghannam C, Siaume-Perez S, Chabardes D. Effect of prostaglandin E2 on agonist-stimulated cAMP accumulation in the distal convoluted tubule isolated from the rabbit kidney. Pflugers Archiv: European journal of physiology. 1993; 422:577–584. [PubMed: 7682323]

175. Grimm PR, Foutz RM, Brenner R, Sansom SC. Identification and localization of BK-beta subunits in the distal nephron of the mouse kidney. Am J Physiol Renal Physiol. 2007; 293:F350–359. [PubMed: 17459953]

176. Grimm PR, Taneja TK, Liu J, Coleman R, Chen YY, Delpire E, Wade JB, Welling PA. SPAK isoforms and OSR1 regulate sodium-chloride co-transporters in a nephron-specific manner. J Biol Chem. 2012; 287:37673–37690. [PubMed: 22977235]

177. Grimm PR, Taneja TK, Liu J, Coleman R, Chen YY, Delpire E, Wade JB, Welling PA. SPAK isoforms and OSR1 regulate sodium-chloride co-transporters in a nephron-specific manner. The Journal of biological chemistry. 2012; 287:37673–37690. [PubMed: 22977235]

178. Groenestege WM, Hoenderop JG, van den Heuvel L, Knoers N, Bindels RJ. The epithelial Mg2+ channel transient receptor potential melastatin 6 is regulated by dietary Mg2+ content and estrogens. J Am Soc Nephrol. 2006; 17:1035–1043. [PubMed: 16524949]

179. Groenestege WM, Thebault S, van der Wijst J, van den Berg D, Janssen R, Tejpar S, van den Heuvel LP, van Cutsem E, Hoenderop JG, Knoers NV, Bindels RJ. Impaired basolateral sorting of pro-EGF causes isolated recessive renal hypomagnesemia. J Clin Invest. 2007; 117:2260–2267. [PubMed: 17671655]

180. Gross JB, Imai M, Kokko JP. A functional comparison of the cortical collecting tubule and the distal convoluted tubule. JClinInvest. 1975; 55:1284–1294.

181. Hadchouel J, Soukaseum C, Busst C, Zhou XO, Baudrie V, Zurrer T, Cambillau M, Elghozi JL, Lifton RP, Loffing J, Jeunemaitre X. Decreased ENaC expression compensates the increased NCC activity following inactivation of the kidney-specific isoform of WNK1 and prevents hypertension. Proceedings of the National Academy of Sciences of the United States of America. 2010; 107:18109–18114. [PubMed: 20921400]

182. Harbarth S, Pestotnik SL, Lloyd JF, Burke JP, Samore MH. The epidemiology of nephrotoxicity associated with conventional amphotericin B therapy. Am J Med. 2001; 111:528–534. [PubMed: 11705428]

183. Hays SR, Baum M, Kokko JP. Effects of protein kinase C activation on sodium, potassium, chloride, and total CO2 transport in the rabbit cortical collecting tubule. J Clin Invest. 1987; 80:1561–1570. [PubMed: 3680514]

184. Hayslett JP, Boulpaep EL, Kashgarian M, Giebisch G. Electrical characteristics of the mamalian distal tubule: comparison of Ling-Gerard and macroelectrodes. Kidney Int. 1977; 12:324–331. [PubMed: 604621]

185. He G, Wang HR, Huang SK, Huang CL. Intersectin links WNK kinases to endocytosis of ROMK1. J Clin Invest. 2007; 117:1078–1087. [PubMed: 17380208]

186. Heering P, Degenhardt S, Grabensee B. Tubular dysfunction following kidney transplantation. Nephron. 1996; 74:501–511. [PubMed: 8938672]

187. Heidemann HT, Gerkens JF, Spickard WA, Jackson EK, Branch RA. Amphotericin B nephrotoxicity in humans decreased by salt repletion. AmJMed. 1983; 75:476–481.

188. Heidet L, Decramer S, Pawtowski A, Moriniere V, Bandin F, Knebelmann B, Lebre AS, Faguer S, Guigonis V, Antignac C, Salomon R. Spectrum of HNF1B mutations in a large cohort of patients who harbor renal diseases. Clinical journal of the American Society of Nephrology: CJASN. 2010; 5:1079–1090. [PubMed: 20378641]

189. Heo NJ, Son MJ, Lee JW, Jung JY, Kim S, Oh YK, Na KY, Yoon HJ, Joo KW, Han JS. Effect of estradiol on the expression of renal sodium transporters in rats. Climacteric: the journal of the International Menopause Society. 2013; 16:265–273. [PubMed: 22668026]

190. Hierholzer K, Wiederholt M, Holzgreve H, Giebisch G, Klose RM, Windhager EE. Micropuncture study of renal transtubular concentration gradients of sodium and potassium in adrenalectomized rats. Pflügers Arch. 1965; 285:193.

191. Higgins R, Ramaiyan K, Dasgupta T, Kanji H, Fletcher S, Lam F, Kashi H. Hyponatraemia and hyperkalaemia are more frequent in renal transplant recipients treated with tacrolimus than with cyclosporin. Further evidence for differences between cyclosporin and tacrolimus nephrotoxicities. Nephrology, dialysis, transplantation: official publication of the European Dialysis and Transplant Association - European Renal Association. 2004; 19:444–450.

192. Hoenderop JG, Dardenne O, Van Abel M, Van Der Kemp AW, Van Os CH, St-Arnaud R, Bindels RJ. Modulation of renal Ca2+ transport protein genes by dietary Ca2+ and 1,25-dihydroxyvitamin D3 in 25-hydroxyvitamin D3-1alpha-hydroxylase knockout mice. FASEB journal: official publication of the Federation of American Societies for Experimental Biology. 2002; 16:1398–1406. [PubMed: 12205031]

193. Hoenderop JG, Muller D, Van Der Kemp AW, Hartog A, Suzuki M, Ishibashi K, Imai M, Sweep F, Willems PH, Van Os CH, Bindels RJ. Calcitriol controls the epithelial calcium channel in kidney. J Am Soc Nephrol. 2001; 12:1342–1349. [PubMed: 11423563]

194. Hoenderop JG, Nilius B, Bindels RJ. Calcium absorption across epithelia. Physiol Rev. 2005; 85:373–422. [PubMed: 15618484]

195. Hoenderop JG, van Leeuwen JP, van der Eerden BC, Kersten FF, van der Kemp AW, Merillat AM, Waarsing JH, Rossier BC, Vallon V, Hummler E, Bindels RJ. Renal Ca2+ wasting, hyperabsorption, and reduced bone thickness in mice lacking TRPV5. J Clin Invest. 2003; 112:1906–1914. [PubMed: 14679186]

196. Hofmeister MV, Fenton RA, Praetorius J. Fluorescence isolation of mouse late distal convoluted tubules and connecting tubules: effects of vasopressin and vitamin D3 on Ca2+ signaling. Am J Physiol Renal Physiol. 2009; 296:F194–203. [PubMed: 18987111]

197. Holden S, Cox J, Raymond FL. Cloning, genomic organization, alternative splicing and expression analysis of the human gene WNK3 (PRKWNK3). Gene. 2004; 335:109–119. [PubMed: 15194194]

198. Holla VR, Makita K, Zaphiropoulos PG, Capdevila JH. The kidney cytochrome P-450 2C23 arachidonic acid epoxygenase is upregulated during dietary salt loading. J Clin Invest. 1999; 104:751–760. [PubMed: 10491410]

199. Hoorn EJ, Walsh SB, McCormick JA, Fürstenberg A, Yang C-L, Roeschel T, Paliege A, Howie AJ, Conley J, Bachmann S, Unwin RJ, Ellison DH. The calcineurin inhibitor tacrolimus activates the renal sodium chloride cotransporter to cause hypertension. Nature Medicine. 2011; 17:1304–1309.

200. Hoover RS, Poch E, Monroy A, Vazquez N, Nishio T, Gamba G, Hebert SC. N-Glycosylation at two sites critically alters thiazide binding and activity of the rat thiazide-sensitive Na(+):Cl(−) cotransporter. J Am Soc Nephrol. 2003; 14:271–282. [PubMed: 12538726]

201. Hou J, Goodenough DA. Claudin-16 and claudin-19 function in the thick ascending limb. Current opinion in nephrology and hypertension. 2010; 19:483–488. [PubMed: 20616717]

202. Hou J, Rajagopal M, Yu AS. Claudins and the kidney. Annu Rev Physiol. 2013; 75:479–501. [PubMed: 23140368]

203. Hropot M, Fowler NB, Karlmark B, Giebisch G. Tubular action of diuretics: distal effects on electrolyte transport and acidification. Kidney Int. 1985; 28:477–489. [PubMed: 4068482]

204. Hrushesky WJM, Shimp W, Kennedy BJ. Lack of age-dependent cisplatin nephrotoxicity. AmJMed. 1984; 76:579–584.

205. Hsu YJ, Dimke H, Schoeber JP, Hsu SC, Lin SH, Chu P, Hoenderop JG, Bindels RJ. Testosterone increases urinary calcium excretion and inhibits expression of renal calcium transport proteins. Kidney Int. 2010; 77:601–608. [PubMed: 20090667]

206. Hsu YJ, Hoenderop JG, Bindels RJ. TRP channels in kidney disease. Biochimica et biophysica acta. 2007; 1772:928–936. [PubMed: 17346947]

207. Huang C, Sindic A, Hill CE, Hujer KM, Chan KW, Sassen M, Wu Z, Kurachi Y, Nielsen S, Romero MF, Miller RT. Interaction of the Ca2+-sensing receptor with the inwardly rectifying potassium channels Kir4.1 and Kir4.2 results in inhibition of channel function. Am J Physiol Renal Physiol. 2007; 292:F1073–1081. [PubMed: 17122384]

208. Huang CL, Feng S, Hilgemann DW. Direct activation of inward rectifier potassium channels by PIP2 and its stabilization by Gbetagamma. Nature. 1998; 391:803–806. [PubMed: 9486652]

209. Hudecova S, Sedlakova B, Kvetnansky R, Ondrias K, Krizanova O. Modulation of the sodium-calcium exchanger in the rat kidney by different sequential stressors. Stress. 2010; 13:15–21. [PubMed: 19658027]

210. Hunter RW, Craigie E, Homer NZ, Mullins JJ, Bailey MA. Acute inhibition of NCC does not activate distal electrogenic Na+ reabsorption or kaliuresis. American journal of physiology Renal physiology. 2014; 306:F457–467. [PubMed: 24402096]

211. Huybers S, Naber TH, Bindels RJ, Hoenderop JG. Prednisolone-induced Ca2+ malabsorption is caused by diminished expression of the epithelial Ca2+ channel TRPV6. American journal of physiology Gastrointestinal and liver physiology. 2007; 292:G92–97. [PubMed: 16901990]

212. Ikari A, Okude C, Sawada H, Yamazaki Y, Sugatani J, Miwa M. TRPM6 expression and cell proliferation are up-regulated by phosphorylation of ERK1/2 in renal epithelial cells. Biochemical and biophysical research communications. 2008; 369:1129–1133. [PubMed: 18339311]

213. Ikari A, Sanada A, Okude C, Sawada H, Yamazaki Y, Sugatani J, Miwa M. Up-regulation of TRPM6 transcriptional activity by AP-1 in renal epithelial cells. Journal of cellular physiology. 2010; 222:481–487. [PubMed: 19937979]

214. Ikari A, Sanada A, Sawada H, Okude C, Tonegawa C, Sugatani J. Decrease in transient receptor potential melastatin 6 mRNA stability caused by rapamycin in renal tubular epithelial cells. Biochimica et biophysica acta. 2011; 1808:1502–1508. [PubMed: 21073857]

215. Imai M. The connecting tubule: a functional subdivision of the rabbit distal nephron segments. Kidney Int. 1979; 15:346–356. [PubMed: 513494]

216. Imaoka S, Wedlund PJ, Ogawa H, Kimura S, Gonzalez FJ, Kim HY. Identification of CYP2C23 expressed in rat kidney as an arachidonic acid epoxygenase. The Journal of pharmacology and experimental therapeutics. 1993; 267:1012–1016. [PubMed: 8246128]

217. Inoue T, Nonoguchi H, Tomita K. Physiological effects of vasopressin and atrial natriuretic peptide in the collecting duct. Cardiovascular research. 2001; 51:470–480. [PubMed: 11476737]

218. Irnaten M, Blanchard-Gutton N, Praetorius J, Harvey BJ. Rapid effects of 17beta-estradiol on TRPV5 epithelial Ca2+ channels in rat renal cells. Steroids. 2009; 74:642–649. [PubMed: 19463684]

219. Ito M, Inanobe A, Horio Y, Hibino H, Isomoto S, Ito H, Mori K, Tonosaki A, Tomoike H, Kurachi Y. Immunolocalization of an inwardly rectifying K+ channel, K(AB)-2 (Kir4.1), in the basolateral membrane of renal distal tubular epithelia. FEBS letters. 1996; 388:11–15. [PubMed: 8654579]

220. James PA, Oparil S, Carter BL, Cushman WC, Dennison-Himmelfarb C, Handler J, Lackland DT, Lefevre ML, Mackenzie TD, Ogedegbe O, Smith SC Jr, Svetkey LP, Taler SJ, Townsend RR, Wright JT Jr, Narva AS, Ortiz E. 2014 Evidence-Based Guideline for the Management of High Blood Pressure in Adults: Report From the Panel Members Appointed to the Eighth Joint National Committee (JNC 8). JAMA. 2013

221. Jayakumar A, Cheng L, Liang CT, Sacktor B. Sodium gradient-dependent calcium uptake in renal basolateral membrane vesicles. Effect of parathyroid hormone. J Biol Chem. 1984; 259:10827–10833. [PubMed: 6469984]

222. Jiang Y, Ferguson WB, Peng JB. WNK4 enhances TRPV5-mediated calcium transport: potential role in hypercalciuria of familial hyperkalemic hypertension caused by gene mutation of WNK4. American journal of physiology Renal physiology. 2007; 292:F545–554. [PubMed: 17018846]

223. Jin Y, Wang Z, Zhang Y, Yang B, Wang WH. PGE2 inhibits apical K channels in the CCD through activation of the MAPK pathway. Am J Physiol Renal Physiol. 2007; 293:F1299–1307. [PubMed: 17686952]

224. Kahle KT, Rinehart J, de Los Heros P, Louvi A, Meade P, Vazquez N, Hebert SC, Gamba G, Gimenez I, Lifton RP. WNK3 modulates transport of Cl- in and out of cells: implications for control of cell volume and neuronal excitability. Proc Natl Acad Sci U S A. 2005; 102:16783–16788. [PubMed: 16275911]

225. Kahle KT, Wilson FH, Leng Q, Lalioti MD, O'Connell AD, Dong K, Rapson AK, MacGregor GG, Giebisch G, Hebert SC, Lifton RP. WNK4 regulates the balance between renal NaCl reabsorption and K+ secretion. Nature genetics. 2003; 35:372–376. [PubMed: 14608358]

226. Kaissling B. Cellular heterogeneity of the distal nephron and its relation to function. Klin Wochenschr. 1985 Sep 16.63:868–876. [PubMed: 4057916]

227. Kaissling B. Structural adaptation to altered electrolyte metabolism by cortical distal segments. Fed Proc. 1985; 44:2710–2716. [PubMed: 3894055]

228. Kaissling B. Structural aspects of adaptive changes in renal electrolyte excretion. AmJPhysiol. 1982; 243:F211–F226.

229. Kaissling B. Ultrastructural organization of the transition from the distal nephron to the collecting duct in the desert rodent Psammomys obesus. Cell Tissue Res. 1980; 212:475–495. [PubMed: 7006826]

230. Kaissling B, Bachmann S, Kriz W. Structural adaptation of the distal convoluted tubule to prolonged furosemide treatment. AmJPhysiol. 1985; 248:F374–F381.

231. Kaissling B, Kriz W. Structural analysis of the rabbit kidney. Advances in anatomy, embryology, and cell biology. 1979; 56:1–123.

232. Kaissling B, Kriz W. Structural analysis of the rabbit kidney. Adv Anat Embryol Cell Biol. 1979; 56:1–123. [PubMed: 443090]

233. Kaissling B, Le Hir M. Distal tubular segments of the rabbit kidney after adaptation to altered Na- and K-intake. Cell Tissue Res. 1982; 224:469–492. [PubMed: 7116409]

234. Kaissling B, Stanton BA. Adaptation of distal tubule and collecting duct to increased sodium delivery. I. Ultrastructure. AmJPhysiol. 1988; 255:F1256–F1268.

235. Kaissling, B., Stanton, BA. Structure-function correlation in electrolyte transporting epithelia. In: Seldin, DW., Giebisch, G., editors. The Kidney: Physiology and Pathophysiology. New York: Raven Press, Ltd; 1992. p. 779-801.

236. Kashgarian M, Biemesderfer D, Caplan M, Forbush B III. Monoclonal antibody to Na, K-ATPase: Immunocytochemical localization along nephron segments. Kidney Int. 1985; 28:899–913. [PubMed: 3003443]

237. Kashgarian M, Stöckle H, Gottschalk CW, Ullrich KJ. Transtubular electrochemical potentials of sodium and chloride in proximal and distal renal tubules of rats during antidiuresis and water diuresis (diabetes insipidus). Pflügers Arch. 1963; 277:89–106.

238. Katz AI, Doucet A, Morel F. Na-K-ATPase activity along the rabbit, rat, and mouse nephron. AmJPhysiol. 1979:114–120.

239. Khan O, Riazi S, Hu X, Song J, Wade JB, Ecelbarger CA. Regulation of the renal thiazide-sensitive Na-Cl cotransporter, blood pressure, and natriuresis in obese Zucker rats treated with rosiglitazone. American journal of physiology Renal physiology. 2005; 289:F442–450. [PubMed: 15814531]

240. Khuri RN, Wiederholt M, Strieder N, Giebisch G. Effects of flow rate and potassium intake on distal tubular potassium transfer. AmJPhysiol. 1975; 228:1249–1261.

241. Khuri RN, Wiederholt M, Strieder N, Giebisch G. Effects of graded solute diuresis on renal tubular sodium transport in the rat. AmJPhysiol. 1975; 228:1262–1268.

242. Kieferle S, Fong P, Bens M, Vandewalle A, Jentsch TJ. Two highly homologous members of the ClC chloride channel family in both rat and human kidney. ProcNatlAcadSciUSA. 1994; 91:6943–6947.

243. Kim GH, Martin SW, Fernandez-Llama P, Masilamani S, Packer RK, Knepper MA. Long-term regulation of renal Na-dependent cotransporters and ENaC: response to altered acid-base intake. American journal of physiology Renal physiology. 2000 Sep.279:F459–467. [PubMed: 10966925]
244. Kim GH, Masilamani S, Turner R, Mitchell C, Wade JB, Knepper MA. The thiazide-sensitive Na-Cl cotransporter is an aldosterone-induced protein. Proceedings of the National Academy of Sciences of the United States of America. 1998 Nov 24.95:14552–14557. [PubMed: 9826738]
245. Kim YH, Kwon TH, Frische S, Kim J, Tisher CC, Madsen KM, Nielsen S. Immunocytochemical localization of pendrin in intercalated cell subtypes in rat and mouse kidney. Am J Physiol Renal Physiol. 2002; 283:F744–754. [PubMed: 12217866]
246. Kishore BK, Mandon B, Oza NB, DiGiovanni SR, Coleman RA, Ostrowski NL, Wade JB, Knepper MA. Rat renal arcade segment expresses vasopressin-regulated water channel and vasopressin V2 receptor. JClinInvest. 1996; 97:2763–2771.
247. Kleyman TR, Roberts C, Ling BN. A mechanism for pentamidine-induced hyperkalemia: Inhibition of distal nephron sodium transport. AnnInternMed. 1995; 122:103–106.
248. Knoers NV, Levtchenko EN. Gitelman syndrome. Orphanet J Rare Dis. 2008; 3:22. [PubMed: 18667063]
249. Kobayashi S, Clemmons DR, Nogami H, Roy AK, Venkatachalam MA. Tubular hypertrophy due to work load induced by furosemide is associated with increses of IGF-1 and IGFBP-1. Kidney Int. 1995; 47:818–828. [PubMed: 7538611]
250. Kohan DE, Knox FG. Localization of the nephron sites responsible for mineralocorticoid escape in rats. The American journal of physiology. 1980 Aug.239:F149–153. [PubMed: 7406045]
251. Komers R, Rogers S, Oyama TT, Xu B, Yang CL, McCormick J, Ellison DH. Enhanced phosphorylation of Na+-Cl- co-transporter in experimental metabolic syndrome: role of insulin. Clinical science. 2012; 123:635–647. [PubMed: 22651238]
252. Korovkina VP, England SK. Molecular diversity of vascular potassium channel isoforms. Clinical and experimental pharmacology & physiology. 2002; 29:317–323. [PubMed: 11985543]
253. Koster HP, Hartog A, Van Os CH, Bindels RJ. Calbindin-D28K facilitates cytosolic calcium diffusion without interfering with calcium signaling. Cell Calcium. 1995; 18:187–196. [PubMed: 8529259]
254. Kriz, W., Kaissling, B. Structural organization of the mammalian kidney. In: Seldin, DW., Giebisch, G., editors. The Kidney: Physiology and Pathophysiology. New York: Raven Press; 1992. p. 779-802.
255. Kubo Y, Adelman JP, Clapham DE, Jan LY, Karschin A, Kurachi Y, Lazdunski M, Nichols CG, Seino S, Vandenberg CA. International Union of Pharmacology. LIV. Nomenclature and molecular relationships of inwardly rectifying potassium channels. Pharmacological reviews. 2005; 57:509–526. [PubMed: 16382105]
256. Kumar R, Schaefer J, Grande JP, Roche PC. Immunolocalization of calcitriol receptor, 24-hydroxylase cytochrome P- 450, and calbindin D28k in human kidney. The American journal of physiology. 1994 Mar.266 F477-485SB - M.
257. Kunau RT Jr, Webb HL, Borman SC. Characteristics of sodium reabsorption in the loop of Henle and distal tubule. AmJPhysiol. 1974; 227:1181–1191.
258. Kunau RT Jr, Weller DR, Webb HL. Clarification of the site of action of chlorothiazide in the rat nephron. J Clin Invest. 1975; 56:401–407. [PubMed: 1150878]
259. Kunchaparty S, Palcso M, Berkman J, Velázquez H, Bernstein P, Reilly RF, Ellison DH. Defective processing and expression of the thiazide-sensitive Na-Cl cotransporter as a cause Gitelman's Syndrome. Am J Physiol Renal Physiol. 1999; 277:F643–F649.
260. Kurtzberg J, Dennis VW, Kinney TR. Cisplatinum-induced renal salt wasting. Med Pediatr Oncol. 1984; 12:150–154. [PubMed: 6538257]
261. Kwon TH, Nielsen J, Kim YH, Knepper MA, Frokiaer J, Nielsen S. Regulation of sodium transporters in the thick ascending limb of rat kidney: response to angiotensin II. Am J Physiol Renal Physiol. 2003; 285:F152–165. [PubMed: 12657563]

262. Kwon TH, Nielsen J, Knepper MA, Frokiaer J, Nielsen S. Angiotensin II AT1 receptor blockade decreases vasopressin-induced water reabsorption and AQP2 levels in NaCl-restricted rats. Am J Physiol Renal Physiol. 2005; 288:F673–684. [PubMed: 15585668]

263. Lai L, Feng X, Liu D, Chen J, Zhang Y, Niu B, Gu Y, Cai H. Dietary salt modulates the sodium chloride cotransporter expression likely through an aldosterone-mediated WNK4-ERK1/2 signaling pathway. Pflugers Archiv: European journal of physiology. 2012; 463:477–485. [PubMed: 22200850]

264. Lajeunesse D, Bouhtiauy I, Brunette MG. Parathyroid hormone and hydrochlorothiazide increase calcium transport by the luminal membrane of rabbit distal nephron segments through different pathways. Endocrinology. 1994; 134:35–41. [PubMed: 7506210]

265. Lalioti MD, Zhang J, Volkman HM, Kahle KT, Hoffmann KE, Toka HR, Nelson-Williams C, Ellison DH, Flavell R, Booth CJ, Lu Y, Geller DS, Lifton RP. Wnk4 controls blood pressure and potassium homeostasis via regulation of mass and activity of the distal convoluted tubule. Nat Genet. 2006; 38:1124–1132. [PubMed: 16964266]

266. Lambers TT, Mahieu F, Oancea E, Hoofd L, de Lange F, Mensenkamp AR, Voets T, Nilius B, Clapham DE, Hoenderop JG, Bindels RJ. Calbindin-D28K dynamically controls TRPV5-mediated Ca2+ transport. EMBO J. 2006; 25:2978–2988. [PubMed: 16763551]

267. Lambers TT, Oancea E, de Groot T, Topala CN, Hoenderop JG, Bindels RJ. Extracellular pH dynamically controls cell surface delivery of functional TRPV5 channels. Molecular and cellular biology. 2007; 27:1486–1494. [PubMed: 17178838]

268. Lassiter WE, Gottschalk CW, Mylle M. Micropuncture study of renal tubular reabsorption of calcium in normal rodents. AmJPhysiol. 1963; 204:771–775.

269. Lau K, Bourdeau JE. Evidence for cAMP-dependent protein kinase in mediating the parathyroid hormone-stimulated rise in cytosolic free calcium in rabbit connecting tubules. J Biol Chem. 1989; 264:4028–4032. [PubMed: 2537302]

270. Lazrak A, Liu Z, Huang CL. Antagonistic regulation of ROMK by long and kidney-specific WNK1 isoforms. Proc Natl Acad Sci U S A. 2006; 103:1615–1620. [PubMed: 16428287]

271. Le Hir M, Dubach UC. The cellular specificity of lectin binding in the kidney. I. A light microscopical study in the rat. Histochem. 1982; 74:521–530.

272. Ledeganck KJ, Boulet GA, Horvath CA, Vinckx M, Bogers JJ, Van Den Bossche R, Verpooten GA, De Winter BY. Expression of renal distal tubule transporters TRPM6 and NCC in a rat model of cyclosporine nephrotoxicity and effect of EGF treatment. American journal of physiology Renal physiology. 2011; 301:F486–493. [PubMed: 21653632]

273. Lee CT, Shang S, Lai LW, Yong KC, Lien YH. Effect of thiazide on renal gene expression of apical calcium channels and calbindins. American journal of physiology Renal physiology. 2004; 287:F1164–1170. [PubMed: 15265769]

274. Lee DH, Maunsbach AB, Riquier-Brison AD, Nguyen MT, Fenton RA, Bachmann S, Yu AS, McDonough AA. Effects of ACE inhibition and ANG II stimulation on renal Na-Cl cotransporter distribution, phosphorylation, and membrane complex properties. American journal of physiology Cell physiology. 2013; 304:C147–163. [PubMed: 23114965]

275. Lee DH, Riquier AD, Yang LE, Leong PK, Maunsbach AB, McDonough AA. Acute hypertension provokes acute trafficking of distal tubule Na-Cl cotransporter (NCC) to subapical cytoplasmic vesicles. American journal of physiology Renal physiology. 2009; 296:F810–818. [PubMed: 19144688]

276. Lee J, Cha SK, Sun TJ, Huang CL. PIP2 activates TRPV5 and releases its inhibition by intracellular Mg2+ The Journal of general physiology. 2005; 126:439–451. [PubMed: 16230466]

277. Lee K, Brown D, Urena P, Ardaillou N, Ardaillou R, Deeds J, Segre GV. Localization of parathyroid hormone/parathyroid hormone-related peptide receptor mRNA in kidney. The American journal of physiology. 1996 Jan.270:F186–191. [PubMed: 8769838]

278. Leng Q, Kahle KT, Rinehart J, MacGregor GG, Wilson FH, Canessa CM, Lifton RP, Hebert SC. WNK3, a kinase related to genes mutated in hereditary hypertension with hyperkalaemia, regulates the K+ channel ROMK1 (Kir1.1). The Journal of physiology. 2006; 571:275–286. [PubMed: 16357011]

279. Lennon EJ, Piering WF. A comparison of the effects of glucose ingestion and NH4Cl acidosis on urinary calcium and magnesium excretion in man. J Clin Invest. 1970; 49:1458–1465. [PubMed: 5432375]

280. Leviel F, Hubner CA, Houillier P, Morla L, El Moghrabi S, Brideau G, Hassan H, Parker MD, Kurth I, Kougioumtzes A, Sinning A, Pech V, Riemondy KA, Miller RL, Hummler E, Shull GE, Aronson PS, Doucet A, Wall SM, Chambrey R, Eladari D. The Na+-dependent chloride-bicarbonate exchanger SLC4A8 mediates an electroneutral Na+ reabsorption process in the renal cortical collecting ducts of mice. J Clin Invest. 2010; 120:1627–1635. [PubMed: 20389022]

281. Li J, Wang DH. Function and regulation of epithelial sodium transporters in the kidney of a salt-sensitive hypertensive rat model. Journal of hypertension. 2007; 25:1065–1072. [PubMed: 17414671]

282. Li M, Du J, Jiang J, Ratzan W, Su LT, Runnels LW, Yue L. Molecular determinants of Mg2+ and Ca2+ permeability and pH sensitivity in TRPM6 and TRPM7. J Biol Chem. 2007; 282:25817–25830. [PubMed: 17599911]

283. Li M, Jiang J, Yue L. Functional characterization of homo- and heteromeric channel kinases TRPM6 and TRPM7. The Journal of general physiology. 2006; 127:525–537. [PubMed: 16636202]

284. Li WY, Huey CL, Yu AS. Expression of claudin-7 and -8 along the mouse nephron. American journal of physiology Renal physiology. 2004; 286:F1063–1071. [PubMed: 14722018]

285. Liapis H, Nag M, Kaji DM. K-Cl cotransporter expression in the human kidney. The American journal of physiology. 1998 Dec.275:C1432–1437. [PubMed: 9843703]

286. Lin D, Kamsteeg EJ, Zhang Y, Jin Y, Sterling H, Yue P, Roos M, Duffield A, Spencer J, Caplan M, Wang WH. Expression of tetraspan protein CD63 activates protein-tyrosine kinase (PTK) and enhances the PTK-induced inhibition of ROMK channels. J Biol Chem. 2008; 283:7674–7681. [PubMed: 18211905]

287. Lin D, Sterling H, Lerea KM, Giebisch G, Wang WH. Protein kinase C (PKC)-induced phosphorylation of ROMK1 is essential for the surface expression of ROMK1 channels. J Biol Chem. 2002; 277:44278–44284. [PubMed: 12221079]

288. Lin DH, Sterling H, Lerea KM, Welling P, Jin L, Giebisch G, Wang WH. K depletion increases protein tyrosine kinase-mediated phosphorylation of ROMK. Am J Physiol Renal Physiol. 2002; 283:F671–677. [PubMed: 12217858]

289. Lin DH, Yue P, Rinehart J, Sun P, Wang Z, Lifton R, Wang WH. Protein phosphatase 1 modulates the inhibitory effect of With-no-Lysine kinase 4 on ROMK channels. American journal of physiology Renal physiology. 2012; 303:F110–119. [PubMed: 22513846]

290. Lin SH, Cheema-Dhadli S, Gowrishankar M, Marliss EB, Kamel KS, Halperin ML. Control of excretion of potassium: lessons from studies during prolonged total fasting in human subjects. American Journal of Physiology. 1997; 273:F796–800. [PubMed: 9374844]

291. Lin SH, Shiang JC, Huang CC, Yang SS, Hsu YJ, Cheng CJ. Phenotype and genotype analysis in Chinese patients with Gitelman's syndrome. The Journal of clinical endocrinology and metabolism. 2005; 90:2500–2507. [PubMed: 15687331]

292. Lin SH, Yu IS, Jiang ST, Lin SW, Chu P, Chen A, Sytwu HK, Sohara E, Uchida S, Sasaki S, Yang SS. Impaired phosphorylation of Na(+)-K(+)-2Cl(−) cotransporter by oxidative stress-responsive kinase-1 deficiency manifests hypotension and Bartter-like syndrome. Proceedings of the National Academy of Sciences of the United States of America. 2011; 108:17538–17543. [PubMed: 21972418]

293. Liou HH, Zhou SS, Huang CL. Regulation of ROMK1 channel by protein kinase A via a phosphatidylinositol 4,5-bisphosphate-dependent mechanism. Proceedings of the National Academy of Sciences of the United States of America. 1999; 96:5820–5825. [PubMed: 10318968]

294. Liu W, Wei Y, Sun P, Wang WH, Kleyman TR, Satlin LM. Mechanoregulation of BK channel activity in the mammalian cortical collecting duct: role of protein kinases A and C. Am J Physiol Renal Physiol. 2009; 297:F904–915. [PubMed: 19656909]

295. Liu W, Xu S, Woda C, Kim P, Weinbaum S, Satlin LM. Effect of flow and stretch on the [Ca2+]i response of principal and intercalated cells in cortical collecting duct. American journal of physiology Renal physiology. 2003; 285:F998–F1012. [PubMed: 12837680]

296. Liu Z, Wang HR, Huang CL. Regulation of ROMK channel and K+ homeostasis by kidney-specific WNK1 kinase. J Biol Chem. 2009; 284:12198–12206. [PubMed: 19244242]

297. Liu Z, Xie J, Wu T, Truong T, Auchus RJ, Huang CL. Downregulation of NCC and NKCC2 cotransporters by kidney-specific WNK1 revealed by gene disruption and transgenic mouse models. Human molecular genetics. 2011; 20:855–866. [PubMed: 21131289]

298. Loffing J, Kaissling B. Sodium and calcium transport pathways along the mammalian distal nephron: from rabbit to human. Am J Physiol Renal Physiol. 2003 Apr.284:F628–643. [PubMed: 12620920]

299. Loffing J, Le Hir M, Kaissling B. Modulation of salt transport rate affects DNA synthesis in vivo in rat renal tubules. Kidney Int. 1995; 47:1615–1623. [PubMed: 7643530]

300. Loffing J, Loffing-Cueni D, Hegyi I, Kaplan MR, Hebert SC, Le Hir M, Kaissling B. Thiazide treatment of rats provokes apoptosis in distal tubule cells. Kidney international. 1996; 50:1180–1190. [PubMed: 8887276]

301. Loffing J, Loffing-Cueni D, Valderrabano V, Klausli L, Hebert SC, Rossier BC, Hoenderop JG, Bindels RJ, Kaissling B. Distribution of transcellular calcium and sodium transport pathways along mouse distal nephron. Am J Physiol Renal Physiol. 2001; 281:F1021–1027. [PubMed: 11704552]

302. Loffing J, Pietri L, Aregger F, Bloch-Faure M, Ziegler u, Meneton p, Rossier BC, Kaissling B. Differential subcellular localization of ENaC subunits in mouse kidney in response to high- and low- sodium diets. AmJPhysiol Renal Physiol. 2000; 279:F252–F258.

303. Loffing J, Vallon V, Loffing-Cueni D, Aregger F, Richter K, Pietri L, Bloch-Faure M, Hoenderop JG, Shull GE, Meneton P, Kaissling B. Altered renal distal tubule structure and renal Na(+) and Ca(2+) handling in a mouse model for Gitelman's syndrome. Journal of the American Society of Nephrology: JASN. 2004; 15:2276–2288. [PubMed: 15339977]

304. Loon NR, Wilcox CS, Unwin RJ. Mechanism of impaired natriuretic response to furosemide during prolonged therapy. Kidney Int. 1989; 36:682–689. [PubMed: 2811065]

305. Louis-Dit-Picard H, Barc J, Trujillano D, Miserey-Lenkei S, Bouatia-Naji N, Pylypenko O, Beaurain G, Bonnefond A, Sand O, Simian C, Vidal-Petiot E, Soukaseum C, Mandet C, Broux F, Chabre O, Delahousse M, Esnault V, Fiquet B, Houillier P, Bagnis CI, Koenig J, Konrad M, Landais P, Mourani C, Niaudet P, Probst V, Thauvin C, Unwin RJ, Soroka SD, Ehret G, Ossowski S, Caulfield M, Bruneval P, Estivill X, Froguel P, Hadchouel J, Schott JJ, Jeunemaitre X. KLHL3 mutations cause familial hyperkalemic hypertension by impairing ion transport in the distal nephron. Nature genetics. 2012; 44:456–460. S451–453. [PubMed: 22406640]

306. Lourdel S, Paulais M, Cluzeaud F, Bens M, Tanemoto M, Kurachi Y, Vandewalle A, Teulon J. An inward rectifier K(+) channel at the basolateral membrane of the mouse distal convoluted tubule: similarities with Kir4-Kir5.1 heteromeric channels. The Journal of physiology. 2002; 538:391–404. [PubMed: 11790808]

307. Lourdel S, Paulais M, Marvao P, Nissant A, Teulon J. A chloride channel at the basolateral membrane of the distal-convoluted tubule: a candidate ClC-K channel. The Journal of general physiology. 2003; 121:287–300. [PubMed: 12668733]

308. Lu X, Roksnoer LC, Danser AH. The intrarenal renin-angiotensin system: does it exist? Implications from a recent study in renal angiotensin-converting enzyme knockout mice. Nephrology, dialysis, transplantation: official publication of the European Dialysis and Transplant Association - European Renal Association. 2013; 28:2977–2982.

309. Ma J, Qu W, Scarborough PE, Tomer KB, Moomaw CR, Maronpot R, Davis LS, Breyer MD, Zeldin DC. Molecular cloning, enzymatic characterization, developmental expression, and cellular localization of a mouse cytochrome P450 highly expressed in kidney. J Biol Chem. 1999; 274:17777–17788. [PubMed: 10364221]

310. Madala Halagappa VK, Tiwari S, Riazi S, Hu X, Ecelbarger CM. Chronic candesartan alters expression and activity of NKCC2, NCC, and ENaC in the obese Zucker rat. American journal of physiology Renal physiology. 2008; 294:F1222–1231. [PubMed: 18305093]

311. Magyar CE, White KE, Rojas R, Apodaca G, Friedman PA. Plasma membrane Ca2+-ATPase and NCX1 Na+/Ca2+ exchanger expression in distal convoluted tubule cells. Am J Physiol Renal Physiol. 2002; 283:F29–40. [PubMed: 12060584]

312. Maki N, Komatsuda A, Wakui H, Ohtani H, Kigawa A, Aiba N, Hamai K, Motegi M, Yamaguchi A, Imai H, Sawada K. Four novel mutations in the thiazide-sensitive Na-Cl co-transporter gene in Japanese patients with Gitelman's syndrome. Nephrology, dialysis, transplantation: official publication of the European Dialysis and Transplant Association - European Renal Association. 2004; 19:1761–1766.

313. Malnic G, Giebisch G. Some electrical properties of distal tubular epithelium in the rat. AmJPhysiol. 1972; 223:797–808.

314. Malnic G, Klose RM, Giebisch G. Micropuncture study of distal tubular potassium and sodium transport in rat nephron. The American journal of physiology. 1966; 211:529–547. [PubMed: 5927880]

315. Mangray M, Vella JP. Hypertension after kidney transplant. American journal of kidney diseases: the official journal of the National Kidney Foundation. 2011; 57:331–341. [PubMed: 21251543]

316. Martin HE, Jones R. The effect of ammonium chloride and sodium bicarbonate on the urinary excretion of magnesium, calcium, and phosphate. American heart journal. 1961; 62:206–210. [PubMed: 13767354]

317. Masilamani S, Wang X, Kim GH, Brooks H, Nielsen J, Nielsen S, Nakamura K, Stokes JB, Knepper MA. Time course of renal Na-K-ATPase, NHE3, NKCC2, NCC, and ENaC abundance changes with dietary NaCl restriction. Am J Physiol Renal Physiol. 2002; 283:F648–657. [PubMed: 12217855]

318. Matsusaka T, Niimura F, Shimizu A, Pastan I, Saito A, Kobori H, Nishiyama A, Ichikawa I. Liver angiotensinogen is the primary source of renal angiotensin II. Journal of the American Society of Nephrology: JASN. 2012; 23:1181–1189. [PubMed: 22518004]

319. Mavichak V, Coppin CM, Wong NL, Dirks JH, Walker V, Sutton RA. Renal magnesium wasting and hypocalciuria in chronic cis-platinum nephropathy in man. Clin Sci (Lond). 1988; 75:203–207. [PubMed: 3409636]

320. Mayan H, Attar-Herzberg D, Shaharabany M, Holtzman EJ, Farfel Z. Increased urinary Na-Cl cotransporter protein in familial hyperkalaemia and hypertension. Nephrol Dial Transplant. 2007

321. Mayan H, Munter G, Shaharabany M, Mouallem M, Pauzner R, Holtzman EJ, Farfel Z. Hypercalciuria in familial hyperkalemia and hypertension accompanies hyperkalemia and precedes hypertension: description of a large family with the Q565E WNK4 mutation. The Journal of clinical endocrinology and metabolism. 2004; 89:4025–4030. [PubMed: 15292344]

322. Mayan H, Vered I, Mouallem M, Tzadok-Witkon M, Pauzner R, Farfel Z. Pseudohypoaldosteronism type II: marked sensitivity to thiazides, hypercalciuria, normomagnesemia, and low bone mineral density. J Clin Endocrinol Metab. 2002; 87:3248–3254. [PubMed: 12107233]

323. Mazzitelli LR, Adamo HP. The phosphatase activity of the plasma membrane Ca2+ pump. Activation by acidic lipids in the absence of Ca2+ increases the apparent affinity for Mg2+ Biochimica et biophysica acta. 2007; 1768:1777–1783. [PubMed: 17540337]

324. McCormick JA, Bhalla V, Pao AC, Pearce D. SGK1: a rapid aldosterone-induced regulator of renal sodium reabsorption. Physiology (Bethesda). 2005; 20:134–139. [PubMed: 15772302]

325. McCormick JA, Ellison DH. The WNKs: atypical protein kinases with pleiotropic actions. Physiol Rev. 2010

326. McCormick JA, Mutig K, Nelson JH, Saritas T, Hoorn EJ, Yang C-L, Rogers S, Curry J, Delpire E, Bachmann S, Ellison DH. A SPAK isoform switch modulates renal salt transport and blood pressure. Cell Metab. 2011; 14:352–364. [PubMed: 21907141]

327. McManus OB, Helms LM, Pallanck L, Ganetzky B, Swanson R, Leonard RJ. Functional role of the beta subunit of high conductance calcium-activated potassium channels. Neuron. 1995; 14:645–650. [PubMed: 7695911]

328. McNulty S, Fonfria E. The role of TRPM channels in cell death. Pflugers Archiv: European journal of physiology. 2005; 451:235–242. [PubMed: 16025303]

329. Mederle K, Mutig K, Paliege A, Carota I, Bachmann S, Castrop H, Oppermann M. Loss of WNK3 is compensated for by the WNK1/SPAK axis in the kidney of the mouse. Am J Physiol Renal Physiol. 2013; 304:F1198–1209. [PubMed: 23427142]

330. Mederle K, Mutig K, Paliege A, Carota I, Bachmann S, Castrop H, Oppermann M. Loss of WNK3 is compensated for by the WNK1/SPAK axis in the kidney of the mouse. American journal of physiology Renal physiology. 2013; 304:F1198–1209. [PubMed: 23427142]

331. Meij IC, Koenderink JB, van Bokhoven H, Assink KF, Groenestege WT, de Pont JJ, Bindels RJ, Monnens LA, van den Heuvel LP, Knoers NV. Dominant isolated renal magnesium loss is caused by misrouting of the Na(+), K(+)-ATPase gamma-subunit. Nature genetics. 2000; 26:265–266. [PubMed: 11062458]

332. Melo Z, Cruz-Rangel S, Bautista R, Vazquez N, Castaneda-Bueno M, Mount DB, Pasantes-Morales H, Mercado A, Gamba G. Molecular evidence for a role for K(+)-Cl(−) cotransporters in the kidney. American journal of physiology Renal physiology. 2013; 305:F1402–1411. [PubMed: 24089410]

333. Menaa C, Devlin RD, Reddy SV, Gazitt Y, Choi SJ, Roodman GD. Annexin II increases osteoclast formation by stimulating the proliferation of osteoclast precursors in human marrow cultures. J Clin Invest. 1999; 103:1605–1613. [PubMed: 10359570]

334. Meneton P, Loffing J, Warnock DG. Sodium and potassium handling by the aldosterone-sensitive distal nephron: the pivotal role of the distal and connecting tubule. Am J Physiol Renal Physiol. 2004; 287:F593–601. [PubMed: 15345493]

335. Mennitt PA, Wade JB, Ecelbarger CA, Palmer LG, Frindt G. Localization of ROMK channels in the rat kidney. J Am Soc Nephrol. 1997; 8:1823–1830. [PubMed: 9402083]

336. Merino A, Kalplan MR, Hole AE, Hebert SC, Gamba G. Electroneutral Na-(K)-Cl cotransporters transcript expression in the kidney with furosemide administration. JAmSocNephrol. 1995:346.

337. Meyer TE, Verwoert GC, Hwang SJ, Glazer NL, Smith AV, van Rooij FJ, Ehret GB, Boerwinkle E, Felix JF, Leak TS, Harris TB, Yang Q, Dehghan A, Aspelund T, Katz R, Homuth G, Kocher T, Rettig R, Ried JS, Gieger C, Prucha H, Pfeufer A, Meitinger T, Coresh J, Hofman A, Sarnak MJ, Chen YD, Uitterlinden AG, Chakravarti A, Psaty BM, van Duijn CM, Kao WH, Witteman JC, Gudnason V, Siscovick DS, Fox CS, Kottgen A. Genetic Factors for Osteoporosis C, Meta Analysis of G, Insulin Related Traits C. Genome-wide association studies of serum magnesium, potassium, and sodium concentrations identify six Loci influencing serum magnesium levels. PLoS genetics. 2010; 6

338. Monroy A, Plata C, Hebert SC, Gamba G. Characterization of the thiazide-sensitive Na(+)- Cl(−) cotransporter: a new model for ions and diuretics interaction. American journal of physiology Renal physiology. 2000 Jul.279:F161–169. [PubMed: 10894798]

339. Morel F. Sites of hormone action in the mammalian nephron. AmJPhysiol. 1981; 240:F159–F164.

340. Morel F, Chabardès D, Imbert M. Functional segmentation of the rabbit distal tubule by microdissection of hormone-dependent adenylate cyclase activity. Kidney Int. 1976; 9:264–277. [PubMed: 940269]

341. Moreno G, Merino A, Mercado A, Herrera JP, Gonzalez-Salazar J, Correa-Rotter R, Hebert SC, Gamba G. Electroneutral Na-coupled cotransporter expression in the kidney during variations of NaCl and water metabolism. Hypertension. 1998 Apr.31:1002–1006. [PubMed: 9535427]

342. Morgan B, Robertson WG. The urinary excretion of calcium. An analysis of the distribution of values in relation to sex, age and calcium deprivation. Clinical orthopaedics and related research. 1974:254–267.

343. Moriguchi T, Urushiyama S, Hisamoto N, Iemura SI, Uchida S, Natsume T, Matsumoto K, Shibuya H. WNK1 regulates phosphorylation of cation-chloride-coupled cotransporters via the STE20-related kinases, SPAK and OSR1. J Biol Chem. 2005; 280:42685–42693. [PubMed: 16263722]

344. Morris RG, Hoorn EJ, Knepper MA. Hypokalemia in a mouse model of Gitelman's syndrome. Am J Physiol Renal Physiol. 2006; 290:F1416–1420. [PubMed: 16434571]

345. Morsing P, Velazquez H, Ellison D, Wright FS. Resetting of tubuloglomerular feedback by interrupting early distal flow. Acta PhysiolScand. 1993; 148:63–68.

346. Morsing P, Velazquez H, Wright FS, Ellison DH. Adaptation of distal convoluted tubule of rats. II. Effects of chronic thiazide infusion. The American journal of physiology. 1991; 261:F137–143. [PubMed: 1858894]

347. Mu S, Shimosawa T, Ogura S, Wang H, Uetake Y, Kawakami-Mori F, Marumo T, Yatomi Y, Geller DS, Tanaka H, Fujita T. Epigenetic modulation of the renal beta-adrenergic-WNK4 pathway in salt-sensitive hypertension. Nature medicine. 2011; 17:573–580.

348. Murthy M, Cope G, O'Shaughnessy KM. The acidic motif of WNK4 is crucial for its interaction with the K channel ROMK. Biochemical and biophysical research communications. 2008; 375:651–654. [PubMed: 18755144]

349. Mutig K, Paliege A, Kahl T, Jons T, Muller-Esterl W, Bachmann S. Vasopressin V2 receptor expression along rat, mouse, and human renal epithelia with focus on TAL. American journal of physiology Renal physiology. 2007; 293:F1166–1177. [PubMed: 17626156]

350. Mutig K, Saritas T, Uchida S, Kahl T, Borowski T, Paliege A, Bohlick A, Bleich M, Shan Q, Bachmann S. Short-term stimulation of the thiazide-sensitive Na+-Cl- cotransporter by vasopressin involves phosphorylation and membrane translocation. Am J Physiol Renal Physiol. 2010; 298:F502–509. [PubMed: 20007345]

351. Muto S, Yasoshima K, Yoshitomi K, Imai M, Asano Y. Electrophysiological identification of a- and b-intercalated cells and their distribution along the rabbit distal nephron segments. JClinInvest. 1990; 86:1829–1839.

352. Naziroglu M. New molecular mechanisms on the activation of TRPM2 channels by oxidative stress and ADP-ribose. Neurochemical research. 2007; 32:1990–2001. [PubMed: 17562166]

353. Needham PG, Mikoluk K, Dhakarwal P, Khadem S, Snyder AC, Subramanya AR, Brodsky JL. The thiazide-sensitive NaCl cotransporter is targeted for chaperone-dependent endoplasmic reticulum-associated degradation. The Journal of biological chemistry. 2011; 286:43611–43621. [PubMed: 22027832]

354. Nguyen MT, Lee DH, Delpire E, McDonough AA. Differential regulation of Na+ transporters along nephron during ANG II-dependent hypertension: distal stimulation counteracted by proximal inhibition. American journal of physiology Renal physiology. 2013; 305:F510–519. [PubMed: 23720346]

355. Nijenhuis T, Hoenderop JG, Bindels RJ. Downregulation of Ca(2+) and Mg(2+) transport proteins in the kidney explains tacrolimus (FK506)-induced hypercalciuria and hypomagnesemia. Journal of the American Society of Nephrology: JASN. 2004; 15:549–557. [PubMed: 14978156]

356. Nijenhuis T, Hoenderop JG, Loffing J, van der Kemp AW, van Os CH, Bindels RJ. Thiazide-induced hypocalciuria is accompanied by a decreased expression of Ca2+ transport proteins in kidney. Kidney international. 2003; 64:555–564. [PubMed: 12846750]

357. Nijenhuis T, Renkema KY, Hoenderop JG, Bindels RJ. Acid-base status determines the renal expression of Ca2+ and Mg2+ transport proteins. Journal of the American Society of Nephrology: JASN. 2006; 17:617–626. [PubMed: 16421227]

358. Nijenhuis T, Renkema KY, Hoenderop JG, Bindels RJ. Acid-base status determines the renal expression of Ca2+ and Mg2+ transport proteins. J Am Soc Nephrol. 2006; 17:617–626. [PubMed: 16421227]

359. Nijenhuis T, Vallon V, van der Kemp AW, Loffing J, Hoenderop JG, Bindels RJ. Enhanced passive Ca2+ reabsorption and reduced Mg2+ channel abundance explains thiazide-induced hypocalciuria and hypomagnesemia. J Clin Invest. 2005; 115:1651–1658. [PubMed: 15902302]

360. Nijenhuis T, Vallon V, van der Kemp AW, Loffing J, Hoenderop JG, Bindels RJ. Enhanced passive Ca2+ reabsorption and reduced Mg2+ channel abundance explains thiazide-induced hypocalciuria and hypomagnesemia. J Clin Invest. 2005; 115:1651–1658. [PubMed: 15902302]

361. Nilius B, Prenen J, Vennekens R, Hoenderop JG, Bindels RJ, Droogmans G. Modulation of the epithelial calcium channel, ECaC, by intracellular Ca2+ Cell calcium. 2001; 29:417–428. [PubMed: 11352507]

362. Nilius B, Weidema F, Prenen J, Hoenderop JG, Vennekens R, Hoefs S, Droogmans G, Bindels RJ. The carboxyl terminus of the epithelial Ca(2+) channel ECaC1 is involved in Ca(2+)-dependent inactivation. Pflugers Archiv: European journal of physiology. 2003; 445:584–588. [PubMed: 12634930]

363. Nishida H, Sohara E, Nomura N, Chiga M, Alessi DR, Rai T, Sasaki S, Uchida S. Phosphatidylinositol 3-kinase/Akt signaling pathway activates the WNK-OSR1/SPAK-NCC phosphorylation cascade in hyperinsulinemic db/db mice. Hypertension. 2012; 60:981–990. [PubMed: 22949526]

364. O'Reilly M, Marshall E, Macgillivray T, Mittal M, Xue W, Kenyon CJ, Brown RW. Dietary Electrolyte-Driven Responses in the Renal WNK Kinase Pathway In Vivo. J Am Soc Nephrol. 2006; 17:2402–2413. [PubMed: 16899520]

365. O'Reilly M, Marshall E, Speirs HJ, Brown RW. WNK1, a Gene within a Novel Blood Pressure Control Pathway, Tissue-Specifically Generates Radically Different Isoforms with and without a Kinase Domain. Journal of the American Society of Nephrology: JASN. 2003; 14:2447–2456. [PubMed: 14514722]

366. Obermuller N, Bernstein P, Velazquez H, Reilly R, Moser D, Ellison DH, Bachmann S. Expression of the thiazide-sensitive Na-Cl cotransporter in rat and human kidney. The American journal of physiology. 1995; 269:F900–910. [PubMed: 8594886]

367. Obermüller N, Bernstein PL, Velázquez H, Reilly R, Moser D, Ellison DH, Bachmann S. Expression of the thiazide-sensitive Na-Cl cotransporter in rat and human kidney. Am J Physiol. 1995; 269:F900–F910. [PubMed: 8594886]

368. Ohno M, Uchida K, Ohashi T, Nitta K, Ohta A, Chiga M, Sasaki S, Uchida S. Immunolocalization of WNK4 in mouse kidney. Histochemistry and cell biology. 2011; 136:25–35. [PubMed: 21660484]

369. Ohta A, Rai T, Yui N, Chiga M, Yang SS, Lin SH, Sohara E, Sasaki S, Uchida S. Targeted disruption of the Wnk4 gene decreases phosphorylation of Na-Cl cotransporter, increases Na excretion, and lowers blood pressure. Hum Mol Genet. 2009

370. Ohta A, Schumacher FR, Mehellou Y, Johnson C, Knebel A, Macartney TJ, Wood NT, Alessi DR, Kurz T. The CUL3-KLHL3 E3 ligase complex mutated in Gordon's hypertension syndrome interacts with and ubiquitylates WNK isoforms: disease-causing mutations in KLHL3 and WNK4 disrupt interaction. Biochem J. 2013; 451:111–122. [PubMed: 23387299]

371. Oi K, Sohara E, Rai T, Misawa M, Chiga M, Alessi DR, Sasaki S, Uchida S. A minor role of WNK3 in regulating phosphorylation of renal NKCC2 and NCC co-transporters in vivo. Biology open. 2012; 1:120–127. [PubMed: 23213404]

372. Oi K, Sohara E, Rai T, Misawa M, Chiga M, Alessi DR, Sasaki S, Uchida S. A minor role of WNK3 in regulating phosphorylation of renal NKCC2 and NCC co-transporters in vivo. Biology open. 2012; 1:120–127. [PubMed: 23213404]

373. Okusa, MD., Ellison, DH. Physiology and pathophysiology of diuretic action. In: Alpern, RJ., Hebert, SC., editors. The Kidney: Physiology and Pathophysiology. Amsterdam: Elsevier; 2008. p. 1051-1984.

374. Okusa MD, Velazquez H, Ellison DH, Wright FS. Luminal calcium regulates potassium transport by the renal distal tubule. The American journal of physiology. 1990; 258:F423–428. [PubMed: 2309896]

375. Okusa MD, Velazquez H, Ellison DH, Wright FS. Luminal calcium regulates potassium transport by the renal distal tubule. The American journal of physiology. 1990 Feb.258:F423–428. [PubMed: 2309896]

376. Pacheco-Alvarez D, Cristobal PS, Meade P, Moreno E, Vazquez N, Munoz E, Diaz A, Juarez ME, Gimenez I, Gamba G. The Na+:Cl- cotransporter is activated and phosphorylated at the amino-terminal domain upon intracellular chloride depletion. J Biol Chem. 2006; 281:28755–28763. [PubMed: 16887815]

377. Palmer LG. Epithelial Na channels: The nature of the conducting pore. Renal PhysiolBiochem. 1990; 13:51–58.

378. Panichpisal K, Angulo-Pernett F, Selhi S, Nugent KM. Gitelman-like syndrome after cisplatin therapy: a case report and literature review. BMC Nephrol. 2006; 7:10. [PubMed: 16723030]

379. Pathare G, Hoenderop JG, Bindels RJ, San-Cristobal P. A molecular update on Pseudohypoaldosteronism type II. American journal of physiology Renal physiology. 2013

380. Patschan D, Loddenkemper K, Buttgereit F. Molecular mechanisms of glucocorticoid-induced osteoporosis. Bone. 2001; 29:498–505. [PubMed: 11728918]

381. Paver WK, Pauline GJ. Hypertension and hyperpotassemia without renal disease in a young male. Med J Aust. 1964; 2:305–306. [PubMed: 14194482]
382. Pedersen NB, Hofmeister MV, Rosenbaek LL, Nielsen J, Fenton RA. Vasopressin induces phosphorylation of the thiazide-sensitive sodium chloride cotransporter in the distal convoluted tubule. Kidney international. 2010; 78:160–169. [PubMed: 20445498]
383. Pedersen NB, Hofmeister MV, Rosenbaek LL, Nielsen J, Fenton RA. Vasopressin induces phosphorylation of the thiazide-sensitive sodium chloride cotransporter in the distal convoluted tubule. Kidney Int. 2010; 78:160–169. [PubMed: 20445498]
384. Peng JB, Bell PD. Cellular mechanisms of WNK4-mediated regulation of ion transport proteins in the distal tubule. Kidney Int. 2006; 69:2116–2118. [PubMed: 16761023]
385. Peterson LN, Wright FS. Effect of sodium intake on renal potassium excretion. AmJPhysiol. 1977; 233:F225–F234.
386. Petty KJ, Kokko JP, Marver D. Secondary effect of aldosterone on Na-K ATPase activity in the rabbit cortical collecting tubule. JClinInvest. 1981; 68:1514–1521.
387. Picard N, Van Abel M, Campone C, Seiler M, Bloch-Faure M, Hoenderop JG, Loffing J, Meneton P, Bindels RJ, Paillard M, Alhenc-Gelas F, Houillier P. Tissue kallikrein-deficient mice display a defect in renal tubular calcium absorption. J Am Soc Nephrol. 2005; 16:3602–3610. [PubMed: 16251243]
388. Piechotta K, Lu J, Delpire E. Cation chloride cotransporters interact with the stress-related kinases Ste20-related proline-alanine-rich kinase (SPAK) and oxidative stress response 1 (OSR1). J Biol Chem. 2002 Dec 27.277:50812–50819. [PubMed: 12386165]
389. Pitt B. Effect of aldosterone blockade in patients with systolic left ventricular dysfunction: implications of the RALES and EPHESUS studies. Molecular and cellular endocrinology. 2004; 217:53–58. [PubMed: 15134801]
390. Plotkin MD, Kaplan MR, Verlander JW, Lee W-S, Brown D, Poch E, Gullans SR, Hebert SC. Localization of the thiazide sensitive Na-Cl cotransporter, rTSC1, in the rat kidney. Kidney Int. 1996; 50:174–183. [PubMed: 8807586]
391. Pluznick JL, Wei P, Grimm PR, Sansom SC. BK-{beta}1 subunit: immunolocalization in the mammalian connecting tubule and its role in the kaliuretic response to volume expansion. Am J Physiol Renal Physiol. 2005; 288:F846–854. [PubMed: 15613616]
392. Quamme GA. Effect of calcitonin on calcium and magnesium transport in rat nephron. The American journal of physiology. 1980 Jun.238:E573–578. [PubMed: 7386624]
393. Quamme GA. Renal magnesium handling: new insights in understanding old problems. Kidney Int. 1997; 52:1180–1195. [PubMed: 9350641]
394. Quamme GA, Dirks JH. Intraluminal and contraluminal magnesium on magnesium and calcium transfer in the rat nephron. The American journal of physiology. 1980 Mar.238:F187–198. [PubMed: 7369360]
395. Quamme GA, Dirks JH. Magnesium transport in the nephron. The American journal of physiology. 1980 Nov.239:F393–401. [PubMed: 7435614]
396. Rafiqi FH, Zuber AM, Glover M, Richardson C, Fleming S, Jovanovic S, Jovanovic A, O'Shaughnessy KM, Alessi DR. Role of the WNK-activated SPAK kinase in regulating blood pressure. EMBO Mol Med. 2010
397. Reichold M, Zdebik AA, Lieberer E, Rapedius M, Schmidt K, Bandulik S, Sterner C, Tegtmeier I, Penton D, Baukrowitz T, Hulton SA, Witzgall R, Ben-Zeev B, Howie AJ, Kleta R, Bockenhauer D, Warth R. KCNJ10 gene mutations causing EAST syndrome (epilepsy, ataxia, sensorineural deafness, and tubulopathy) disrupt channel function. Proceedings of the National Academy of Sciences of the United States of America. 2010; 107:14490–14495. [PubMed: 20651251]
398. Reid IR. Glucocorticoid osteoporosis--mechanisms and management. European journal of endocrinology/European Federation of Endocrine Societies. 1997; 137:209–217.
399. Reif MC, Troutman SL, Schafer JA. Sodium transport by rat cortical collecting tubule. effects of vasopressin and desoxycorticosterone. JClinInvest. 1986; 1986
400. Reilly RF, Ellison DH. Mammalian distal tubule: physiology, pathophysiology, and molecular anatomy. Physiol Rev. 2000; 80:277–313. [PubMed: 10617770]

401. Reilly RF, Huang CL. The mechanism of hypocalciuria with NaCl cotransporter inhibition. Nature reviews Nephrology. 2011; 7:669–674. [PubMed: 21947122]

402. Rempe DA, Takano T, Nedergaard M. TR(I)Pping towards treatment for ischemia. Nature neuroscience. 2009; 12:1215–1216. [PubMed: 19783978]

403. Rengarajan S, Lee DH, Oh YT, Delpire E, Youn JH, McDonough AA. Increasing Plasma [K+] by Intravenous Potassium Infusion Reduces NCC Phosphorylation and Drives Kaliuresis and Natriuresis. American journal of physiology Renal physiology. 2014

404. Rhoten WB, Bruns ME, Christakos S. Presence and localization of two vitamin D-dependent calcium binding proteins in kidneys of higher vertebrates. Endocrinology. 1985 Aug.117:674–683. [PubMed: 3926460]

405. Riazi S, Madala-Halagappa VK, Hu X, Ecelbarger CA. Sex and body-type interactions in the regulation of renal sodium transporter levels, urinary excretion, and activity in lean and obese Zucker rats. Gender medicine. 2006; 3:309–327. [PubMed: 17582372]

406. Riazi S, Maric C, Ecelbarger CA. 17-beta Estradiol attenuates streptozotocin-induced diabetes and regulates the expression of renal sodium transporters. Kidney Int. 2006; 69:471–480. [PubMed: 16514430]

407. Riccardi D, Lee W-S, Lee K, Segre GV, Brown EM, Hebert SC. Localization of the extracellular Ca2+-sensing receptor and PTH/PTHrP receptor in rat kidney. AmJPhysiol. 1996; 271:F951–F956.

408. Richardson C, Rafiqi FH, Karlsson HK, Moleleki N, Vandewalle A, Campbell DG, Morrice NA, Alessi DR. Activation of the thiazide-sensitive Na+-Cl- cotransporter by the WNK-regulated kinases SPAK and OSR1. J Cell Sci. 2008; 121:675–684. [PubMed: 18270262]

409. Richardson C, Sakamoto K, de Los Heros P, Deak M, Campbell DG, Prescott AR, Alessi DR. Regulation of the NKCC2 ion cotransporter by SPAK-OSR1-dependent and -independent pathways. J Cell Sci. 2011; 124:789–800. [PubMed: 21321328]

410. Rieg T, Tang T, Uchida S, Hammond HK, Fenton RA, Vallon V. Adenylyl cyclase 6 enhances NKCC2 expression and mediates vasopressin-induced phosphorylation of NKCC2 and NCC. The American journal of pathology. 2013; 182:96–106. [PubMed: 23123217]

411. Rinehart J, Kahle KT, de Los Heros P, Vazquez N, Meade P, Wilson FH, Hebert SC, Gimenez I, Gamba G, Lifton RP. WNK3 kinase is a positive regulator of NKCC2 and NCC, renal cation-Cl-cotransporters required for normal blood pressure homeostasis. Proc Natl Acad Sci U S A. 2005; 102:16777–16782. [PubMed: 16275913]

412. Ring AM, Cheng SX, Leng Q, Kahle KT, Rinehart J, Lalioti MD, Volkman HM, Wilson FH, Hebert SC, Lifton RP. WNK4 regulates activity of the epithelial Na+ channel in vitro and in vivo. Proc Natl Acad Sci U S A. 2007; 104:4020–4024. [PubMed: 17360470]

413. Rivard CJ, Almeida NE, Berl T, Capasso JM. The gamma subunit of Na/K-ATPase: an exceptional, small transmembrane protein. Front Biosci. 2005; 10:2604–2610. [PubMed: 15970522]

414. Rodan AR, Cheng CJ, Huang CL. Recent advances in distal tubular potassium handling. Am J Physiol Renal Physiol. 2011; 300:F821–827. [PubMed: 21270092]

415. Ronzaud C, Loffing-Cueni D, Hausel P, Debonneville A, Malsure SR, Fowler-Jaeger N, Boase NA, Perrier R, Maillard M, Yang B, Stokes JB, Koesters R, Kumar S, Hummler E, Loffing J, Staub O. Nedd4-2 deficiency in the nephron causes elevated salt-dependent blood pressure involving thiazide-sensitive Na-Cl-cotransport. J Clin Invest. 2013; 123:657–665. [PubMed: 23348737]

416. Ronzaud C, Loffing-Cueni D, Hausel P, Debonneville A, Malsure SR, Fowler-Jaeger N, Boase NA, Perrier R, Maillard M, Yang B, Stokes JB, Koesters R, Kumar S, Hummler E, Loffing J, Staub O. Renal tubular NEDD4-2 deficiency causes NCC-mediated salt-dependent hypertension. J Clin Invest. 2013; 123:657–665. [PubMed: 23348737]

417. Rosenbaek LL, Kortenoeven ML, Aroankins TS, Fenton RA. Phosphorylation Decreases Ubiquitylation of the Thiazide-sensitive Co-transporter NCC and Subsequent Clathrin-mediated Endocytosis. The Journal of biological chemistry. 2014

418. Royaux IE, Wall SM, Karniski LP, Everett LA, Suzuki K, Knepper MA, Green ED. Pendrin, encoded by the Pendred syndrome gene, resides in the apical region of renal intercalated cells

and mediates bicarbonate secretion. Proceedings of the National Academy of Sciences of the United States of America. 2001; 98:4221–4226. [PubMed: 11274445]

419. Rozansky DJ, Cornwall T, Subramanya AR, Rogers S, Yang YF, David LL, Zhu X, Yang CL, Ellison DH. Aldosterone mediates activation of the thiazide-sensitive Na-Cl cotransporter through an SGK1 and WNK4 signaling pathway. J Clin Invest. 2009; 119:2601–2612. [PubMed: 19690383]
420. Runyan AL, Sun Y, Bhattacharya SK, Ahokas RA, Chhokar VS, Gerling IC, Weber KT. Responses in extracellular and intracellular calcium and magnesium in aldosteronism. The Journal of laboratory and clinical medicine. 2005; 146:76–84. [PubMed: 16099237]
421. Sabath E, Meade P, Berkman J, de los Heros P, Moreno E, Bobadilla NA, Vazquez N, Ellison DH, Gamba G. Pathophysiology of functional mutations of the thiazide-sensitive Na-Cl cotransporter in Gitelman disease. American journal of physiology Renal physiology. 2004; 287:F195–203. [PubMed: 15068971]
422. Sala-Rabanal M, Kucheryavykh LY, Skatchkov SN, Eaton MJ, Nichols CG. Molecular mechanisms of EAST/SeSAME syndrome mutations in Kir4.1 (KCNJ10). J Biol Chem. 2010; 285:36040–36048. [PubMed: 20807765]
423. San-Cristobal P, Pacheco-Alvarez D, Richardson C, Ring AM, Vazquez N, Rafiqi FH, Chari D, Kahle KT, Leng Q, Bobadilla NA, Hebert SC, Alessi DR, Lifton RP, Gamba G. Angiotensin II signaling increases activity of the renal Na-Cl cotransporter through a WNK4-SPAK-dependent pathway. Proceedings of the National Academy of Sciences of the United States of America. 2009; 106:4384–4389. [PubMed: 19240212]
424. Sandberg MB, Maunsbach AB, McDonough AA. Redistribution of distal tubule Na+-Cl- cotransporter (NCC) in response to a high-salt diet. Am J Physiol Renal Physiol. 2006; 291:F503–508. [PubMed: 16554416]
425. Sandberg MB, Maunsbach AB, McDonough AA. Redistribution of distal tubule Na+-Cl- cotransporter (NCC) in response to a high-salt diet. Am J Physiol Renal Physiol. 2006; 291:F503–508. [PubMed: 16554416]
426. Sandberg MB, Riquier AD, Pihakaski-Maunsbach K, McDonough AA, Maunsbach AB. ANG II provokes acute trafficking of distal tubule Na+-Cl cotransporter to apical membrane. Am J Physiol Renal Physiol. 2007; 293:F662–669. [PubMed: 17507603]
427. Sansom SC, Stockand JD. Physiological role of large, Ca2+-activated K+ channels in human glomerular mesangial cells. Clinical and experimental pharmacology & physiology. 1996; 23:76–82. [PubMed: 8713500]
428. Saritas T, Borschewski A, McCormick JA, Paliege A, Dathe C, Uchida S, Terker A, Himmerkus N, Bleich M, Demaretz S, Laghmani K, Delpire E, Ellison DH, Bachmann S, Mutig K. SPAK differentially mediates vasopressin effects on sodium cotransporters. J Am Soc Nephrol. 2013; 24:407–418. [PubMed: 23393317]
429. Scherzer P, Wald H, Popovtzer MM. Enhanced glomerular filtration and Na+-K+-ATPase with furosemide administration. AmJPhysiol. 1987; 252:F910–F915.
430. Schlanger LE, Kleyman TR, Ling BN. K(+)-sparing actions of trimethoprim: inhibition of Na + channels in A6 distal nephron cells. Kidney Int. 1994; 45:1070–1076. [PubMed: 8007576]
431. Schlatter E, Schafer JA. Electrophysiological studies in pricipal cells of rat cortical collecting tubules: ADH increases the apical membrane Na+-conductance. Pflügers Archives. 1987; 409:81–92. [PubMed: 2441357]
432. Schlingmann KP, Weber S, Peters M, Niemann Nejsum L, Vitzthum H, Klingel K, Kratz M, Haddad E, Ristoff E, Dinour D, Syrrou M, Nielsen S, Sassen M, Waldegger S, Seyberth HW, Konrad M. Hypomagnesemia with secondary hypocalcemia is caused by mutations in TRPM6, a new member of the TRPM gene family. Nature genetics. 2002; 31:166–170. [PubMed: 12032568]
433. Schmidt U, Dubach UC. Activity of (Na+ K+)-stimulated adenosintriphospatase in the rat nephron. Pflügers Arch. 1969; 306:219–226. [PubMed: 4238475]
434. Schmitt R, Ellison DH, Farman N, Rossier B, Reilly RF, Kunchaparty S, Reeves WB, Oberbäumer I, Tapp R, Bachmann S. Developmental expression of sodium entry pathways in rat distal nephron. Am J Physiol. 1999; 276:F367–F381. [PubMed: 10070160]

435. Schnermann J, Briggs JP, Schubert G. In situ studies of the distal convoluted tubule in the rat. I. Evidence for NaCl secretion. AmJPhysiol. 1982; 243:F160–F166.

436. Scholl UI, Choi M, Liu T, Ramaekers VT, Hausler MG, Grimmer J, Tobe SW, Farhi A, Nelson-Williams C, Lifton RP. Seizures, sensorineural deafness, ataxia, mental retardation, and electrolyte imbalance (SeSAME syndrome) caused by mutations in KCNJ10. Proceedings of the National Academy of Sciences of the United States of America. 2009; 106:5842–5847. [PubMed: 19289823]

437. Schreiner DS, Jande SS, Parkes CO, Lawson DE, Thomasset M. Immunocytochemical demonstration of two vitamin D-dependent calcium- binding proteins in mammalian kidney. Acta Anat (Basel). 1983; 117:1–14. [PubMed: 6356760]

438. Schrier RW. Aldosterone 'escape' vs 'breakthrough'. Nature reviews Nephrology. 2010; 6:61.

439. Schultheis PJ, Lorenz JN, Meneton P, Nieman ML, Riddle TM, Flagella M, Duffy JJ, Doetschman T, Miller ML, Shull GE. Phenotype resembling Gitelman's syndrome in mice lacking the apical Na+-Cl- cotransporter of the distal convoluted tubule. JBiolChem. 1998 Oct 30.273:29150–29155.

440. Schultheis PJ, Lorenz JN, Meneton P, Nieman ML, Riddle TM, Flagella M, Duffy JJ, Doetschman T, Miller ML, Shull GE. Phenotype resembling Gitelman's syndrome in mice lacking the apical Na+-Cl-cotransporter of the distal convoluted tubule. J Biol Chem. 1998; 273:29150–29155. [PubMed: 9786924]

441. Schweigel M, Martens H. Magnesium transport in the gastrointestinal tract. Frontiers in bioscience: a journal and virtual library. 2000; 5:D666–677. [PubMed: 10922297]

442. Schweigel M, Vormann J, Martens H. Mechanisms of Mg(2+) transport in cultured ruminal epithelial cells. American journal of physiology Gastrointestinal and liver physiology. 2000; 278:G400–408. [PubMed: 10712259]

443. Scoble JE, Mills S, Hruska KA. Calcium transport in canine renal basolateral membrane vesicles. Effects of parathyroid hormone. J Clin Invest. 1985; 75:1096–1105. [PubMed: 3988932]

444. Seyberth HW, Schlingmann KP. Bartter- and Gitelman-like syndromes: salt-losing tubulopathies with loop or DCT defects. Pediatric nephrology. 2011; 26:1789–1802. [PubMed: 21503667]

445. Shao L, Lang Y, Wang Y, Gao Y, Zhang W, Niu H, Liu S, Chen N. High-frequency variant p.T60M in NaCl cotransporter and blood pressure variability in Han Chinese. American journal of nephrology. 2012; 35:515–519. [PubMed: 22627394]

446. Shao L, Ren H, Wang W, Zhang W, Feng X, Li X, Chen N. Novel SLC12A3 mutations in Chinese patients with Gitelman's syndrome. Nephron Physiology. 2008; 108:p29–36. [PubMed: 18287808]

447. Shapiro RJ, Yong CK, Quamme GA. Influence of chronic dietary acid on renal tubular handling of magnesium. Pflugers Archiv: European journal of physiology. 1987; 409:492–498. [PubMed: 3627965]

448. Shekarabi M, Girard N, Riviere JB, Dion P, Houle M, Toulouse A, Lafreniere RG, Vercauteren F, Hince P, Laganiere J, Rochefort D, Faivre L, Samuels M, Rouleau GA. Mutations in the nervous system-specific HSN2 exon of WNK1 cause hereditary sensory neuropathy type II. J Clin Invest. 2008

449. Shibata S, Zhang J, Puthumana J, Stone KL, Lifton RP. Kelch-like 3 and Cullin 3 regulate electrolyte homeostasis via ubiquitination and degradation of WNK4. Proceedings of the National Academy of Sciences of the United States of America. 2013; 110:7838–7843. [PubMed: 23576762]

450. Shibata S, Zhang J, Puthumana J, Stone KL, Lifton RP. Kelch-like 3 and Cullin 3 regulate electrolyte homeostasis via ubiquitination and degradation of WNK4. Proceedings of the National Academy of Sciences of the United States of America. 2013

451. Shimizu T, Nakamura M, Yoshitomi K, Imai M. Effects of prostaglandin E2 on membrane voltage of the connecting tubule and cortical collecting duct from rabbits. J Physiol (Lond). 1993 Mar. 462:275–289. [PubMed: 8331584]

452. Shimizu T, Nakamura M, Yoshitomi K, Imai M. Interaction of trichlormethiazide or amiloride with PTH in stimulating Ca2+ absorption in rabbit CNT. AmJPhysiol. 1991; 261:F36–F43.

453. Shimizu T, Yoshitomi K, Nakamura M, Imai M. Effects of PTH, calcitonin, and cAMP on calcium transport in rabbit distal nephron segments. The American journal of physiology. 1990; 259:F408–414. [PubMed: 1697736]
454. Shimizu T, Yoshitomi K, Nakamura M, Imai M. Site and mechanism of action of trichlormethiazide in rabbit distal nephron segments perfused in vitro. JClinInvest. 1988; 82:721–730.
455. Simon DB, Karet FE, Rodriguez-Soriano J, Hamdan JH, DiPietro A, Trachtman H, Sanjad SA, Lifton RP. Genetic heterogeneity of Bartter's syndrome revealed by mutations in the K+ channel, ROMK. Nature genetics. 1996; 14:152–156. [PubMed: 8841184]
456. Simon DB, Lu Y, Choate KA, Velazquez H, Al-Sabban E, Praga M, Casari G, Bettinelli A, Colussi G, Rodriguez-Soriano J, McCredie D, Milford D, Sanjad S, Lifton RP. Paracellin-1, a renal tight junction protein required for paracellular Mg2+ resorption [see comments]. Science. 1999 Jul 2.285:103–106. [PubMed: 10390358]
457. Simon DB, Nelson-Williams C, Bia MJ, Ellison D, Karet FE, Molina AM, Vaara I, Iwata F, Cushner HM, Koolen M, Gainza FJ, Gitleman HJ, Lifton RP. Gitelman's variant of Bartter's syndrome, inherited hypokalaemic alkalosis, is caused by mutations in the thiazide-sensitive Na-Cl cotransporter. Nature genetics. 1996; 12:24–30. [PubMed: 8528245]
458. Singer JD, Gurian-West M, Clurman B, Roberts JM. Cullin-3 targets cyclin E for ubiquitination and controls S phase in mammalian cells. Genes & development. 1999; 13:2375–2387. [PubMed: 10500095]
459. Sohara E, Rai T, Yang SS, Ohta A, Naito S, Chiga M, Nomura N, Lin SH, Vandewalle A, Ohta E, Sasaki S, Uchida S. Acute insulin stimulation induces phosphorylation of the Na-Cl cotransporter in cultured distal mpkDCT cells and mouse kidney. PloS one. 2011; 6:e24277. [PubMed: 21909387]
460. Soleimani M, Barone S, Xu J, Shull GE, Siddiqui F, Zahedi K, Amlal H. Double knockout of pendrin and Na-Cl cotransporter (NCC) causes severe salt wasting, volume depletion, and renal failure. Proceedings of the National Academy of Sciences of the United States of America. 2012; 109:13368–13373. [PubMed: 22847418]
461. Somasekharan S, Tanis J, Forbush B. Loop diuretic and ion-binding residues revealed by scanning mutagenesis of transmembrane helix 3 (TM3) of Na-K-Cl cotransporter (NKCC1). J Biol Chem. 2012; 287:17308–17317. [PubMed: 22437837]
462. Song J, Hu X, Khan O, Tian Y, Verbalis JG, Ecelbarger CA. Increased blood pressure, aldosterone activity, and regional differences in renal ENaC protein during vasopressin escape. Am J Physiol Renal Physiol. 2004; 287:F1076–1083. [PubMed: 15226153]
463. Sontia B, Montezano AC, Paravicini T, Tabet F, Touyz RM. Downregulation of renal TRPM7 and increased inflammation and fibrosis in aldosterone-infused mice: effects of magnesium. Hypertension. 2008; 51:915–921. [PubMed: 18268139]
464. Sorensen MV, Grossmann S, Roesinger M, Gresko N, Todkar AP, Barmettler G, Ziegler U, Odermatt A, Loffing-Cueni D, Loffing J. Rapid dephosphorylation of the renal sodium chloride cotransporter in response to oral potassium intake in mice. Kidney international. 2013; 83:811–824. [PubMed: 23447069]
465. Sperber J. Studies of the mammalian kidney. ZoolBidrag. 1944; 22:249–431.
466. Stanton BA, Biemesderfer D, Wade JB, Giebisch G. Structural and functional study of the rat distal nephron: effects of potassium adaptation and depletion. Kidney Int. 1981; 19:36–48. [PubMed: 7218667]
467. Stanton BA, Giebisch G. Effects of pH on potassium transport by renal distal tubule. AmJPhysiol. 1982; 242:F544–F551.
468. Stanton BA, Giebisch G. Potassium transport by the renal distal tubule: effects of potassium loading. AmJPhysiol. 1982; 243:F487–F493.
469. Stanton BA, Kaissling B. Adaptation of distal tubule and collecting duct to increased sodium delivery. II. Na+ and K+ transport. AmJPhysiol. 1988; 255:F1269–F1275.
470. Stanton BA, Kaissling B. Regulation of renal ion transport and cell growth by sodium. AmJPhysiol. 1989; 257:F1–F10.

471. Staruschenko A. Regulation of transport in the connecting tubule and cortical collecting duct. Compr Physiol. 2012; 2:1541–1584. [PubMed: 23227301]
472. Stevens CF, Williams JH. "Kiss and run" exocytosis at hippocampal synapses. Proceedings of the National Academy of Sciences of the United States of America. 2000; 97:12828–12833. [PubMed: 11050187]
473. Stockand JD, Sansom SC. Glomerular mesangial cells: electrophysiology and regulation of contraction. Physiol Rev. 1998; 78:723–744. [PubMed: 9674692]
474. Stokes JB. Sodium chloride absorption by the urinary bladder of the winter flounder: a thiazide-sensitive electrically neutral transport system. JClinInvest. 1984; 74:7–16.
475. Strehler EE, Caride AJ, Filoteo AG, Xiong Y, Penniston JT, Enyedi A. Plasma membrane Ca2+ ATPases as dynamic regulators of cellular calcium handling. Ann N Y Acad Sci. 2007; 1099:226–236. [PubMed: 17446463]
476. Subramanya AR, Ellison DH. Sorting out Lysosomal Trafficking of the Thiazide-Sensitive Na-Cl Co-transporter. Journal of the American Society of Nephrology: JASN. 2009
477. Subramanya AR, Ellison DH. Sorting out lysosomal trafficking of the thiazide-sensitive Na-Cl Co-transporter. Journal of the American Society of Nephrology: JASN. 2010; 21:7–9. [PubMed: 19959708]
478. Subramanya AR, Liu J, Ellison DH, Wade JB, Welling PA. WNK4 Diverts the Thiazide-sensitive NaCl Cotransporter to the Lysosome and Stimulates AP-3 Interaction. The Journal of biological chemistry. 2009; 284:18471–18480. [PubMed: 19401467]
479. Subramanya AR, Yang CL, Zhu X, Ellison DH. Dominant-negative regulation of WNK1 by its kidney-specific kinase-defective isoform. Am J Physiol Renal Physiol. 2006; 290:F619–624. [PubMed: 16204408]
480. Sugimoto Y, Namba T, Shigemoto R, Negishi M, Ichikawa A, Narumiya S. Distinct cellular localization of mRNAs for three subtypes of prostaglandin E receptor in kidney. The American journal of physiology. 1994; 266:F823–828. [PubMed: 8203567]
481. Sun HS, Jackson MF, Martin LJ, Jansen K, Teves L, Cui H, Kiyonaka S, Mori Y, Jones M, Forder JP, Golde TE, Orser BA, Macdonald JF, Tymianski M. Suppression of hippocampal TRPM7 protein prevents delayed neuronal death in brain ischemia. Nature neuroscience. 2009; 12:1300–1307. [PubMed: 19734892]
482. Sun P, Lin DH, Wang T, Babilonia E, Wang Z, Jin Y, Kemp R, Nasjletti A, Wang WH. Low Na intake suppresses expression of CYP2C23 and arachidonic acid-induced inhibition of ENaC. Am J Physiol Renal Physiol. 2006; 291:F1192–1200. [PubMed: 16849695]
483. Sun P, Liu W, Lin DH, Yue P, Kemp R, Satlin LM, Wang WH. Epoxyeicosatrienoic acid activates BK channels in the cortical collecting duct. J Am Soc Nephrol. 2009; 20:513–523. [PubMed: 19073823]
484. Susa K, Kita S, Iwamoto T, Yang SS, Lin SH, Ohta A, Sohara E, Rai T, Sasaki S, Alessi DR, Uchida S. Effect of heterozygous deletion of WNK1 on the WNK-OSR1/SPAK-NCC/NKCC1/NKCC2 signal cascade in the kidney and blood vessels. Clinical and experimental nephrology. 2012; 16:530–538. [PubMed: 22294159]
485. Sutton RA, Wong NL, Dirks JH. Effects of metabolic acidosis and alkalosis on sodium and calcium transport in the dog kidney. Kidney Int. 1979; 15:520–533. [PubMed: 480784]
486. Suzuki Y, Ichikawa Y, Saito E, Homma M. Importance of increased urinary calcium excretion in the development of secondary hyperparathyroidism of patients under glucocorticoid therapy. Metabolism: clinical and experimental. 1983; 32:151–156. [PubMed: 6298567]
487. Takahashi D, Mori T, Nomura N, Khan MZ, Araki Y, Zeniya M, Sohara E, Rai T, Sasaki S, Uchida S. WNK4 is the major WNK kinase positively regulating NCC in the mouse kidney. Bioscience reports. 2014
488. Tang X, Hang D, Sand A, Kofuji P. Variable loss of Kir4.1 channel function in SeSAME syndrome mutations. Biochemical and biophysical research communications. 2010; 399:537–541. [PubMed: 20678478]
489. Taniguchi J, Imai M. Flow-dependent activation of maxi K+ channels in apical membrane of rabbit connecting tubule. J Membr Biol. 1998; 164:35–45. [PubMed: 9636242]

490. Taylor AN, McIntosh JE, Bourdeau JE. Immunocytochemical localization of vitamin D-dependent calcium-binding protein in renal tubules of rabbit, rat, and chick. Kidney international. 1982 May.21:765–773. [PubMed: 6180216]

491. Tejpar S, Piessevaux H, Claes K, Piront P, Hoenderop JG, Verslype C, Van Cutsem E. Magnesium wasting associated with epidermal-growth-factor receptor-targeting antibodies in colorectal cancer: a prospective study. Lancet Oncol. 2007; 8:387–394. [PubMed: 17466895]

492. Terada Y, Knepper MA. Thiazide-sensitive NaCl absorption in rat cortical collecting duct. Am J Physiol Renal, Fluid Electrolyte Physiol. 1990; 259:F519–F528.

493. Terker AS, Yang C-L, McCormick JA, Meermeier NP, Rogers SL, Grossman S, Trompf K, Delpire E, Loffing J, Ellison DH. Sympathetic stimulation of thiazide-sensitive sodium chloride cotransport in the generation of salt-sensitive hypertension. Hypertension. 2014

494. Thannickal VJ, Fanburg BL. Reactive oxygen species in cell signaling. American journal of physiology Lung cellular and molecular physiology. 2000; 279:L1005–1028. [PubMed: 11076791]

495. Thastrup JO, Rafiqi FH, Vitari AC, Pozo-Guisado E, Deak M, Mehellou Y, Alessi DR. SPAK/OSR1 regulate NKCC1 and WNK activity: analysis of WNK isoform interactions and activation by T-loop trans-autophosphorylation. The Biochemical journal. 2012; 441:325–337. [PubMed: 22032326]

496. Thebault S, Alexander RT, Tiel Groenestege WM, Hoenderop JG, Bindels RJ. EGF increases TRPM6 activity and surface expression. J Am Soc Nephrol. 2009; 20:78–85. [PubMed: 19073827]

497. Thebault S, Cao G, Venselaar H, Xi Q, Bindels RJ, Hoenderop JG. Role of the alpha-kinase domain in transient receptor potential melastatin 6 channel and regulation by intracellular ATP. J Biol Chem. 2008; 283:19999–20007. [PubMed: 18490453]

498. Touyz RM, Yao G. Inhibitors of Na+/Mg2+ exchange activity attenuate the development of hypertension in angiotensin II-induced hypertensive rats. Journal of hypertension. 2003; 21:337–344. [PubMed: 12569264]

499. Tran JM, Farrell MA, Fanestil DD. Effect of ions on binding of the thiazide-type diuretic metolazone to kidney membrane. AmJPhysiol. 1990; 258:F908–F915.

500. Tsuruoka S, Nishiki K, Ioka T, Ando H, Saito Y, Kurabayashi M, Nagai R, Fujimura A. Defect in parathyroid-hormone-induced luminal calcium absorption in connecting tubules of Klotho mice. Nephrology, dialysis, transplantation: official publication of the European Dialysis and Transplant Association - European Renal Association. 2006; 21:2762–2767.

501. Turban S, Wang XY, Knepper MA. Regulation of NHE3, NKCC2, and NCC abundance in kidney during aldosterone escape phenomenon: role of NO. Am J Physiol Renal Physiol. 2003; 285:F843–851. [PubMed: 12837683]

502. Uchida S, Sasaki S, Nitta K, Uchida K, Horita S, Nihei H, Marumo F. Localization and functional characterization of rat kidney-specific chloride channel, CIC-K1. JClinInvest. 1995; 95:104–113.

503. Vallon V, Schroth J, Lang F, Kuhl D, Uchida S. Expression and phosphorylation of the Na+-Cl-cotransporter NCC in vivo is regulated by dietary salt, potassium, and SGK1. American journal of physiology Renal physiology. 2009; 297:F704–712. [PubMed: 19570885]

504. Van Abel M, Hoenderop JG, Dardenne O, St Arnaud R, Van Os CH, Van Leeuwen HJ, Bindels RJ. 1,25-dihydroxyvitamin D(3)-independent stimulatory effect of estrogen on the expression of ECaC1 in the kidney. J Am Soc Nephrol. 2002; 13:2102–2109. [PubMed: 12138142]

505. van Abel M, Hoenderop JG, van der Kemp AW, Friedlaender MM, van Leeuwen JP, Bindels RJ. Coordinated control of renal Ca(2+) transport proteins by parathyroid hormone. Kidney Int. 2005; 68:1708–1721. [PubMed: 16164647]

506. van Angelen AA, Glaudemans B, van der Kemp AW, Hoenderop JG, Bindels RJ. Cisplatin-induced injury of the renal distal convoluted tubule is associated with hypomagnesaemia in mice. Nephrology, dialysis, transplantation: official publication of the European Dialysis and Transplant Association - European Renal Association. 2013; 28:879–889.

507. Van Cromphaut SJ, Dewerchin M, Hoenderop JG, Stockmans I, Van Herck E, Kato S, Bindels RJ, Collen D, Carmeliet P, Bouillon R, Carmeliet G. Duodenal calcium absorption in vitamin D

receptor-knockout mice: functional and molecular aspects. Proceedings of the National Academy of Sciences of the United States of America. 2001; 98:13324–13329. [PubMed: 11687634]

508. Van Cromphaut SJ, Rummens K, Stockmans I, Van Herck E, Dijcks FA, Ederveen AG, Carmeliet P, Verhaeghe J, Bouillon R, Carmeliet G. Intestinal calcium transporter genes are upregulated by estrogens and the reproductive cycle through vitamin D receptor-independent mechanisms. Journal of bone and mineral research: the official journal of the American Society for Bone and Mineral Research. 2003; 18:1725–1736.
509. van de Graaf SF, Chang Q, Mensenkamp AR, Hoenderop JG, Bindels RJ. Direct interaction with Rab11a targets the epithelial Ca2+ channels TRPV5 and TRPV6 to the plasma membrane. Molecular and cellular biology. 2006; 26:303–312. [PubMed: 16354700]
510. van de Graaf SF, Hoenderop JG, Gkika D, Lamers D, Prenen J, Rescher U, Gerke V, Staub O, Nilius B, Bindels RJ. Functional expression of the epithelial Ca(2+) channels (TRPV5 and TRPV6) requires association of the S100A10-annexin 2 complex. The EMBO journal. 2003; 22:1478–1487. [PubMed: 12660155]
511. van de Graaf SF, Rescher U, Hoenderop JG, Verkaart S, Bindels RJ, Gerke V. TRPV5 is internalized via clathrin-dependent endocytosis to enter a Ca2+-controlled recycling pathway. J Biol Chem. 2008; 283:4077–4086. [PubMed: 18077461]
512. van der Lubbe N, Lim CH, Fenton RA, Meima ME, Jan Danser AH, Zietse R, Hoorn EJ. Angiotensin II induces phosphorylation of the thiazide-sensitive sodium chloride cotransporter independent of aldosterone. Kidney Int. 2011; 79:66–76. [PubMed: 20720527]
513. van der Lubbe N, Lim CH, Meima ME, van Veghel R, Rosenbaek LL, Mutig K, Danser AH, Fenton RA, Zietse R, Hoorn EJ. Aldosterone does not require angiotensin II to activate NCC through a WNK4-SPAK-dependent pathway. Pflugers Archiv: European journal of physiology. 2012; 463:853–863. [PubMed: 22549242]
514. van der Lubbe N, Moes AD, Rosenbaek LL, Schoep S, Meima ME, Danser AH, Fenton RA, Zietse R, Hoorn EJ. K+-induced natriuresis is preserved during Na+ depletion and accompanied by inhibition of the Na+-Cl- cotransporter. American journal of physiology Renal physiology. 2013; 305:F1177–1188. [PubMed: 23986520]
515. van der Wijst J, Glaudemans B, Venselaar H, Nair AV, Forst AL, Hoenderop JG, Bindels RJ. Functional analysis of the Kv1.1 N255D mutation associated with autosomal dominant hypomagnesemia. J Biol Chem. 2010; 285:171–178. [PubMed: 19903818]
516. Vandewalle A, Cluzeaud F, Bens M, Kieferle S, Steinmeyer K, Jentsch TJ. Localization and induction by dehydration of ClC-K chloride channels in the rat kidney. The American journal of physiology. 1997 May.272:F678–688. [PubMed: 9176380]
517. Velázquez H, Bartiss A, Bernstein PL, Ellison DH. Adrenal steroids stimulate thiazide-sensitive NaCl transport by the rat renal distal tubule. AmJPhysiol. 1996; 270:F211–F219.
518. Velázquez H, Ellison DH, Wright FS. Chloride-dependent potassium secretion in early and late renal distal tubule. AmJPhysiol. 1987; 253:F555–F562.
519. Velázquez H, Good DW, Wright FS. Mutual dependence of sodium and chloride absorption by renal distal tubule. AmJPhysiol. 1984; 247:F904–F911.
520. Velázquez H, Naray-Fejes-Tóth A, Silva T, Andújar E, Reilly RF, Desir GV, Ellison DH. The distal convoluted tubule of the rabbit coexpresses NaCl cotransporter and 11b-hydroxysteroid dehydrogenase. Kidney Int. 1998; 54:464–472. [PubMed: 9690213]
521. Velazquez H, Perazella MA, Wright FS, Ellison DH. Renal mechanism of trimethoprim-induced hyperkalemia. Annals of internal medicine. 1993; 119:296–301. [PubMed: 8328738]
522. Velázquez H, Perazella MA, Wright FS, Ellison DH. Renal mechanism of trimethoprim-induced hyperkalemia. AnnInternMed. 1993; 119:296–301.
523. Velazquez H, Silva T. Cloning and localization of KCC4 in rabbit kidney: expression in distal convoluted tubule. American journal of physiology Renal physiology. 2003; 285:F49–58. [PubMed: 12709395]
524. Velázquez H, Silva T, Andujar E. The rabbit DCT does not express ENaC (amiloride-sensitive) activity. JAmSocNephrol. 1998:47A.

525. Velazquez H, Silva T, Andujar E, Desir GV, Ellison DH, Greger R. The distal convoluted tubule of rabbit kidney does not express a functional sodium channel. American journal of physiology Renal physiology. 2001; 280:F530–539. [PubMed: 11181416]

526. Velázquez H, Wright FS. Effects of diuretic drugs on Na, Cl, and K transport by rat renal distal tubule. AmJPhysiol. 1986; 250:F1013–F1023.

527. Velázquez H, Wright FS, Good DW. Luminal influences on potassium secretion: chloride replacement with sulfate. AmJPhysiol. 1982; 242:F46–F55.

528. Vennekens R, Voets T, Bindels RJ, Droogmans G, Nilius B. Current understanding of mammalian TRP homologues. Cell Calcium. 2002; 31:253–264. [PubMed: 12098215]

529. Verlander JW, Tran TM, Zhang L, Kaplan MR, Hebert SC. Estradiol enhances thiazide-sensitive NaCl cotransporter density in the apical plasma membrane of the distal convoluted tubule in ovariectomized rats. JClinInvest. 1998 Apr 15.101:1661–1669.

530. Vidal-Petiot E, Cheval L, Faugeroux J, Malard T, Doucet A, Jeunemaitre X, Hadchouel J. A new methodology for quantification of alternatively spliced exons reveals a highly tissue-specific expression pattern of WNK1 isoforms. PloS one. 2012; 7:e37751. [PubMed: 22701532]

531. Vidal-Petiot E, Elvira-Matelot E, Mutig K, Soukaseum C, Baudrie V, Wu S, Cheval L, Huc E, Cambillau M, Bachmann S, Doucet A, Jeunemaitre X, Hadchouel J. WNK1-related Familial Hyperkalemic Hypertension results from an increased expression of L-WNK1 specifically in the distal nephron. Proceedings of the National Academy of Sciences of the United States of America. 2013; 110:14366–14371. [PubMed: 23940364]

532. Vitari AC, Deak M, Morrice NA, Alessi DR. The WNK1 and WNK4 protein kinases that are mutated in Gordon's hypertension syndrome phosphorylate and activate SPAK and OSR1 protein kinases. Biochem J. 2005; 391:17–24. [PubMed: 16083423]

533. Vitzthum H, Seniuk A, Schulte LH, Muller ML, Hetz H, Ehmke H. Functional coupling of renal K+ and Na+ handling causes high blood pressure in Na+ replete mice. The Journal of physiology. 2014

534. Voets T, Nilius B, Hoefs S, van der Kemp AW, Droogmans G, Bindels RJ, Hoenderop JG. TRPM6 forms the Mg2+ influx channel involved in intestinal and renal Mg2+ absorption. The Journal of biological chemistry. 2004; 279:19–25. [PubMed: 14576148]

535. Wade JB, Fang L, Coleman RA, Liu J, Grimm PR, Wang T, Welling PA. Differential regulation of ROMK (Kir1.1) in distal nephron segments by dietary potassium. American journal of physiology Renal physiology. 2011; 300:F1385–1393. [PubMed: 21454252]

536. Wade JB, Fang L, Liu J, Li D, Yang CL, Subramanya AR, Maouyo D, Mason A, Ellison DH, Welling PA. WNK1 kinase isoform switch regulates renal potassium excretion. Proceedings of the National Academy of Sciences of the United States of America. 2006; 103:8558–8563. [PubMed: 16709664]

537. Wakabayashi M, Mori T, Isobe K, Sohara E, Susa K, Araki Y, Chiga M, Kikuchi E, Nomura N, Mori Y, Matsuo H, Murata T, Nomura S, Asano T, Kawaguchi H, Nonoyama S, Rai T, Sasaki S, Uchida S. Impaired KLHL3-mediated ubiquitination of WNK4 causes human hypertension. Cell reports. 2013; 3:858–868. [PubMed: 23453970]

538. Wald H, Scherzer P, Popovtzer MM. Inhibition of thick ascending limb Na+-K+-ATPase activity in salt-loaded rats by furosemide. AmJPhysiol. 1989; 256:F549–F555.

539. Walder RY, Landau D, Meyer P, Shalev H, Tsolia M, Borochowitz Z, Boettger MB, Beck GE, Englehardt RK, Carmi R, Sheffield VC. Mutation of TRPM6 causes familial hypomagnesemia with secondary hypocalcemia. Nature genetics. 2002; 31:171–174. [PubMed: 12032570]

540. Walder RY, Shalev H, Brennan TM, Carmi R, Elbedour K, Scott DA, Hanauer A, Mark AL, Patil S, Stone EM, Sheffield VC. Familial hypomagnesemia maps to chromosome 9q, not to the X chromosome: genetic linkage mapping and analysis of a balanced translocation breakpoint. Hum Mol Genet. 1997; 6:1491–1497. [PubMed: 9285786]

541. Wall SM, Hassell KA, Royaux IE, Green ED, Chang JY, Shipley GL, Verlander JW. Localization of pendrin in mouse kidney. American Journal of Physiology - Renal Physiology. 2003; 284:F229–241. [PubMed: 12388426]

542. Wang H, D'Ambrosio MA, Garvin JL, Ren Y, Carretero OA. Connecting tubule glomerular feedback mediates acute tubuloglomerular feedback resetting. American journal of physiology Renal physiology. 2012; 302:F1300–1304. [PubMed: 22357913]
543. Wang H, Garvin JL, D'Ambrosio MA, Ren Y, Carretero OA. Connecting tubule glomerular feedback antagonizes tubuloglomerular feedback in vivo. American journal of physiology Renal physiology. 2010; 299:F1374–1378. [PubMed: 20826574]
544. Wang HR, Liu Z, Huang CL. Domains of WNK1 kinase in the regulation of ROMK1. American journal of physiology Renal physiology. 2008
545. Wang T, Giebisch G. Effects of angiotensin II on electrolyte transport in the early and late distal tubule in rat kidney. AmJPhysiolRenal, Fluid Electrolyte Physiol. 1996; 271:F143–F149.
546. Wang T, Malnic G, Giebisch G, Chan YL. Renal bicarbonate reabsorption in the rat. IV. Bicarbonate transport mechanisms in the early and late distal tubule. JClinInvest. 1993; 91:2776–2784.
547. Wang WH. Two types of K+ channel in thick ascending limb of rat kidney. The American journal of physiology. 1994; 267:F599–605. [PubMed: 7943358]
548. Wang WH, Giebisch G. Dual modulation of renal ATP-sensitive K+ channel by protein kinases A and C. Proceedings of the National Academy of Sciences of the United States of America. 1991; 88:9722–9725. [PubMed: 1946394]
549. Wang WH, Yue P, Sun P, Lin DH. Regulation and function of potassium channels in aldosterone-sensitive distal nephron. Current opinion in nephrology and hypertension. 2010; 19:463–470. [PubMed: 20601877]
550. Wang XY, Masilamani S, Nielsen J, Kwon TH, Brooks HL, Nielsen S, Knepper MA. The renal thiazide-sensitive Na-Cl cotransporter as mediator of the aldosterone-escape phenomenon. J Clin Invest. 2001 Jul.108:215–222. [PubMed: 11457874]
551. Wei Y, Bloom P, Lin D, Gu R, Wang WH. Effect of dietary K intake on apical small-conductance K channel in CCD: role of protein tyrosine kinase. Am J Physiol Renal Physiol. 2001; 281:F206–212. [PubMed: 11457712]
552. Weinstein AM. A mathematical model of distal nephron acidification: diuretic effects. American journal of physiology Renal physiology. 2008; 295:F1353–1364. [PubMed: 18715938]
553. Weinstein AM. A mathematical model of rat collecting duct. I. Flow effects on transport and urinary acidification. American journal of physiology Renal physiology. 2002 Dec.283:F1237–1251. [PubMed: 12388378]
554. Weinstein AM. A mathematical model of rat distal convoluted tubule (I): cotransporter function in early DCT. American journal of physiology Renal physiology. 2005
555. Weinstein AM. A mathematical model of rat distal convoluted tubule (II): Potassium secretion along the connecting segment. American journal of physiology Renal physiology. 2005
556. Weinstein AM. Potassium excretion during antinatriuresis: perspective from a distal nephron model. American journal of physiology Renal physiology. 2012; 302:F658–673. [PubMed: 22114205]
557. Welling PA, Ho K. A comprehensive guide to the ROMK potassium channel: form and function in health and disease. Am J Physiol Renal Physiol. 2009; 297:F849–863. [PubMed: 19458126]
558. Wenzel U. Aldosterone antagonists: silver bullet or just sodium excretion and potassium retention? Kidney Int. 2007; 71:374–376. [PubMed: 17315004]
559. Wilcox CS, Mitch WE, Kelly RA, Freidman PA, Souney PF, et al. Factors affecting potassium balance during frusemide administration. Clin Sci. 1984; 67:195–203. [PubMed: 6378491]
560. Wilson FH, Disse-Nicodeme S, Choate KA, Ishikawa K, Nelson-Williams C, Desitter I, Gunel M, Milford DV, Lipkin GW, Achard JM, Feely MP, Dussol B, Berland Y, Unwin RJ, Mayan H, Simon DB, Farfel Z, Jeunemaitre X, Lifton RP. Human hypertension caused by mutations in WNK kinases. Science. 2001; 293:1107–1112. [PubMed: 11498583]
561. Wilson FH, Kahle KT, Sabath E, Lalioti MD, Rapson AK, Hoover RS, Hebert SC, Gamba G, Lifton RP. Molecular pathogenesis of inherited hypertension with hyperkalemia: the Na-Cl cotransporter is inhibited by wild-type but not mutant WNK4. Proc Natl Acad Sci U S A. 2003; 100:680–684. [PubMed: 12515852]

562. Wong NL, Quamme GA, Dirks JH. Effects of acid-base disturbances on renal handling of magnesium in the dog. Clinical science. 1986; 70:277–284. [PubMed: 3948477]

563. Woudenberg-Vrenken TE, Sukinta A, van der Kemp AW, Bindels RJ, Hoenderop JG. Transient receptor potential melastatin 6 knockout mice are lethal whereas heterozygous deletion results in mild hypomagnesemia. Nephron Physiology. 2011; 117:p11–19. [PubMed: 20814221]

564. Wright FS. Flow dependent transport processes: filtration, absorption, secretion. AmJPhysiol. 1982; 243:F1–F11.

565. Wright FS. Increasing magnitude of electrical potential along the renal distal tubule. AmJPhysiol. 1971; 220:624–638.

566. Wright FS. Sites and mechanisms of potassium transport along the renal tubule. Kidney Int. 1977; 11:415–432. [PubMed: 875263]

567. Wright FS, Bomsztyk K. Calcium transport by the proximal tubule. Adv Exp Med Biol. 1986; 208:165–170. [PubMed: 3551526]

568. Wright, FS., Giebisch, G. The Kidney: Physiology and Pathophysiology. New York: Raven Press, Ltd; 1992. Regulation of potassium excretion; p. 2209-2247.

569. Wright FS, Strieder N, Fowler NB, Giebisch G. Potassium secretion by distal tubule after potassium adaptation. AmJPhysiol. 1971; 221:437–448.

570. Wu G, Peng JB. Disease-causing mutations in KLHL3 impair its effect on WNK4 degradation. FEBS Lett. 2013; 587:1717–1722. [PubMed: 23665031]

571. Xi Q, Wang S, Ye Z, Liu J, Yu X, Zhu Z, Su S, Bai J, Li C. Adenovirus-delivered microRNA targeting the vitamin D receptor reduces intracellular Ca(2)(+) concentrations by regulating the expression of Ca(2)(+)-transport proteins in renal epithelial cells. BJU international. 2011; 107:1314–1319. [PubMed: 20553254]

572. Xie J, Wu T, Xu K, Huang IK, Cleaver O, Huang CL. Endothelial-Specific Expression of WNK1 Kinase Is Essential for Angiogenesis and Heart Development in Mice. The American journal of pathology. 2009

573. Xu B, English JM, Wilsbacher JL, Stippec S, Goldsmith EJ, Cobb MH. WNK1, a novel mammalian serine/threonine protein kinase lacking the catalytic lysine in subdomain II. J Biol Chem. 2000; 275:16795–16801. [PubMed: 10828064]

574. Xu JZ, Hall AE, Peterson LN, Bienkowski MJ, Eessalu TE, Hebert SC. Localization of the ROMK protein on the apical membranes of rat kidney nephron segments. AmJPhysiol. 1997; 273:F739–F748.

575. Xu ZC, Yang Y, Hebert SC. Phosphorylation of the ATP-sensitive, inwardly rectifying K+ channel, ROMK, by cyclic AMP-dependent protein kinase. J Biol Chem. 1996; 271:9313–9319. [PubMed: 8621594]

576. Yang C-L, Zhu X, Ellison DH. The thiazide-sensitive Na-Cl cotransporter is regulated by a WNK kinase signaling complex. J Clin Invest. 2007; 117:3403–3411. [PubMed: 17975670]

577. Yang CL, Angell J, Mitchell R, Ellison DH. WNK kinases regulate thiazide-sensitive Na-Cl cotransport. J Clin Invest. 2003; 111:1039–1045. [PubMed: 12671053]

578. Yang CL, Angell J, Mitchell R, Ellison DH. WNK kinases regulate thiazide-sensitive Na-Cl cotransport. J Clin Invest. 2003; 111:1039–1045. [PubMed: 12671053]

579. Yang CL, Zhu X, Ellison DH. The thiazide-sensitive Na-Cl cotransporter is regulated by a WNK kinase signaling complex. J Clin Invest. 2007; 117:3403–3411. [PubMed: 17975670]

580. Yang CL, Zhu X, Wang Z, Subramanya AR, Ellison DH. Mechanisms of WNK1 and WNK4 interaction in the regulation of thiazide-sensitive NaCl cotransport. J Clin Invest. 2005; 115:1379–1387. [PubMed: 15841204]

581. Yang SS, Fang YW, Tseng MH, Chu PY, Yu IS, Wu HC, Lin SW, Chau T, Uchida S, Sasaki S, Lin YF, Sytwu HK, Lin SH. Phosphorylation regulates NCC stability and transporter activity in vivo. Journal of the American Society of Nephrology: JASN. 2013; 24:1587–1597. [PubMed: 23833262]

582. Yang SS, Lo YF, Wu CC, Lin SW, Yeh CJ, Chu P, Sytwu HK, Uchida S, Sasaki S, Lin SH. SPAK-Knockout Mice Manifest Gitelman Syndrome and Impaired Vasoconstriction. J Am Soc Nephrol. 2010; 21:1868–1877. [PubMed: 20813865]

583. Yang SS, Lo YF, Wu CC, Lin SW, Yeh CJ, Chu P, Sytwu HK, Uchida S, Sasaki S, Lin SH. SPAK-knockout mice manifest Gitelman syndrome and impaired vasoconstriction. J Am Soc Nephrol. 2010; 21:1868–1877. [PubMed: 20813865]

584. Yang SS, Lo YF, Yu IS, Lin SW, Chang TH, Hsu YJ, Chao TK, Sytwu HK, Uchida S, Sasaki S, Lin SH. Generation and analysis of the thiazide-sensitive Na+-Cl-cotransporter (Ncc/Slc12a3) Ser707X knockin mouse as a model of Gitelman syndrome. Human mutation. 2010; 31:1304–1315. [PubMed: 20848653]

585. Yang SS, Morimoto T, Rai T, Chiga M, Sohara E, Ohno M, Uchida K, Lin SH, Moriguchi T, Shibuya H, Kondo Y, Sasaki S, Uchida S. Molecular Pathogenesis of Pseudohypoaldosteronism Type II: Generation and Analysis of a Wnk4(D561A/+) Knockin Mouse Model. Cell Metab. 2007; 5:331–344. [PubMed: 17488636]

586. Yang TX, Huang YNG, Singh I, Schnermann J, Briggs JP. Localization of bumetanide- and thiazide-sensitive Na-K-Cl cotransporters along the rat nephron. AmJPhysiolRenal, Fluid Electrolyte Physiol. 1996; 271:F931–F939.

587. Yeh BI, Sun TJ, Lee JZ, Chen HH, Huang CL. Mechanism and molecular determinant for regulation of rabbit transient receptor potential type 5 (TRPV5) channel by extracellular pH. J Biol Chem. 2003; 278:51044–51052. [PubMed: 14525991]

588. Yogi A, Callera GE, O'Connor SE, He Y, Correa JW, Tostes RC, Mazur A, Touyz RM. Dysregulation of renal transient receptor potential melastatin 6/7 but not paracellin-1 in aldosterone- induced hypertension and kidney damage in a model of hereditary hypomagnesemia. Journal of hypertension. 2011; 29:1400–1410. [PubMed: 21602712]

589. Yoo D, Kim BY, Campo C, Nance L, King A, Maouyo D, Welling PA. Cell surface expression of the ROMK (Kir 1.1) channel is regulated by the aldosterone-induced kinase, SGK-1, and protein kinase A. The Journal of biological chemistry. 2003; 278:23066–23075. [PubMed: 12684516]

590. Yoshikawa M, Uchida S, Yamauchi A, Miyai A, Tanaka Y, Sasaki S, Marumo F. Localization of rat CLC-K2 chloride channel mRNA in the kidney. The American journal of physiology. 1999 Apr.276:F552–F558. [PubMed: 10198414]

591. Yue P, Lin DH, Pan CY, Leng Q, Giebisch G, Lifton RP, Wang WH. Src family protein tyrosine kinase (PTK) modulates the effect of SGK1 and WNK4 on ROMK channels. Proceedings of the National Academy of Sciences of the United States of America. 2009; 106:15061–15066. [PubMed: 19706464]

592. Zambrowicz BP, Abuin A, Ramirez-Solis R, Richter LJ, Piggott J, BeltrandelRio H, Buxton EC, Edwards J, Finch RA, Friddle CJ, Gupta A, Hansen G, Hu Y, Huang W, Jaing C, Key BW Jr, Kipp P, Kohlhauff B, Ma ZQ, Markesich D, Payne R, Potter DG, Qian N, Shaw J, Schrick J, Shi ZZ, Sparks MJ, Van Sligtenhorst I, Vogel P, Walke W, Xu N, Zhu Q, Person C, Sands AT. Wnk1 kinase deficiency lowers blood pressure in mice: a gene-trap screen to identify potential targets for therapeutic intervention. Proc Natl Acad Sci U S A. 2003; 100:14109–14114. [PubMed: 14610273]

593. Zeng WZ, Li XJ, Hilgemann DW, Huang CL. Protein kinase C inhibits ROMK1 channel activity via a phosphatidylinositol 4,5-bisphosphate-dependent mechanism. J Biol Chem. 2003; 278:16852–16856. [PubMed: 12615924]

594. Zhang C, Wang L, Thomas S, Wang K, Lin DH, Rinehart J, Wang WH. Src family protein tyrosine kinase regulates the basolateral K channel in the distal convoluted tubule (DCT) by phosphorylation of KCNJ10 protein. The Journal of biological chemistry. 2013; 288:26135–26146. [PubMed: 23873931]

595. Zheng W, Verlander JW, Lynch IJ, Cash M, Shao J, Stow LR, Cain BD, Weiner ID, Wall SM, Wingo CS. Cellular distribution of the potassium channel KCNQ1 in normal mouse kidney. Am J Physiol Renal Physiol. 2007; 292:F456–466. [PubMed: 16896189]

596. Zheng W, Xie Y, Li G, Kong J, Feng JQ, Li YC. Critical role of calbindin-D28k in calcium homeostasis revealed by mice lacking both vitamin D receptor and calbindin-D28k. The Journal of biological chemistry. 2004; 279:52406–52413. [PubMed: 15456794]

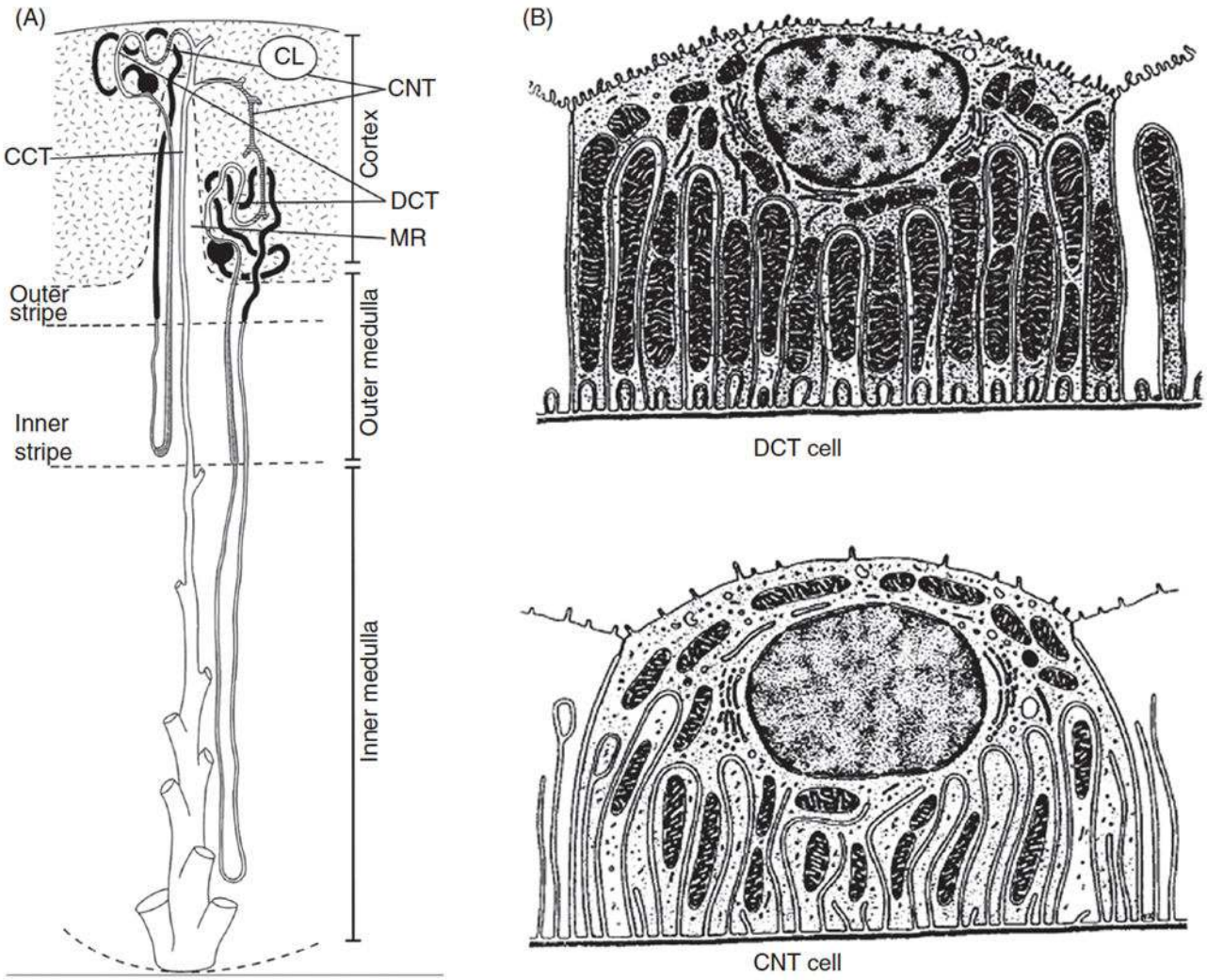

Figure 1.

Panel A: Structure of mammalian nephron: organization of nephron including distal tubule. Two types of nephrons are shown. A superficial nephron, at *left*, contains proximal and distal tubules that ascend to kidney surface and possess short loops of Henle. Loops and collecting ducts of superficial nephrons are located within medullary rays (MR). In superficial nephrons, distal tubule comprises distal convoluted tubule (DCT, shown in white), a short connecting tubule (CNT, shown as hatched), and a portion of collecting duct epithelium (shown in white) that begins proximal to junction to form collecting duct. A juxtamedullary nephron (such as that shown at *right*) has long loops of Henle that descend into renal medulla. Distal tubules comprise only a DCT and CNT segment. In juxtamedullary nephrons, CNT join to form branched arcades that ascend through cortical labyrinth (CL) before emptying into collecting duct (CCT). [Modified from Kriz and Kaissling (230)]. Panel B: Models of DCT and CNT cells. Note the extensive basolateral amplification and multiple mitochondria of DCT cells.

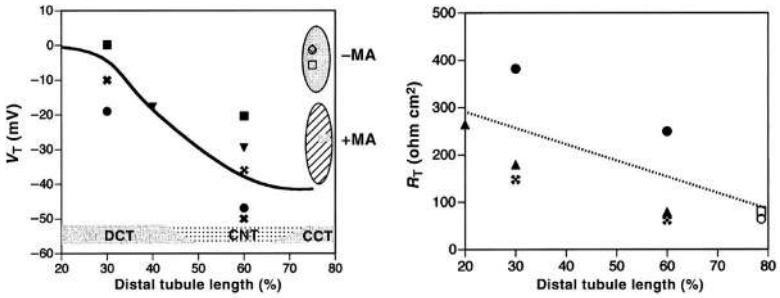

Figure 2.

Left: Transepithelial voltage (*V*T, in mV) along rat distal tubule. Data obtained during *in vivo* micropuncture are indicated by solid symbols and plotted as a percentage of total distal tubule length [×(564); λ(313); ν(22) τ(183); E(89)]. Data obtained by microperfusing cortical collecting ducts *in vitro* are presented as open or gray symbols within 2 ovals. Data collected without mineralocorticoid hormone treatment are shown in the grey oval [–MA; ▼ (431); μ(399); θ(431)]. Data collected in presence of mineralocorticoid hormone treatment are shown in the hatched oval [+MA; ■, (498); ●, (399)]. Location of DCT, CNT; and CCT is inferred from percentage length along distal tubule (104). *Right:* transepithelial resistance (RT) along rat renal distal tubule. Data obtained during *in vivo* micropuncture are indicated by solid symbols (references as in *top panel).* Data obtained by microperfusion *in vitro* are indicated by open symbols (references as in top panel).

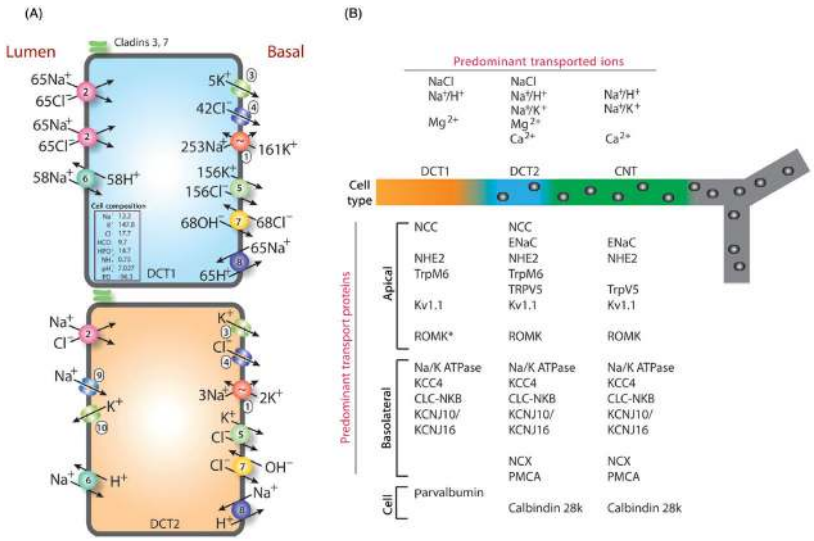

Figure 3.

Ion transport pathways in the DCT1 and DCT2. Panel A: Each channel or transporter is shown schematically and is numbered, according to the scheme in Table 1. The estimated solute fluxes (in pmol·min^{-1}·mm^{-1}) through each pathway are adapted from Weinstein (554). In the present scheme, however, ENaC (9) and ROMK (10) are restricted to the DCT2, and the luminal KCl cotransport has been omitted. Additionally, Weinstein models OH^- traversing Cl^- channels. Big potassium (BK) channels are also likely to be present in this segment, but are not shown. The solute concentrations, pH, and membrane voltage of modeled DCT cells are shown in the box. Concentrations are in mmol/L. Net solute fluxes are not given for the DCT2, as this segment has not been modeled, but are likely to be lower, at baseline. Panel B: Schematic of predominant transported ions, cell types (intercalated cells are indicated by gray circles), and predominant transport proteins. Asterisk indicates that, although ROMK has been detected in the DCT1 by immunohistochemical techniques, it has not been detected in apical patches along this segment.

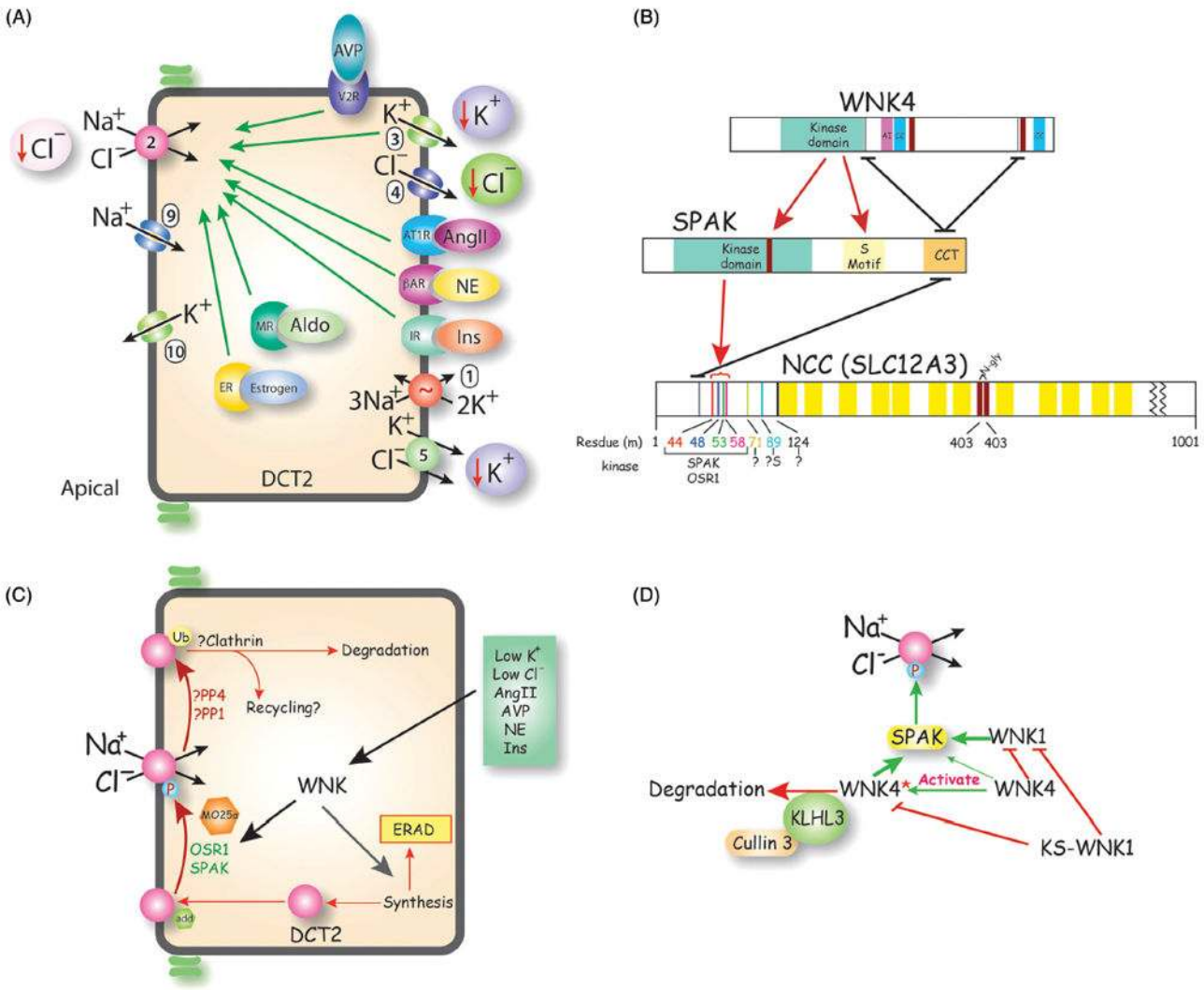

Figure 4.

Regulation of sodium and chloride transport along The DCT. Panel A: Major factors known to regulate NCC along the DCT are shown. Note that regulation of ENaC and ROMK is omitted, as it is similar to regulation along the CNT and CD, Various peptide (Angll, insulin, and AVP) and steroid (aldosterone and estrogen) hormones, as well as norepinephrine (NE), stimulate NaCl transport primarily by enhancing NCC activity, although effects on other transporters are also likely. NCC is stimulated by low paracellular [K^+], perhaps directly via Kir4.1/5.1 channels, but also perhaps by stimulating cell chloride depletion via KCC4. Transporters are identified by numbers shown in Table 1. Panel B: highly simplified scheme of NCC regulation by WNK kinases (WNK4 is shown]. NCC is activated, via phosphorylation (red arrow), by SPAK, at conserved sites as shown. The specific SPAK phosphorylation sites are given according to rodent residue number. Other sites are also shown, which may be phosphorylated by other kinases. Two N-linked glycosylation sites are shown. SPAK In turn is activated by WNKs. Both WNK1 and WNK4 can activate SPAK. Sites of protein-protein interaction are shown by black lines. The conserved C terminus

(CCT) of SPAK binds to an RFXT motif on NCC, shown as a vertical grey bar. In WNK4, there are autoinhibitory (AI) and coiled coil (CC) domains. Panel C: shows a highly simplified diagram of NCC activation by various stimuli, acting via a WNK and SPAK or OSR1. Note that MO25 can facilitate the action of SPAK on NCC. NCC is dephosphorylated by PP1 and PP4. After synthesis, NCC can be degraded by endoplasmic reticulum mediated decay (ERAD). Panel D: simplified scheme of current views of NCC regulation by WNKs and KLHL3 and cullin 3. As noted, WNKs interact to exert complex stimulatory and inhibitory effects. As KS-WNK1 lacks kinase activity, it appears to be predominantly an inhibitory WNK. WNK4, which is a less potent kinase at baseline, can bind to, and inhibit, WNK1. In the presence of angiotensin II, however, WNK4 becomes more active, stimulating SPAK directly. WNK4, and likely WNK1, are targeted for degradation by KLHL3 and cullin 3, as discussed in the text. Much of this scheme remains speculative and incomplete. Note that WNK kinases also have effects on NCC, ROMK, and ENaC that appear related to degradative activity (as shown in Panel C). These are omitted here for clarity.

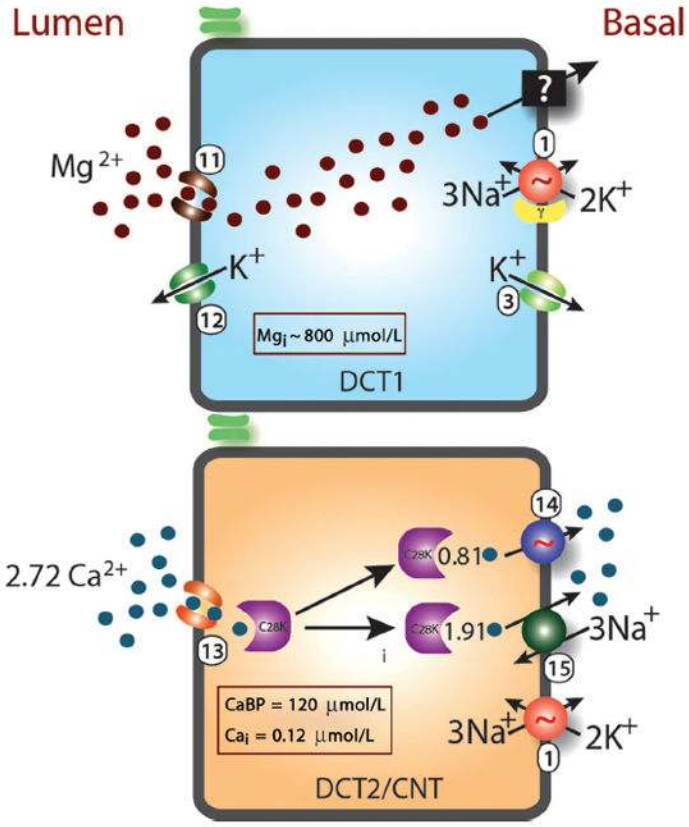

Figure 5.

Calcium and magnesium reabsorptive pathways in the DCT1 and DCT2 (and connecting tubule). The majority of magnesium traverses the DCT1, as shown, whereas the majority of calcium traverses pathways in the DCT2/CNT. Each channel or transporter is numbered according to the scheme in Table 1. The solute fluxes of calcium are adapted from Bonny and Edwards (40), as are the intracellular concentrations of calcium and Calbindin D28K (CaBP). Note that the presence of this buffer keeps intracellular calcium very low, permitting appropriate signal transduction, despite ongoing transepithelial flux. The intracellular magnesium concentration is from Glaudemans (162), and is much higher. For this reason, intracellular buffering does not appear necessary. Additional details are given in the text.

Table 1

Transporters and channels in the DCT

Number	Protein	Gene	Cytogenetic location
1	Na^+-K^+-ATPase	*ATP1A2*	1q23.2
2	NCC	*SLC12A3*	16q13
3	Kir4.1/Kir5.1	*KCNJ10/KCNJ16*	17q24.3/1q23.2
4	CLCNKB	*CLCNKB*	1p36.13
5	KCC4	*SLC12A7*	5p15.33
6	NHE2	*SLC9A2*	2q12.1
7	AE2	*SLC4A2*	7q36.1
8	NHE1	*SLC9A1*	1p36.11
9	ENaC	*SCNN1A/SCNN1B/SCNN1G*	12p13.31/16p12.2/16p12.2
10	ROMK/Kir1.1	*KCNJ1*	11q24.3
11	TRPM6	*TRPM6*	9q21.13
12	Kv1.1	*KCNA1*	12p13.32
13	ECaC/TRPV5	*TRPV5*	7q34
14	PMCA1b*	*ATP2B1*	12q21.33
15	NCX1	*NCX1*	2p22.1

The numbers in the left column correspond to numbers identifying transporters and channels in Figures 3 and 5.

* indicates that there are reports of PMCA4b in kidney as well. The exact isoform of the basolateral NCX is not fully established.

Table 2

Genetic Diseases of the Distal Convoluted Tubule

			Plasma					Urine						
Disease	**Gene**	**Protein**	**Na^+**	**K^+**	**Ca^{2+}**	**Mg^{2+}**	**pH**	**Mg^{2+}**	**Ca^{2+}**	**K^+**	**Na^+**	**BP**	**Other**	**Ref.**
Gitelman	*SLC12A3*	NCC	⇔	↓↓	⇔	↓	↑	↑	↓↓	↑*	⇔ or ↑	⇔ or ↓	Increased bone density	(92, 457)
EAST/SeSAME	*KCNJ10*	Kir4.1	⇔	↓↓	⇔	↓	↑↑	↓↓	↑*	⇔ or ↑		⇔ or ↓	Epilepsy, ataxia, sensorineural deafness	(37, 436)
HSH	*TRPM6*	TRPM6	⇔	⇔	↓	↓↓	⇔	⇔	⇔	NR	NR	⇔	Mental retardation	(432, 539, 540)
HOMG4	*EGF*	EGF	⇔	⇔	⇔	↓↓	⇔	⇔	⇔	NR	NR	⇔	Mental retardation	(179)
Autosomal-dominant hypomagnesemia	*KCNA1*	Kv1.1	⇔	⇔	⇔	↓↓	⇔	⇔	⇔	NR	NR	⇔	Episodic ataxia 1; myokymia	(164)
Isolated dominant hypomagnesemia	*FXYD2*	γNa^+/K^+- ATPase	⇔	⇔	⇔	↓↓	⇔	↑↑	↓↓	NR	NR	⇔		(331)
MODY with hypomagnesemia	*HNF-1b*	HNF1B	NR	NR	⇔	↓	NR	↑	↓	NR	NR	⇔	Cystic kidneys, diabetes mellitus	(4)
FHHt1/PHA2/Gordon	*WNK1*	WNK1	⇔	↑	⇔	NR	↓	NR	⇔	↓*	⇔	⇔ or ↑		(2, 560)
FHHt2/PHA2/Gordon	*WNK4*	WNK4	⇔	↑↑	⇔	⇔	↓	⇔	↑	↓*	⇔	↑	Low bone density	(322, 560)
FHHt3/PHA2/Gordon	*KLHL3*	Kelch-like 3	⇔	↑↑	⇔	NR	↓	NR	NR	↓*	⇔	↑		(46, 305)
	CUL3	Cullin 3	⇔	↑↑↑	⇔	NR	↓↓	NR	NR	↓*	⇔	↑↑		(46)

Full disease names are given in the text.

*for Gitelman and EAST syndrome, excretion of potassium may be normal and reflect dietary intake, but the fractional excretion is always high. In many individuals, dietary consumption is high, leading to increased absolute excretion rates. The converse is true for FHHt.